Title
The Role of Lysosomal Cholesterol Transport in Cellular Nutrient Sensing and Organelle Homeostasis

Author
Davis, Oliver Brayer

Publication Date
2020

Peer reviewed|Thesis/dissertation

The Role of Lysosomal Cholesterol Transport in Cellular Nutrient Sensing and Organelle Homeostasis

by

Oliver Brayer Davis

A dissertation submitted in partial satisfaction of the

requirement for the degree of

Doctor of Philosophy

in

Molecular and Cell Biology

in the

Graduate Division

of the

University of California, Berkeley

Committee in charge:

Professor Roberto Zoncu, Chair
Professor Jeremy W. Thorner
Professor Elçin Ünal
Professor Daniel K. Nomura

Summer 2020

Abstract

The Role of Lysosomal Cholesterol Transport in Cellular Nutrient Sensing and Organelle Homeostasis

by

Oliver Brayer Davis

Doctor of Philosophy in Molecular and Cell Biology

University of California, Berkeley

Professor Roberto Zoncu, Chair

Lysosomes are the main catabolic organelles of a eukaryotic cell and are critical for maintenance of cellular homeostasis. Macromolecules, organelles captured via autophagy, and material taken up by endocytosis are degraded in lysosomes. Consequently, lysosomes concentrate, store, recycle, and distribute metabolites crucial for biosynthetic processes. The lysosome also functions as a platform for regulating and coordinating signaling pathways. In particular, a master regulator of cell growth and proliferation – the mechanistic target of rapamycin complex 1 (mTORC1), an evolutionarily conserved serine/threonine protein kinase – is activated at the surface of the lysosome when nutrients are plentiful (e.g., amino acids potently promote mTORC1 activity). Cholesterol, a key component of biomembranes, also stimulates mTORC1 recruitment and activation at the lysosome. Thus, by integrating its degradative and signaling roles, the lysosome serves as a hub for nutrient sensing.

In diseases known as lysosomal storage disorders, pathogenic levels of a particular metabolite accumulate in the lysosome due to the loss of function of a human gene required for catabolism or transport of a substrate normally digested in the lysosome. In Neimann-Pick type C (NPC) disease, the lysosomal cholesterol exporter, NPC1, is inoperative, causing accumulation of cholesterol within lysosomes, resulting in disruption of lysosomal function, which is propagated to other organelles (e.g., mitochondria) also compromising their function. Ultimately, this damage leads to progressive neurodegeneration in patients. The accumulation of cholesterol caused by loss of NPC1 also chronically hyperactivates mTORC1, further interfering with the regulation of cellular homeostasis.

To increase our understanding of the factors that cause lysosomal failure in NPC disease, I examined the compositional and functional alterations that occur in lysosomes lacking NPC1 activity. Likewise, I studied how NPC1 loss triggers aberrant mTORC1 signaling and how dysregulated mTORC1 contributes to organelle pathogenesis. I first used organelle immuno-isolation in conjunction with proteomic profiling to uncover a pronounced proteolytic impairment of NPC lysosomes that is compounded by depletion of luminal hydrolases and enhanced susceptibility to

membrane damage. I also tested a panel of NPC1 mutants in NPC1-deficient cells and demonstrated that, cholesterol transport by NPC1 is tightly linked to regulation of mTORC1 activity, indicating that lysosomal cholesterol accumulation is the primary underlying cause of mTORC1 hyperactivation in NPC disease. Next, I demonstrated that genetic and pharmacologic mTORC1 inhibition restores lysosomal proteolysis and lysosomal membrane integrity without correcting cholesterol accumulation, implicating mTORC1 hyperactivity as a main driver of downstream pathogenesis, including the loss of mitochondrial quality control and function. In agreement with those conclusions, I showed that mTORC1 inhibition reverses lysosomal and mitochondrial dysfunction in a neuronal model of NPC, extending my findings to a disease-relevant cellular context. Thus, targeting the cholesterol-mTORC1 signaling pathway may represent a novel therapeutic avenue in NPC that could complement or replace current approaches.

Table of Contents

Abstract……..1
Table of Contents…….. i
List of Figures……iii
Acknowledgements…….. iv

Chapter 1: Introduction to Lysosome Structure, Function, and Role in Cellular Cholesterol Sensing by mTORC1

1.1 Lysosome structure and catabolic function in the cell……...2
1.1.1 Structural organization of the lysosome…….. 2
1.1.2 The lysosome is a catabolic hub of the cell……... 3
1.2 Lysosomes and mTORC1…….. 7
1.2.1 Regulation of cellular metabolism by mTORC1……8
1.2.2 Cellular signaling upstream of mTORC1 activation…….. 9
1.3 Lysosomes and Disease…….. 13
1.3.1 Lysosomal Storage Disorders…….. 13
1.3.2 Lysosomal Function, Autophagy, and Neurodegeneration……...13
1.4 Lysosomes and Cholesterol…….. 14
1.4.1 The role and sources of cellular cholesterol…….. 14
1.4.2 NPC1 and NPC2-mediated cholesterol export from the lysosome…….15
1.4.3 Other routes of lysosomal cholesterol transport……16
1.4.4 Cholesterol sensing by mTORC1…….. 18

Chapter 2: NPC1-mTORC1 Signaling Couples Cholesterol Sensing to Organelle Homeostasis and is a Targetable Pathway in Niemann-Pick Type C

2.1 Chapter Summary……21
2.2 Introduction……...21
2.3 Results…….. 23
2.3.1 NPC1-null lysosomes display extensive proteolytic defects…….. 23
2.3.2 NPC1-null lysosomes display increased susceptibility to membrane damage…….. 28
2.3.3 NPC1 regulates mTORC1 via its cholesterol-exporting function……33
2.3.4 mTORC1 inhibition restores integrity and proteolytic function of NPC lysosomes downstream of cholesterol storage……36
2.3.5 mTORC1 inhibition restores lysosomal function in iPSC-derived NPC neuronal cultures…….. 38
2.3.6 mTORC1 inhibition restores defective mitochondrial function in NPC1-null cells……...40
2.4 Discussion…….. 43
2.5 Methods…….. 46

2.5.1 Mammalian Cell Culture……46
2.5.2 Cloning and Generation of Stable Cell Lines……47
2.5.3 Lysosome Immunoprecipitation (Lyso-IP)……47
2.5.4 Proteomics Analysis……48
2.5.5 Immunofluorescence……48
2.5.6 Microscopy……49
2.5.7 Image analysis……49
2.5.8 Measurement of GALC activity……49
2.5.9 Cholesterol starvation and replenishment……50
2.5.10 Cell lysis and immunoblotting……50
2.5.11 Cholesterol labeling in situ with D4H*-mCherry and filipin……50
2.5.12 Measurement of lysosomal permeability……51
2.5.13 hIPSC generation and neuronal differentiation……51
2.5.14 Generation of NPC1 knock-out hIPSCs……51

Chapter 3 Characterization of NPC2 function in regulation of mTORC1 activity

3.1 Chapter Summary……54
3.2 Introduction……54
3.3 Results……55
3.3.1 Loss of NPC2 causes cholesterol accumulation in the lysosomal limiting membrane and render mTORC1 cholesterol insensitive……55
3.3.2 Lysosomal and mitochondrial perturbations caused by loss of NPC2 are remediated by inhibition of mTORC1……56
3.4 Discussion……57
3.5 Methods……59

References……60

List of Figures

Figure 1.1 Structural organization of the lysosome and routes of macromolecular delivery…… 6
Figure 1.2 Logic of the mTORC1 signaling network and its regulation of cellular metabolism…… 8
Figure 1.3 Molecular signaling pathways upstream of mTORC1……...11
Figure 1.4 Cholesterol transport pathways of the endolysosomal system…….. 17
Figure 2.1 Lysosome proteomics reveals a proteolytic defect in NPC1-deficient lysosomes……... 24
Figure 2.2 Immunofluorescence reveals undigested autophagic material in lumen of NPC1-deficient lysosomes……...26
Figure 2.3 Cholesterol export by NPC1 mutants alleviates proteolytic block in NPC1-deficient cells…….. 27
Figure 2.4 NPC1-deficient lysosomes also have reduced levels of luminal hydrolases……..28
Figure 2.5 NPC1-deficient cells have elevated levels of lysosome-associated ESCRT-III……29
Figure 2.6 NPC1-deficient cells are more susceptible to lysosomal rupture……...31
Figure 2.7 Cholesterol export by NPC1 mutants restores lysosomal membrane integrity…… 32
Figure 2.8 Transport by NPC1 controls mTORC1 activity in response to lysosomal cholesterol…… 34
Figure 2.9 Inhibition of mTORC1 activity alleviates lysosomal proteolysis defect associated with loss of NPC1……..35
Figure 2.10 Inhibition of mTORC1 activity reduces ESCRT-III accumulation on NPC1-deficient lysosomes……..37
Figure 2.11 Validation of iPSC-derived neural lineage lines……39
Figure 2.12 Inhibition of mTORC1 corrects lysosomal defects associated with loss of NPC1 in and iPSC-derived neuronal cell model……..40
Figure 2.13 Mitochondrial morphology and function are disrupted by loss of NPC1 and is restored by inhibition of mTORC1…….. 42
Figure 2.14 Model illustrating the relationship between NPC1, lysosomal cholesterol, mTORC1 signaling and organelle homeostasis in both normal and NPC cells……...44
Figure 3.1 NPC2-null cells have dysregulated mTORC1 signaling caused by elevated cholesterol present on the limiting membrane of the lysosome…… 55
Figure 3.2 NPC2-null cells exhibit a block in lysosomal proteolysis and increased mitochondrial fragmentation that are corrected by mTOR inhibition…… 57
Figure 3.3 NPC2-null cells reconstituted with mutant NPC2 isoforms exhibit phenotypic inconsistencies with published results…….. 58

Acknowledgements

The completion of this dissertation would not have been possible without the support of many people. For the sake of brevity, I will not list every person by name, but that should not diminish the importance of anyone's contribution to my success. This is my Oscar's acceptance speech moment, and I can already hear them playing the music to usher me off stage.

First and foremost, I must extend my deepest thanks to Roberto. Without his guidance and encouragement, I would never have accomplished any of this. I have learned much from his critical eye and commitment to rigorous investigation, and he has helped me to become an insightful and a thoughtful scientist. The breadth and depth of his knowledge is astounding, and continues to inspire me to tackle challenging problems, expand my horizons, and to never stop learning.

I am also eternally indebted to the many scientists who I have had the fortune of collaborating with and/or been mentored by throughout my time in graduate school. I must thank all the members of the Zoncu lab, past and present, for their scientific insights and for making the laboratory a truly enjoyable place to work. Thanks as well to all my co-authors, I am forever indebted to you for your help and insights. I am also deeply grateful to my thesis committee both for keeping me on track, and for providing me with much needed encouragement during times when I couldn't see the light at the end of the tunnel.

To my friends and family, I am appreciative of your unconditional love and support. I am truly privileged to have parents that nurtured my inherent curiosity as a child, and who have stood behind me every step of this journey, even when it probably seemed like all I did was move across the country to complain constantly. My mother is my inspiration for pursing a career where I am working every day to improve the human condition. My father is the reason I have the courage to take risks. My sister Harriett is the best confidant I could ask for, and deserves many thanks for validating my feelings and helping me bring balance to my life. Thanks to Ellie and Oren for reminding me to embrace my inner child – I hope I am a good (but not too good of a) role model for you. I have many friends who deserve collective acknowledgment here as well. Thanks for the welcome distractions from the lab, for enriching my life with culture, libations, frequent trips into nature, and for letting me pet your dogs before I had one of my own. Lastly, thanks to Ben. There are no words that will express my gratitude for the love and support you show me every single day. You bring joy to my life and you deserve a doctoral degree just for sticking with me throughout this. I could not ask for a better partner in life.

Chapter 1

Introduction to Lysosome Structure, Function, and Role in Cellular Cholesterol Sensing by mTORC1

Lysosomes are small membrane-bound organelles that are best known as the primary catabolic compartment of eukaryotic cells. Lysosomes were first characterized in 1955 by Christian de Duve. While tracking the biochemical activity of a hydrolytic enzyme, de Duve discovered that this activity, along with hydrolytic activity of several other enzymes, appeared to be enclosed in a membrane-bound structure that maintains an acidic pH supporting optimal enzyme activity (de Duve, 2005). Subsequent electron microscopy and biochemical studies confirmed the existence of these structures, termed “lysosomes” from the Greek for “digestive body”, in eukaryotic cell preparations (de Duve, 2005; Essner and Novikoff, 1961). These two properties – acidic pH and the concentration of hydrolytic enzyme activity – are hallmark characteristics of the lysosome, and have come to define it as simply the “trashcan” of the cell. Recently, a more expansive role for the lysosome in cellular homeostasis and organismal health has been appreciated, and its primary function as a major degradative site in the cell is now thought to exist alongside with and in connection to its newly-found role as a platform for the organization and regulation of cellular metabolism.

1.1 Lysosome structure and catabolic function in the cell

1.1.1 Structural organization of the lysosome

The lysosome is most simplistically divided into two main structural components, the limiting membrane that defines the exterior boundary of the lysosome, and the acidic lumen that is encapsulated by the limiting membrane (Figure 1.1). The lysosomal lumen is home to approximately 60 resident hydrolytic enzymes whose activities are directed at a diverse array of substrates to support the degradation of complex cellular macromolecules, such as proteins, polysaccharides, nucleic acids, and lipids (Perera and Zoncu, 2016; Settembre et al., 2013). Lysosomal hydrolases generally exhibit optimal activity in the low pH environment of the lysosomal lumen, which is a result of the activity of the vacuolar H^+-ATPase (v-ATPase). The v-ATPase is present in the limiting membrane of the lysosome, and uses a rotational mechanism to couple energy provided by ATP hydrolysis to translocate protons from the cytoplasm into the lysosome lumen, resulting in an internal pH between 4.5 and 5.0 (Forgac, 2007; Mindell, 2012).

The lysosomal limiting membrane is a single phospholipid membrane bilayer that contains an array of resident transmembrane proteins, that primarily serves to segregate the harsh acid environment of the lysosome lumen from the rest of the cell (Saftig and Klumperman, 2009; Settembre et al., 2013). One class of transmembrane proteins, comprised of highly abundant proteins such as lysosome-associated membrane protein 1 (LAMP1) and LAMP2, are highly glycosylated on their luminal side and play an important structural role. These glycosylated proteins form a glycocalyx, a protective polysaccharide coating that lines the inner leaflet of the lysosomal membrane, protecting the membrane and other transmembrane proteins from the digestive activity of the resident lysosomal hydrolases (Perera and Zoncu, 2016; Saftig and Klumperman, 2009; Settembre et al., 2013).

Another class of transmembrane proteins present on lysosome membranes are nutrient and metabolite transporters that are responsible for the recycling of cellular building blocks that are the end products of lysosomal degradation. The relevance of this class of proteins was first appreciated in studies of the yeast vacuole – the homologous structure to the mammalian lysosome – which has long been understood to function as a storage site for amino acids, phosphate, and metal ions (Li and Kane, 2009). Yeast vacuoles have multiple families of nutrient transporters and permeases present on their membranes, that allow them to selectively concentrate and mobilize specific metabolite pools from the vacuolar lumen in a proton gradient-dependent manner (Li and Kane, 2009; Russnak et al., 2001; Sekito et al., 2008). Lysosomes in higher eukaryotes also have a diverse cohort of transporters required for export of metabolites such as amino acids, sugars, nucleosides, lipids, polyamines, organic and metal ions from the lysosome lumen (Chapel et al., 2013; Jeźégou et al., 2012; Kalatzis et al., 2001; Liu et al., 2012; Rong et al., 2011; Sagné et al., 2001; Verdon et al., 2017; Wyant et al., 2018). Emerging evidence suggests that as with the yeast vacuole, lysosomes are able to dynamically control the release of specific metabolites in response to changes in cellular environmental conditions (Abu-Remaileh et al., 2017; Verdon et al., 2017).

1.1.2 The lysosome is a catabolic hub of the cell

Because of its catabolic functions, the lysosome is centered in the cell at the terminal steps of several major endosomal routes for degradation (Figure 1.1). The dynamic positioning, tethering, and fusion of lysosomes with target organelles are mediated by distinct proteins and complexes that are embedded in or associated with the lysosomal membrane (Lawrence and Zoncu, 2019). Lysosome transport and positioning along microtubules is regulated by kinesins, which mediate plus-end directed movement towards the cell periphery, and dyneins, which mediate minus-end directed movement towards the nucleus (Lawrence and Zoncu, 2019). Interactions between the lysosome and these molecular motors are formed by proteins on the lysosomal membrane such as the BLOC1-related complex (BORC), and the Rab7-interacting lysosomal protein (RILP), which interact with kinesins and dyneins, respectively (Lawrence and Zoncu, 2019; Pu et al., 2015; Rocha et al., 2009). Tethering of lysosomes to target organelles is mediated by the homotypic fusion and vacuolar protein sorting (HOPS), a multi-subunit complex that is recruited to lysosomes via its interaction with the Rab7 GTPase, and fusion of lysosomes with target organelles involves formation of a *trans*-SNARE complex including the lysosomal R-SNAREs vesicle-associated membrane protein-7 (VAMP7) or VAMP8 (Lawrence and Zoncu, 2019; Luzio et al., 2007).

Both extra- and intracellular cargo destined for degradation in the lysosome are primarily delivered to via vesicular trafficking pathways. Extracellular cargo that is taken up by the cell enters an endosomal trafficking pathway that terminates at the lysosome. Many mechanisms, such as clathrin-dependent and -independent endocytosis, phagocytosis, and macropinocytosis, exist for the uptake of an enormously diverse array of extracellular cargo such as cell surface receptors, extracellular matrix material, and viral and bacterial pathogens (Doherty and McMahon,

2009). Once internalized, endosomes enter a maturation process involving multiple rounds of vesicle fusion and subsequent sorting of material that progressively remodels its protein and lipid composition and decreases luminal pH (Luzio et al., 2009; Perera and Zoncu, 2016; Saftig and Klumperman, 2009). These matured (or "late") endosomes can then either further mature into a lysosome upon delivery of enough luminal hydrolases (typically from Golgi-derived vesicles) (Perera and Zoncu, 2016), or can directly fuse with pre-existing lysosomes to complete degradation of their contents (Luzio et al., 2009; Saftig and Klumperman, 2009).

Lysosomal catabolism is of critical importance for the regulation of the myriad of processes that involve endosomal trafficking and degradation. Destruction of endocytosed cell surface receptors in the lysosome is an important mechanism for long-term attenuation of signaling downstream of these receptors (Goh and Sorkin, 2013). The lysosomal breakdown of extracellular material, scavenged via macropinocytosis, is also important for providing cells in low-nutrient conditions with metabolites required to sustain cellular survival (Davidson and Vander Heiden, 2017; Perera and Bardeesy, 2015). Phagocytosis, another form of cellular uptake that is carried out by specialized cells, is important for clearing extracellular pathogens and apoptotic cell debris, and is also ultimately dependent on the degradative capacity of the lysosome (Luzio et al., 2007).

Intracellular material that is destined for lysosomal degradation is trafficked via the cellular "self-eating" process termed autophagy. Multiple forms of autophagy exist, but the best studied pathway, termed "macroautophagy", involves the capture of cytoplasmic materials and other cellular structures within a double-membrane vesicle termed the autophagosome (He and Klionsky, 2009; Hurley and Schulman, 2014; Yim and Mizushima, 2020; Zhao and Zhang, 2019). In mammalian cells, complex cellular signaling and machinery regulates the initiation, growth, formulation, and closure of this phagophore membrane to form the autophagosome (He and Klionsky, 2009; Hurley and Schulman, 2014; Zhao and Zhang, 2019). The outer membrane of the autophagosome then fuses with a lysosome, forming a hybrid organelle known as an autolysosome, to deliver hydrolytic capacity that degrades the inner membrane and encapsulated contents (He and Klionsky, 2009; Yim and Mizushima, 2020; Zhao and Zhang, 2019). Subsequent to the completion of autophagic degradation, lysosomes can be reformed via a specific pathway that involves tubulation and separation of the lysosome membrane from the autolysosome membrane (Yim and Mizushima, 2020).

Two other mechanisms of autophagic degradation, termed microautophagy and chaperone-mediated autophagy (CMA), have been characterized in mammalian cells. In microautophagy, lysosome or late endosome membranes directly capture cellular material through invaginations in the limiting membrane created by a membrane remodeling complex known as Endosomal Sorting Complex Required for Transport (ESCRT). Polymerization of the ESCRT-III module at the limiting membrane of lysosomes causes the membrane to bud inwardly to form intraluminal vesicles that are subsequently degraded (Luzio et al., 2007; Yim and Mizushima, 2020). The regulation and mechanisms of microautophagy are poorly characterized in mammalian cells, although studies of the yeast vacuole have validated its existence in this organism and shed some light on its mechanistic regulation (Yim and Mizushima, 2020). In contrast to

other forms of autophagy, CMA is a non-vesicular route for lysosomal degradation where protein substrates are bound by the HSC70 chaperone, which may mediate their unfolding, and direct their translocation across the lysosomal membrane through a pore-forming membrane protein that remains to be identified (Cuervo and Dice, 1996; Kaushik and Cuervo, 2018).

While the current understanding of the molecular mechanisms that govern autophagosome formation and maturation is extensive, it was genetic studies of yeast mutants defective in autophagy that first provided the list of the core machinery, which came to be known as the autophagy-related (ATG) genes, involved in this process (Thumm et al., 1994; Tsukada and Ohsumi, 1993). The earliest steps in autophagosome formation rely on the ULK1/2 complex (Atg1 complex in yeast), which is recruited to ER membranes and marks the site of phagophore formation via an incompletely characterized mechanism that relies on the kinase activity of the complex (Hurley and Schulman, 2014; Zhao and Zhang, 2019). Atg9, an integral membrane component, is thought to be involved in shuttling donor membrane vesicles to the growing phagophore (Feng et al., 2014), and in yeast cells the complex of Atg2 and Atg18 (WIPI proteins in mammalian cells) appears to bind to growing ends of the phagophore where it is involved in recycling of Atg9 (Feng et al., 2014; Hurley and Schulman, 2014). Another set of proteins (Vps34, Vps15, Beclin1, and Atg14 in mammals) forms the class III phosphatidylinositol 3-kinase (PI3K) complex that synthesizes phosphatidylinositol 3-phosphate (PI3P) on the growing phagophore, mediating the recruitment of PI3P-binding proteins such as Atg18 to the autophagosome (Feng et al., 2014; Hurley and Schulman, 2014). Two ubiquitin-like proteins (UBLs) are also involved in autophagosome maturation in yeast; Atg8 and Atg12. Like ubiquitin, both Atg8 and Atg12 are activated via an enzymatic cascade that results in their conjugation to other cellular components (Feng et al., 2014; Hurley and Schulman, 2014). Atg12 becomes conjugated to Atg5 (in complex with Atg16) via the sequential activities of Atg7 and Atg10. Atg8 is processed by the sequential activity of Atg4, Atg7, and Atg3 before the Atg12-5 and Atg16 complex then acts as a ligase to conjugate Atg8 to phosphatidylethanolamine (PE) inserted in the autophagosome membrane (Hurley and Schulman, 2014). In mammals a single Atg12 ortholog exists, while there are multiple Atg8 orthologs comprised of the LC3 and GABARAP families of proteins (Feng et al., 2014; Hurley and Schulman, 2014).

In addition to being critical for the recycling of molecular building blocks via non-specific bulk degradation of cellular material, selective autophagy is an important mechanism for cellular quality control and critical for maintenance of cellular homeostasis (Gatica et al., 2018; Singh and Cuervo, 2011). The general mechanism for selective autophagy involves the recognition of a substrate by a specific cargo receptor protein that also binds to Atg8-family proteins that decorate the growing phagophore (Anding and Baehrecke, 2017; Gatica et al., 2018; Hurley and Schulman, 2014). Specific motifs on cargo receptors, termed LC3-interacting regions (LIRs) or ubiquitin-interacting motifs (UIMs), mediate the binding and recruitment of receptors to Atg8-decorated autophagosomes (Behrends et al., 2010; Marshall et al., 2019; Noda et al., 2008). Many cargo receptors, such as p62/SQSTM1 and NBR1, recognize ubiquitinated substrates marked for degradation, and thus can mediate the recruitment

of a diverse range of substrates to the autophagosome (Kim et al., 2008b; Kirkin et al., 2009; Pankiv et al., 2007). Other cargo receptors, such as NCOA4 and FAM134B, appear much more specific in function, and bind directly to substrates (ferritin for NCOA4), or are embedded in target membranes (the ER for FAM134B) (Khaminets et al., 2015; Mancias et al., 2014).

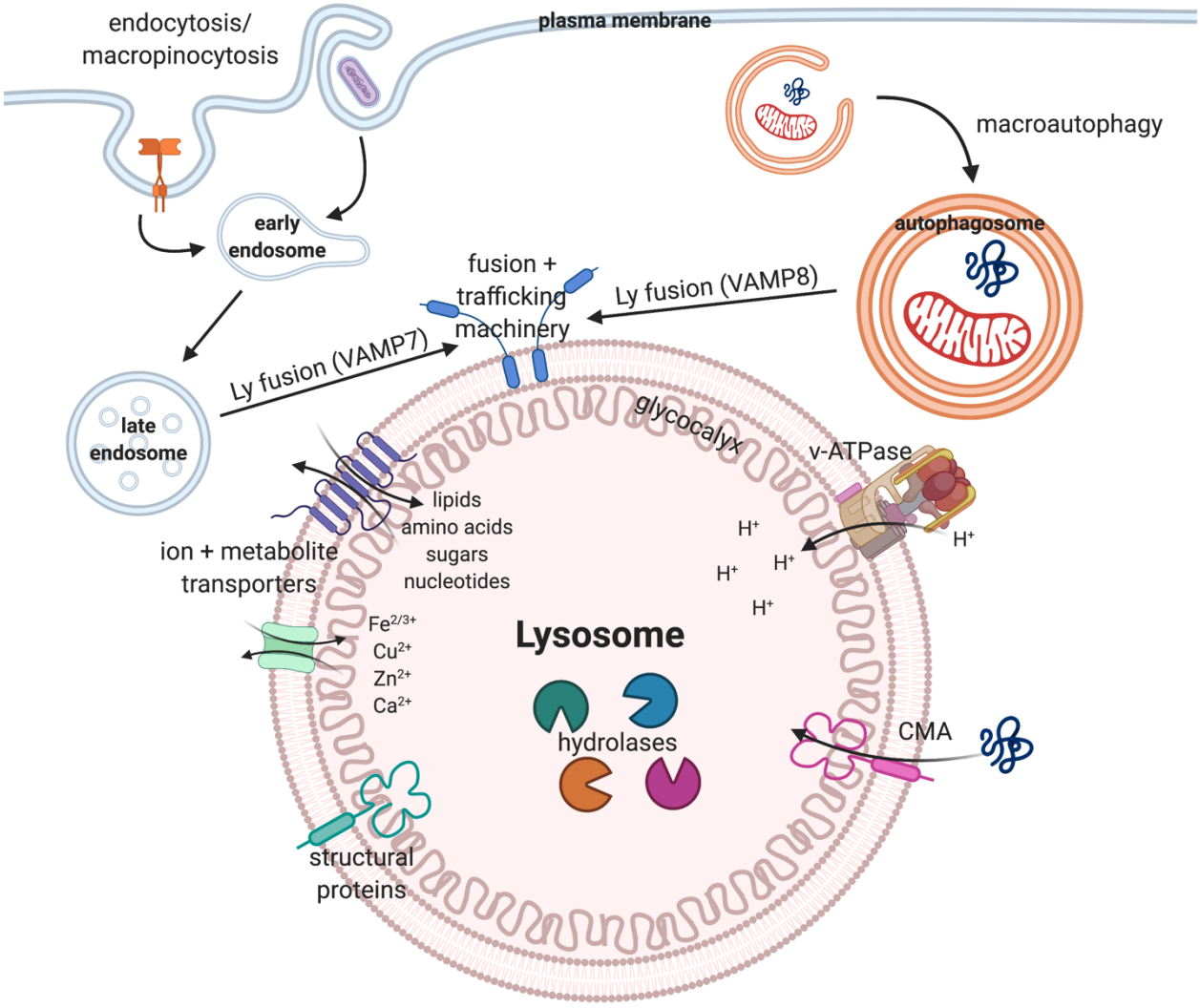

Figure 1.1 Structural organization of the lysosome and routes of macromolecular delivery
The limiting membrane of the lysosome segregates the resident hydrolases present in the lumen from the rest of the cell, and provides a barrier that allows the activity of the v-ATPase to establish and maintain the acidic environment of the lumen. The luminal side of the limiting membrane is lined with a protective glycan layer, the glycocalyx, formed by glycosylations on structural proteins and other proteins embedded in the limiting membrane. A wide array of transporter proteins span the limiting membrane and mediate the exchange of ions and cellular metabolites between the cytoplasm and the lysosomal lumen. Macromolecules, organelles, and extracellular material destined for degradation in the lysosome are captured via endocytosis or macroautophagy and dedicated machinery on the lysosomal membrane mediates the fusion of endosomes and autophagosomes with the lysosome. Cytosolic proteins can also be directly translocated across the lysosomal membrane for degradation via chaperone mediated autophagy (CMA).

Nutrient starvation is one of the most potent activators of autophagy, and consequently proper execution of autophagy is important for metabolic control via the mobilization of cellular stores of lipids, carbohydrates, and iron (Gatica et al., 2018; Mancias et al., 2014; Singh and Cuervo, 2011). Selective autophagy is also involved in the elimination of dysfunctional or unnecessary organelles. Emerging evidence has begun to characterize specific pathways for the autophagic elimination of mitochondria, peroxisomes, endoplasmic reticulum, ribosomes, and even damaged lysosomes (An et al., 2019; Anding and Baehrecke, 2017; Gatica et al., 2018; Maejima et al., 2013; Wyant et al., 2018; Yim and Mizushima, 2020). Some of these pathways involve resident receptors on the respective organelles (i.e. FAM134B and TEX264 for the ER)(An et al., 2019; Khaminets et al., 2015), whereas others seem to be dependent on organelle-associated E3 ligases that ubiquitinate several target proteins on the organelle surface (such as the E3 ligase Parkin in mitophagy), followed by recognition of the ubiquitinated proteins by ubiquitin-binding adaptors like OPTN and NDP52 (Gegg et al., 2010; Lazarou et al., 2015). In addition to organelles, toxic misfolded protein aggregates and pathogenic bacteria and viruses can also be ubiquitinated and cleared from the cell via autophagy (Gatica et al., 2018).

1.2 Lysosomes and mTORC1

A major shift in thinking about the role of the lysosome in the cell has occurred in the past 10 years, subsequent to the discovery that the lysosomal surface is a physical platform that recruits and regulates the activity of the mechanistic target of rapamycin complex 1 (mTORC1), both in metazoan and yeast cells (Binda et al., 2009; Sancak et al., 2010). The mTOR protein is a serine/threonine protein kinase that is a part of the PI3K-related protein kinase (PIKK) family, and was first discovered in the 1990s as pharmacological target of the bacterial macrolide rapamycin, first in yeast, then in mammals (Heitman et al., 1991; Sabatini et al., 1994). mTOR is evolutionarily conserved in eukaryotes, and is the central catalytic member of two distinct kinase complexes, mTORC1 and mTORC2, that are at the nexus of cellular signaling pathways regulating cellular and organismal physiology (Dos D. Sarbassov et al., 2004; Kim et al., 2002; Liu and Sabatini, 2020; Loewith et al., 2002). The activity of both complexes play central roles in promoting anabolism and growth; mTORC1 activates cellular growth and biomass accumulation (Ben-Sahra et al., 2016; Dowling et al., 2010; Düvel et al., 2010; Kim et al., 2002), whereas mTORC2 plays a variety of roles in cytoskeletal organization, insulin signal transduction and sphingolipid homeostasis (Riggi et al., 2019; Rispal et al., 2015; Roelants et al., 2011; Sarbassov et al., 2005) (reviewed in Liu and Sabatini, 2020; Shin and Zoncu, 2020). While the association of mTORC1, a pro-growth master cellular regulator, with the lysosome, the major catabolic center of the cell, might seem counterintuitive, further consideration of the evolutionarily conserved role of the lysosome (or vacuole) as a site of nutrient storage obviates a role for mTORC1 in sensing cellular nutrient availability at this site (Bar-Peled et al., 2013; Chantranupong et al., 2016; Jung et al., 2015; Panchaud et al.,

2013; Péli-Gulli et al., 2015; Rebsamen et al., 2015; Wang et al., 2015; Wolfson et al., 2016; Zoncu et al., 2011).

1.2.1 Regulation of cellular metabolism by mTORC1

mTORC1 controls the balance of cellular metabolism by simultaneously promoting anabolic processes and repressing catabolic processes when it is active (Figure 1.2) (Saxton and Sabatini, 2017; Valvezan and Manning, 2019). A major effect of mTORC1 activation is to upregulate protein synthesis in the cell. mTORC1 phosphorylates the eukaryotic translation initiation factor 4E (eIF4E)-binding proteins (4EBPs), disrupting the interaction of 4EBP and eIF4E, and allowing eIF4E to bind the 5' end 7-methyl-GTP cap on mRNAs to promote translation initiation (Brunn et al., 1997; Gingras et al., 1999; Hara et al., 1997). mTORC1 also promotes mRNA translation by phosphorylating p70 S6 kinase (S6K) (Kuo et al., 1992; Price et al., 1992), which itself phosphorylates multiple translation factors to promote mRNA unwinding, maturation and splicing, and ribosome biogenesis (Liu and Sabatini, 2020; Valvezan and Manning, 2019).

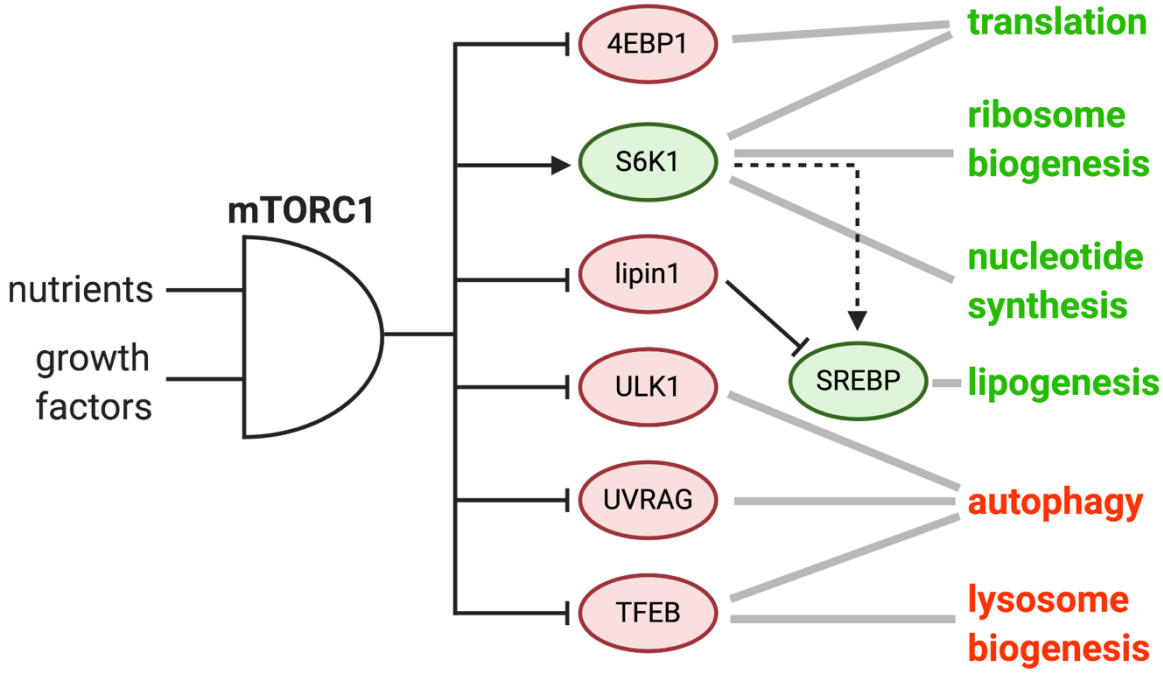

Figure 1.2 Logic of the mTORC1 signaling network and its regulation of cellular metabolism
mTORC1 functions as a molecular 'AND' gate such that the presence of sufficient cellular nutrient and systemic growth factor signals are required for full activation. Select substrates of mTORC1 are shown in ovals and are connected with gray lines to the cellular metabolic processes they regulate. Substrates and metabolic processes are colored green or red according to whether they are promoted or inhibited by mTORC1 activity, respectively.

mTORC1 activity also plays an important role in promoting the production of cellular building blocks required for macromolecular synthesis and cell growth. mTORC1 promotes the synthesis of nucleotides needed to support DNA and rRNA synthesis; it induces *de novo* pyrimidine synthesis via its activation of S6K (Ben-Sahra et al., 2013; Robitaille et al., 2013), and increases purine production by upregulating

the mitochondrial tetrahydrofolate cycle via ATF4-dependent transcription (Ben-Sahra et al., 2016). Synthesis of cellular lipids, the building blocks of new membranes, is also regulated by mTORC1 activity. Several studies have shown that mTORC1 promotes the processing and activation of the sterol responsive element binding protein (SREBP) family of transcription factors, which upregulate cholesterol and lipid synthesis when sterol levels in the ER are low, both in cells and in organisms (Düvel et al., 2010; Li et al., 2010; Peterson et al., 2011; Porstmann et al., 2008). mTORC1-dependent activation of SREBPs occurs both through a poorly defined S6K-dependent mechanism that promotes SREBP activation (Düvel et al., 2010), as well as via the direct phosphorylation of the phosphatidic acid phosphatase lipin1, preventing it from entering the nucleus and suppressing SREBP activity (Peterson et al., 2011). mTORC1 also can stimulate the global remodeling of cellular metabolism to promote glycolytic flux, allowing the cell to utilize glucose to produce biosynthetic intermediates. This occurs primarily through mTORC1's effects on the stability and transcription of the hypoxia inducible factor 1α (HIF1α) (Düvel et al., 2010; He et al., 2018).

In addition to inducing cellular anabolism, active mTORC1 simultaneously represses key catabolic processes of the cell. mTORC1 phosphorylates unc-51-like autophagy-activating kinase 1 (ULK1) and ATG13, two key effectors involved in the initial steps of autophagy, thereby inhibiting them and blocking autophagosome formation (Hosokawa et al., 2009; Kim et al., 2011). mTORC1 also inhibits the later stages of autophagy by phosphorylating UV radiation resistance-associated gene product (UVRAG), a key effector that promotes autophagosome-lysosome fusion (Kim et al., 2015). The basic helix-loop-helix (bHLH) transcription factor EB (TFEB) and its related family members are regulators of key lysosomal and autophagy genes that function to transcriptionally induce lysosome biogenesis and stimulate autophagy by binding to a consensus sequence known as the Coordinated Lysosomal Expression and Regulation (CLEAR) element (Palmieri et al., 2011; Sardiello et al., 2009; Settembre et al., 2011). Phosphorylation of TFEB by mTORC1 inhibits this process by blocking the nuclear import of TFEB (Martina et al., 2012; Roczniak-Ferguson et al., 2012; Settembre et al., 2012).

1.2.2 Cellular signaling upstream of mTORC1 activation

Harmonious with its role as a master regulator of cellular growth and metabolism, many layers of diverse signaling events occur upstream of mTORC1 and are integrated by dedicated factors to promote its activation on the surface of the lysosome (Figure 1.3). Because mTORC1 induces energy- and nutrient-intensive anabolic programs in cells, it is extensively regulated by the abundance of many metabolites, to ensure activity only when sufficient building blocks and energy are available to support cell growth (Liu and Sabatini, 2020; Saxton and Sabatini, 2017; Valvezan and Manning, 2019). Cellular growth also must be highly regulated in multicellular organisms, and thus mTORC1 activity is also highly dependent on the presence of systemic pro-growth signals such as growth factors, hormones, and cytokines (Liu and Sabatini, 2020; Valvezan and Manning, 2019). The circuitry of signaling events upstream of mTORC1 is organized such that it functions as a molecular coincidence detector, where the presence of nutrients, energy, and

exogenous growth signals are simultaneously required for full mTORC1 activation (Valvezan and Manning, 2019). Consequently, the depletion of any single component upstream of mTORC1 activation is sufficient to inhibit this process (Valvezan and Manning, 2019).

On a molecular level, the terminal steps in the activation of mTORC1 are accomplished by two sets of small G proteins, the Rag and Rheb guanosine triphosphatases (GTPases) (Liu and Sabatini, 2020; Valvezan and Manning, 2019). When in its active, GTP-bound form, the Ras-like GTPase Rheb is responsible for directly stimulating the kinase activity of mTORC1 (Inoki et al., 2003a; Tee et al., 2003). At the lysosomal membrane, GTP-Rheb directly binds the mTOR kinase, causing a global rearrangement of the kinase complex to align the catalytic site for optimal activity (Long et al., 2005; Yang et al., 2017). Rheb is potently and specifically regulated by the activity of the tuberous sclerosis complex (TSC), which acts as a GTPase-activating protein (GAP) to inactivate Rheb by accelerating its conversion to the GDP-bound form (Inoki et al., 2003a; Tee et al., 2003). The TSC2 subunit of the TSC complex is directly phosphorylated and inactivated by multiple growth factor-activated kinases, including Akt (Inoki et al., 2002; Manning et al., 2002) and Erk (Ma et al., 2005). Conversely, phosphorylation of TSC2 by glycogen synthase kinase 3 (GSK3, itself inhibited by Wnt signaling) or AMP kinase (activated by high intracellular AMP/ATP ratio), promotes TSC GAP activity (Inoki et al., 2003b, 2006). In this way, signaling downstream of growth factors serves to promote mTORC1 activity, while signals generated by low cellular ATP levels inhibit mTORC1. Mechanistically, the regulation of TSC GAP activity is thought to occur spatially – inhibition of TSC is thought to promote its dissociation from the lysosome, preventing it from acting on the lysosomal pool of GTP-Rheb (Menon et al., 2014).

The physical recruitment of mTORC1 to the lysosomal surface, where it may encounter GTP-Rheb for activation, is mediated by the activity of the heterodimeric Rag GTPases (Kim et al., 2008a; Sancak et al., 2008, 2010). Four Rags are encoded in the mammalian genome, and the Rags function as obligate heterodimers, with RagA or RagB (homologous to yeast Gtr1) bound to RagC or RagD (homologous to yeast Gtr2) (Liu and Sabatini, 2020; Nicastro et al., 2017). The nucleotide bound to the individual Rag monomers influences the affinity of the complex for mTORC1, such that the GTP-bound RagA/B and GDP-bound RagC/D conformation exhibits the strongest binding to mTORC1 (Kim et al., 2008a; Sancak et al., 2008). The Rags are bound to the lysosomal surface via their interaction with a pentameric complex, termed the “Ragulator”, that is lipidated and stably associated with the lysosome (Bar-Peled et al., 2012; Sancak et al., 2010). Recent work has revealed the dynamic nature of Rag-dependent mTORC1 recruitment; the Rags and mTORC1 constantly cycle on and off the lysosomal surface, with the rate of this cycling determined by the nucleotides bound to the Rags, providing a mechanism for cells to finely-tune mTORC1 activity (Lawrence et al., 2018). Recent structural work using cryo-electron microscopy has shed light on the overall architecture of the Ragulator-Rag-mTORC1 supercomplex. These studies validate the biochemical observation that RagA is the main mTORC1-anchoring subunit of the Rags, which directly binds to the mTORC1 component Raptor, whereas RagC appears to play an accessory role. Moreover, these structures provide insight into the

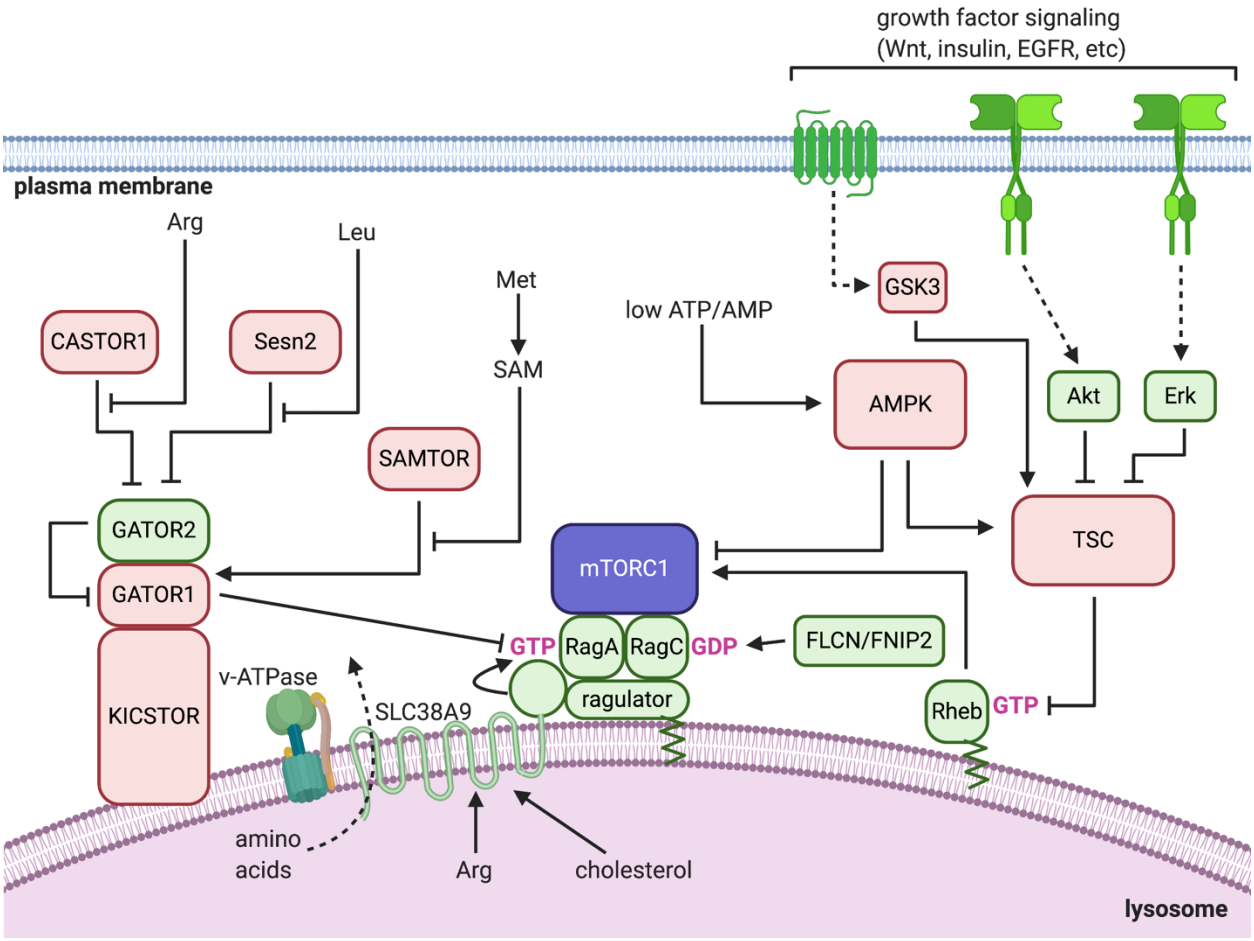

Figure 1.3 Molecular signaling pathways upstream of mTORC1
The major cellular pathways that sense nutrients, energy, and growth factors upstream of mTORC1 are depicted. Positive regulators of mTORC1 activity are shown in green, while negative regulators are shown in red.

orientation of the Ragulator-Rag scaffold with respect to the lysosomal membrane and how this may enable the simultaneous binding of Rheb to mTORC1 (Anandapadamanaban et al., 2019; Rogala et al., 2019).

The Rag-dependent lysosomal recruitment of mTORC1 is broadly regarded as the nutrient-regulated branch of the mTORC1 activation pathway (Liu and Sabatini, 2020; Saxton and Sabatini, 2017). Amino acids in particular have long been known to potently stimulate mTORC1 activity (Hara et al., 1998), and consequently the mechanisms by which they regulate the activity of the Rags are best understood. A dedicated pathway for sensing cytosolic amino acids and related metabolites converges upstream of the Rags at the GAP activity towards the Rags 1 (GATOR1) complex, which as its name suggests acts as a GAP for Rag A/B (Bar-Peled et al., 2013). GATOR1 is conserved in yeast, where it is known as the Seh1-associated (SEA) complex and has GAP activity toward Gtr1 (Dokudovskaya et al., 2011; Panchaud et al., 2013). GATOR1 is localized to the lysosomal surface through its association with another complex, KICSTOR, and has high GAP activity in the absence of amino acids, thus potently inhibiting lysosomal recruitment, and activation, of mTORC1 (Bar-Peled

et al., 2013; Wolfson et al., 2017). Elevated concentrations of the amino acids leucine and arginine in the cytosol are communicated to GATOR1 through separate proteins, Sestrin2 and CASTOR1, that function as sensors for these amino acids (Chantranupong et al., 2016; Wolfson et al., 2016). Binding of leucine and arginine to Sestrin2 and CASTOR1, respectively, relieves inhibitory interactions they have with the GATOR2 complex, which itself appears to functionally inhibit the GAP activity of GATOR1 (Bar-Peled et al., 2013; Chantranupong et al., 2016; Saxton et al., 2016b, 2016a; Wolfson et al., 2016). GATOR1 activity is also promoted by its interaction with a third cytosolic sensor, termed SAMTOR, which is required for mTORC1 to respond to changes in methionine levels. SAMTOR binds s-adenosylmethionine (SAM), a metabolite derived from methionine, causing it to dissociate from GATOR1, inhibiting its activity and promoting mTORC1 activation (Gu et al., 2017).

Additional mechanisms through which the nucleotide binding state and activity of the Rags have been characterized as well. A complex formed by the tumor suppressor gene folliculin (FLCN) and FNIP2, homologous to the yeast Lst4/Lst7 complex, functions as a GAP for RagC/D, and is required for full activation of mTORC1 in response to amino acids (Péli-Gulli et al., 2015; Petit et al., 2013; Tsun et al., 2013). How the activity of FLCN-FNIP2 is regulated and whether or not this is related to nutrient availability or other cellular environmental cues has yet to be determined.

The abundance of amino acids and other nutrients stored in the lysosome is also communicated to mTORC1 through the Rag GTPases. Evidence for this pathway was first demonstrated by studies showing that the activity of the v-ATPase is required for mTORC1 reactivation by amino acids after starvation (Zoncu et al., 2011). Key experiments using cell-free lysosomal preparations showed that when intact organelles were loaded with amino acids they were able to recruit recombinantly produced mTORC1, suggesting an essential role for sensing luminal contents in mTORC1 activation (Zoncu et al., 2011). Additional evidence for a role of the v-ATPase in mTORC1 regulation has come from a recent study reporting the identification of cysteine-reactive compounds that, by covalently modifying the v-ATPase, block its mTORC1-regulating function without affecting its proton-pumping activity (Chung et al., 2019). Subsequently, the amino acid transporter SLC38A9, present in lysosomal membranes, was demonstrated to function as a sensor for arginine stored in the lumen of the lysosome (Jung et al., 2015; Rebsamen et al., 2015; Wang et al., 2015). SLC38A9 binds arginine in the lumen, causing it to efflux neutral amino acids into the cytosol; this both provides cytosolic leucine that can activate mTORC1 through Sestrin2, as well as somehow directly promoting Rag activation, possibly via a non-canonical guanine nucleotide exchange factor (GEF) mechanism involving the cytosolic N-terminal domain of SLC38A9 (Shen and Sabatini, 2018; Wyant et al., 2017).

In addition to amino acids, mTORC1 is known to sense cellular levels of multiple other nutrients, although the mechanisms by which this is accomplished are largely uncharacterized. Cellular glucose levels are known to regulate mTORC1 activity, both via AMPK-dependent regulation of TSC and AMPK-independent regulation of the Rags (Efeyan et al., 2013; Kalender et al., 2010). Very recently, dihydroxyacetone phosphate has been proposed to be the glucose-derived metabolite that directly regulates mTORC1 (Orozco et al., 2020). Purine availability also appears to regulate mTORC1

activity, through a Rag-independent mechanism (Emmanuel et al., 2017; Hoxhaj et al., 2017). Recent work has also characterized the role of lipids, specifically cholesterol present in lysosomes, in promoting mTORC1 activation (Castellano et al., 2017). The mechanisms of lysosomal cholesterol transport and the ways in which it regulates mTORC1 will be discussed in greater detail in subsequent sections.

1.3 Lysosomes and Disease

1.3.1 Lysosomal Storage Disorders

Because the lysosome is a catabolic hub of the cell, as well as functioning as a platform for coordinating cellular nutrient sensing, lysosomal dysfunction is implicated in the pathogenesis of many human diseases. Particular insight into the connection between lysosome function and human disease has come from the study of rare lysosome storage diseases (LSDs) that are caused by mutations in genes required for proper lysosome function. Around 70 LSDs have been characterized, each caused by mutations affecting the proper function or trafficking of lysosomal hydrolases, transporters, or structural proteins (Platt, 2018; Platt et al., 2018). These result in the pathogenic accumulation of undigested substrates or metabolites in the lysosome, causing lysosome dysfunction that eventually leads to cellular dysfunction and death (Platt, 2018; Platt et al., 2018). While the exact pathophysiology of each LSD is unique, the observation that about 70% of identified LSDs result in progressive neurodegeneration highlights the importance of the lysosome for proper functioning of the central nervous system (Perera and Zoncu, 2016; Platt, 2018).

It is also well documented that patients with certain LSDs exhibit hallmarks of, or are at higher risks of developing other neurodegenerative disorders such as Parkinson's or Alzheimer's disease (Perera and Zoncu, 2016). A potent example of this is illustrated by the observation that mutations in GBA, the gene encoding glucocerebrosidase that underlies the LSD known as Gaucher's disease, are among the most common risk factors for the development of Parkinson's disease (Riboldi and Di Fonzo, 2019). Recent genome wide association studies (GWAS) have also indicated that individuals affected with Parkinson's disease have a higher burden of genetic variations associated with LSDs (Robak et al., 2017), and that genetic perturbations to autophagy and lysosomal genes are associated with higher risk of Alzheimer's disease (Gao et al., 2018). Whether or not lysosome dysfunction is a pathogenic driver, or enhanced by other cellular dysfunctions in the neurodegenerative diseases such as Parkinson's and Alzheimer's is an area of active investigation.

1.3.2 Lysosomal Function, Autophagy, and Neurodegeneration

Of particular note is the role that constitutive basal autophagy plays in the maintenance of neuronal cell homeostasis and survival. In addition to frequently manifesting with neurodegeneration, LSDs are also frequently observed to disrupt normal autophagy causing secondary accumulation of undigested protein aggregates (Elrick et al., 2012; Ordonez et al., 2012; Sarkar et al., 2013; Seranova et al., 2017; Settembre et al., 2008a, 2008b). Moreover, mice that lack the essential autophagy

genes for either Atg7 or Atg5 in neural cells develop severe neurodegeneration and die prematurely, even in the absence of any other disease-associated mutations, highlighting the requirement for functional autophagy in maintenance of the central nervous system (Hara et al., 2006; Komatsu et al., 2006). Ubiquitinated protein aggregates accumulate in the brains of mice defective in neural autophagy (Komatsu et al., 2006, 2007), supporting the notion that autophagy plays an important role in clearing toxic protein aggregates that underlie the pathology of diseases such as Alzheimer's and Parkinson's disease, Huntington disease, amyotrophic lateral sclerosis (ALS), and others (Dikic and Elazar, 2018; Menzies et al., 2017). Clearance of damaged mitochondria via mitophagy also is likely involved in preventing neurodegeneration, as damaged mitochondria are known to leak reactive oxygen species (ROS) that can damage other cellular components (Dikic and Elazar, 2018). This is underscored by the observation that inactivating mutations in the PTEN-induced kinase 1 (PINK1) and parkin E3 ligase – the cellular machinery involved in selective mitophagy of damaged mitochondria – cause Parkinson's disease (Kitada et al., 1998; Menzies et al., 2017; Valente et al., 2004).

1.4 Lysosomes and Cholesterol

1.4.1 The role and sources of cellular cholesterol

The diverse roles that lipids play in cells highlights the importance of maintaining proper homeostasis of this class of metabolites. In addition to their role as the major structural component of cellular membranes, lipids have important roles as signaling molecules, in modifying and regulating protein structure and function, and as important sources of cellular energy (Harayama and Riezman, 2018). Lipid composition and distribution within the cell varies according to cell type to support specific biological functions, and thus cells must utilize synthesis, uptake, degradation, storage, and transport of lipids to regulate homeostasis (Harayama and Riezman, 2018; Thelen and Zoncu, 2017). Cholesterol is a lipid of particular importance to the cell. It's rigid four-ring structure imparts it with unique biophysical properties that influence the packing and organization of nearby lipids in a membrane, such that as the concentration of cholesterol in a membrane increases, so does the rigidity of the membrane (Ikonen, 2008). Cholesterol can also modulate the activity of membrane proteins such as G-protein coupled receptors, and metabolic derivatives of cholesterol such as bile acids, steroid hormones, and oxysterols, have important metabolic and signal transduction roles in eukaryotes (Ikonen, 2008). Consequently, cholesterol is distributed asymmetrically in cellular membranes in coordination with their cellular functions, and cholesterol levels and distribution in the cell are tightly controlled (Ikonen, 2008; Meng et al., 2020; Thelen and Zoncu, 2017)

Mammalian cells have two routes by which they can obtain cholesterol; it can be synthesized *de novo* from acetyl-CoA via a multi-step pathway controlled by the master regulator, bHLH transcription factor Sterol Regulatory Element Binding Protein 2 (SREBP2), or exogenous cholesterol can be delivered to cells in the form of a low-density lipoprotein (LDL) particle (Goldstein and Brown, 2015). LDL binds to specific

receptors on the cell surface, that are subsequently endocytosed and trafficked to the lysosome (Goldstein and Brown, 2015). LDL particles primarily contain cholesterol in its esterified form, and once delivered to the lysosome, free cholesterol is liberated from the LDL particle by the action of a luminal protein, the lysosomal acid lipase (LipA/LAL) (Meng et al., 2020; Thelen and Zoncu, 2017). In addition to the cholesterol delivered to the lysosome via LDL, membranes that are captured via autophagy and endocytic sorting also end up in the lysosome where their lipid components (including cholesterol) must be recycled, sorted, and eventually exported to other cellular locations (Meng et al., 2020; Thelen and Zoncu, 2017).

1.4.2 NPC1 and NPC2-mediated cholesterol export from the lysosome

How cholesterol is exported from the lysosome has been the subject of extensive research over the past 25 years, and while much has been learned about this process, many mechanistic details of this process remain undefined. The primary route for cholesterol export from lysosomes is dependent on the activity of two proteins, NPC1 and 2 (Figure 1.4), so named because mutations in the genes encoding these proteins cause the lysosomal cholesterol storage disorder Neimann-Pick type C disease (Patterson and Walkley, 2017; Pfeffer, 2019). NPC2 is a small soluble protein present in the lysosome lumen, and it is thought to first bind free cholesterol present in the lumen, before transferring it to NPC1. NPC1 is a large, 13-pass transmembrane protein present on the limiting membrane of the lysosome, that transports cholesterol received from NPC2 past the glycocalyx for insertion into the limiting membrane and/or export from the lysosome (Meng et al., 2020; Pfeffer, 2019). Mutations causing loss of function in either gene results in a massive accumulation of cholesterol and glycosphingolipids in the lysosome, eventually resulting in premature death (Peake and Vance, 2010; Pfeffer, 2019).

The exact mechanism by which cholesterol is transported out of the lysosome via NPC1 and NPC2 is not fully understood, but structural and biochemical work performed in the past 15 years has elucidated many of the major steps of this process. Cholesterol is first bound by NPC2 in a hydrophobic pocket that shields the majority of the molecule from aqueous surroundings, save for the 3β-hydroxyl group which remains solvent exposed (Friedland et al., 2003; Wang et al., 2010; Xu et al., 2007). NPC1 has a soluble luminal N-terminal domain (NTD) that also binds cholesterol, albeit in the opposite orientation to NPC2, suggesting a mechanism of transfer where NPC2 and the NPC1-NTD “kiss” to facilitate the passive transfer of cholesterol from one pocket to the other (Infante et al., 2008a; Kwon et al., 2009; Wang et al., 2010). This model is further supported by the observation that cholesterol transfer between NPC2 and the NPC1-NTD is bidirectional, as well as structural studies demonstrating that NPC2 binds to another middle luminal domain (MLD) on NPC1 (Infante et al., 2008b), and that this is required for aligning the pockets of NPC2 and NPC1-NTD to promote efficient cholesterol transfer (Deffieu and Pfeffer, 2011; Li et al., 2016).

Multiple studies involving the use of various cholesterol analogs have suggested the presence of additional cholesterol binding sites in the NPC1 protein beyond the pocket in the NTD. The presence of a cholesterol binding site in the sterol-sensing domain (SSD), a transmembrane domain that is homologous to sterol-binding domains

of other proteins involved in cholesterol metabolism, of NPC1 was long thought to be important for cholesterol transport (Thelen and Zoncu, 2017). This was supported by multiple studies showing cholesterol binding to NPC1 that is independent of the NTD, and that mutations in the SSD can block cholesterol binding to NPC1 (Lu et al., 2015; Ohgami et al., 2004; Ohgane et al., 2013; Trinh et al., 2017). Very recent structures of both the yeast and human NPC1 proteins have brought many details of the route of cholesterol transport through the protein to light. All of these structures show the existence of a hydrophobic tunnel extending from the NTD, through the MLD and C-terminal luminal domain (CTD), to the SSD that can accommodate the transfer of a cholesterol molecule (Long et al., 2020; Qian et al., 2020; Winkler et al., 2019). Furthermore, protonatable residues in these structures suggest a H^+-driven mechanism that could possibly drive the transport of cholesterol through the tunnel (Qian et al., 2020; Winkler et al., 2019). Whether or not cholesterol is inserted into the limiting membrane of the lysosome once it reaches the SSD, or if NPC1 actively promotes its export from the lysosome, remains unresolved. The latter possibility is supported by intriguing evidence from a proteomic screen for cholesterol-interacting proteins, that showed a cross-linkable cholesterol derivative bound to peptides of NPC1 located on cytoplasm-facing portions of the protein (Hulce et al., 2013).

1.4.3 Other routes of lysosomal cholesterol transport

A number of other membrane proteins have been reported to play a role in cholesterol export from the lysosome (Figure 1.4). The lysosomal-associated membrane proteins (LAMP) 1 and 2 are abundant, highly glycosylated single-pass transmembrane proteins that are major components of the glycocalyx, were recently shown to bind cholesterol, as well as NPC2 and the NTD of NPC1, in their luminal domains (Li and Pfeffer, 2016). LAMPs have been previously suggested to be required for cholesterol export from the lysosome (Eskelinen et al., 2004; Schneede et al., 2011), and their ability to bind cholesterol is required for them to support cholesterol export from the lysosome (Li and Pfeffer, 2016). Another lysosomal transmembrane protein, lysosomal integral membrane protein 2 (LIMP2), was recently shown to promote cholesterol export from the lysosome as well via a hydrophobic transmembrane channel in its structure (Heybrock et al., 2019). This pathway was suggested to operate in parallel to NPC1/2-mediated cholesterol export, albeit on a much slower timescale (Heybrock et al., 2019).

Beyond the lysosome, cholesterol transport in the cell is also regulated by a distinct class of lipid transfer proteins with soluble cholesterol-binding domains that enable them to shield cholesterol from aqueous environments to transport it through the cytosol (Ikonen, 2008; Meng et al., 2020; Thelen and Zoncu, 2017). Several families of sterol-binding lipid transfer proteins exist, and they are specifically localized at distinct locations within the cell where different organelles come into close physical proximity (5 nm) to support the asymmetric distribution of cholesterol across different cellular membranes (Meng et al., 2020). While vesicular transport likely plays some role in cholesterol export from the lysosome, several lipid transfer proteins have been suggested to play important roles the direct transfer of cholesterol from the limiting membrane as well. ORP5, a member of the oxysterol-binding protein (OSBP) and

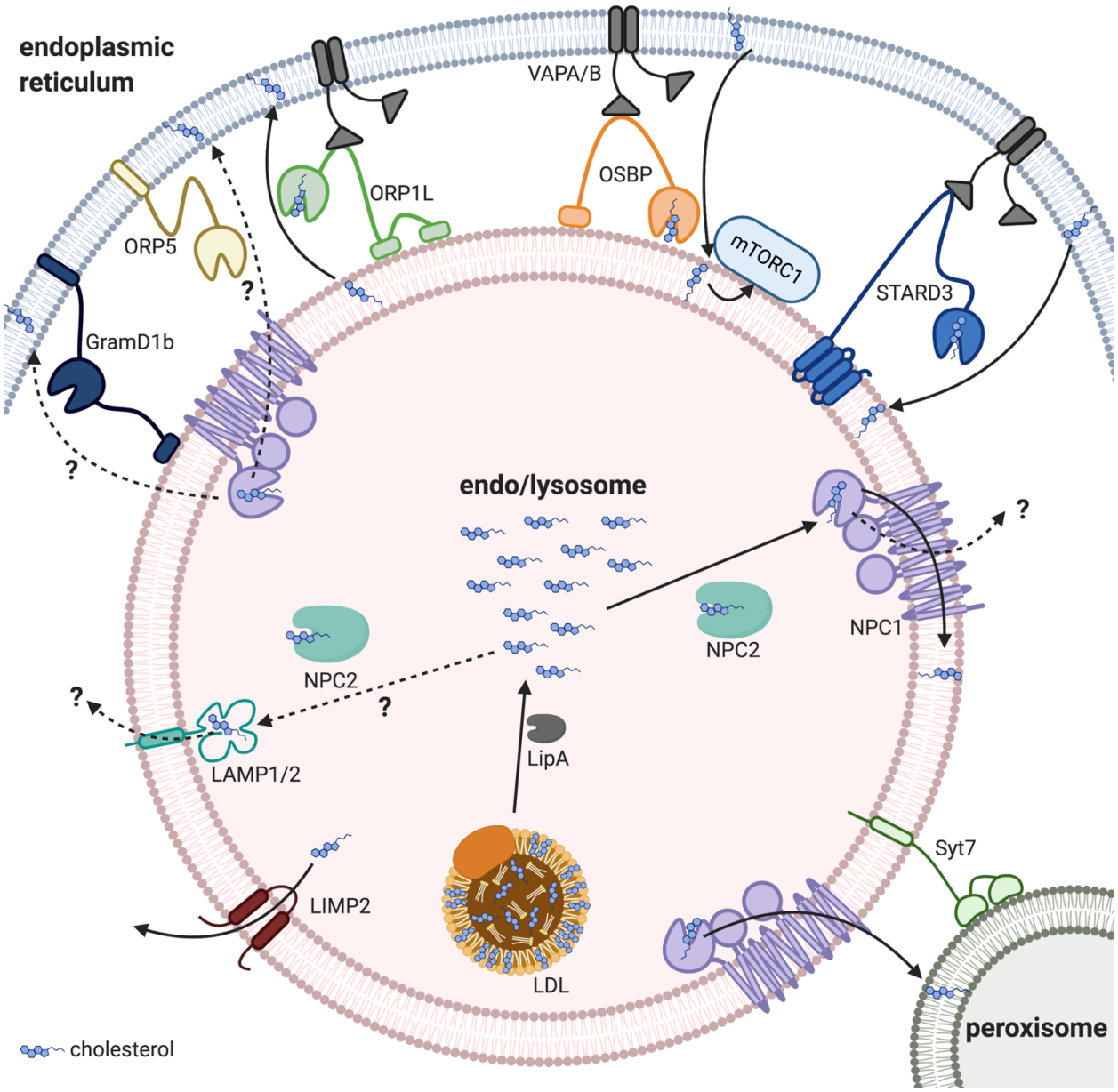

Figure 1.4 Cholesterol transport pathways of the endolysosomal system
Exogenous cholesterol is delivered to the lysosome via an endocytosed LDL particle, in which cholesterol is primarily found in its esterified form. The activity of LipA de-esterifies the LDL-derived cholesterol, and this free pool of cholesterol is then bound by NPC2 and transferred to NPC1 for export from the lysosome. Several other non-vesicular routes of cholesterol export from the lysosome exist, including via other proteins embedded in the lysosomal membrane (LAMP1/2 and LIMP2), as well as via other proteins that can tether lysosomal membranes to other target membranes to either directly (ORP1L, ORP5, GramD1b) or indirectly (Syt7) mediate cholesterol transfer between the opposing membranes. Cholesterol can also be transferred to the lysosomal membrane from other organelles via a similar mechanism (OSBP, STARD3).

OSBP-related protein (ORP) family of lipid transfer proteins, has been proposed to interact with NPC1 to promote cholesterol export from the lysosome (Du et al., 2011), although subsequent studies have failed to replicate these results (Höglinger et al.,

2019). Another ORP family member, ORP1L, has been implicated in transfer of cholesterol from the lysosomal membrane to the ER in mammalian cells as well. Cells lacking ORP1L show a reduction in the rate of LDL-derived cholesterol esterification in the ER, suggesting an impairment of cholesterol export from the lysosome (Zhao and Ridgway, 2017). Direct transfer of LDL-derived cholesterol from lysosomes to peroxisomes has also been proposed, based on evidence that disruption of lysosome-peroxisome contacts by depletion of synaptotagmin VII disrupts cholesterol transfer in an NPC1-dependent manner (Chu et al., 2015). More recently, a correlative study has suggested that NPC1 coordinates with the ER sterol transfer protein of the LAM family, GramD1b, to form ER-lysosome contacts that themselves are required for efficient sterol export from the lysosome (Höglinger et al., 2019). Whether or not one of these proposed routes for cholesterol export predominates over another, how they might be functionally distinct, or if other routes for cholesterol export from the lysosome exist, are important questions that remain to be resolved.

Several mechanisms of cholesterol transfer to endolysosomal membranes from other cellular membranes have also been identified. The cholesterol transfer protein STARD3, a member of the steroidogenic acute regulatory protein (StAR)-related lipid transfer (START) domain family of proteins, has been shown to complex with the ER-localized anchor proteins VAPA and VAPB to form ER-lysosome contacts that serve to promote cholesterol transfer from the ER to the lysosome (Wilhelm et al., 2017). Interestingly, STARD3-mediated cholesterol transfer was not observed to impact cellular cholesterol homeostasis, suggesting it might function on a smaller scale to allow individual organelles to finely adjust their cholesterol levels (Wilhelm et al., 2017). OSBP itself has also been shown to transfer cholesterol from the ER to endosomes in exchange for phosphatidylinositol 4-phosphate (PI4P) via contact sites also established by interactions with the VAPs on the ER (Dong et al., 2016). While OSBP-mediated ER-endosome contacts were first shown to be important for regulating endosomal budding and cargo sorting (Dong et al., 2016), subsequent work (discussed below) has identified OSBP-mediated ER-lysosome contacts as a site for the regulation of mTORC1 activity.

1.4.4 Cholesterol sensing by mTORC1

Cholesterol synthesis is a bioenergetically costly process (Goldstein and Brown, 2015), so it makes sense that cells must properly sense levels of the recycled and LDL-derived cholesterol in the lysosome. Given the myriad of ways that cholesterol is important for integral cellular processes, it is perhaps unsurprising that mTORC1, a critical regulator of cellular homeostasis, is itself regulated by lysosomal cholesterol (Meng et al., 2020; Thelen and Zoncu, 2017). When cells are starved for cholesterol by using cyclodextrins to strip sterols from their membranes, mTORC1 dissociates from the lysosome and its kinase activity is reduced; subsequent refeeding with LDL or exogenous free cholesterol restores mTORC1 activity and its lysosomal localization (Castellano et al., 2017). Similar to amino acids, this process occurs through the Rag-dependent arm of the activation pathway upstream of mTORC1. Cholesterol present in the lysosomal membrane binds to a conserved transmembrane motif in SLC38A9 known to confer cholesterol regulation in other membrane proteins (Derler et al., 2016),

and this appears to be required for it to promote the activation of the Rags (Castellano et al., 2017). Interestingly, this process appears to be negatively regulated by NPC1, as cells lacking NPC1 are unable to turn off mTORC1 signaling in response to cholesterol depletion with the same dynamics as cells with intact NPC1 function (Castellano et al., 2017).

Subsequent work identified ER-lysosome membrane contacts as sites for cholesterol transfer that is required for mTORC1 activation. Blocking cholesterol transfer from the ER to the lysosome, by inhibition of the cholesterol transfer protein OSBP or its ER anchors VAPA and B, results in the inhibition of mTORC1 activity (Lim et al., 2019). Inhibition of OSBP-mediated cholesterol transfer was also able to attenuate aberrant mTORC1 signaling in NPC1-deficient cells, suggesting that the balance of OSBP-mediated cholesterol import with NPC1-dependent export from the lysosome is required for proper mTORC1 regulation (Lim et al., 2019). Of note, this pathway appears to be specific to OSBP, as knockdown of other ORPs and sterol transfer proteins known to transfer cholesterol to and from the lysosome appeared to have no effect on the regulation of mTORC1 activity in response to cholesterol (Lim et al., 2019).

While some light has been shed on the mechanisms by which lysosomal cholesterol is able to regulate the activity of mTORC1, several important questions remain unaddressed. Previous investigations have demonstrated that NPC1 clearly exerts a negative regulatory effect on mTORC1 signaling with respect to cholesterol sensing, but the mechanism by which this occurs, and whether or not NPC1 directly participates in regulating mTORC1 or only does so indirectly via its cholesterol transport activity remains underexplored. Furthermore, the roles that NPC1 and lysosomal cholesterol transport play in maintaining organelle and cellular homeostasis, and how this contributes to pathogenesis in NPC disease has not been comprehensively studied on a subcellular level. And lastly, whether or not mTORC1 dysregulation caused by the loss of NPC1 contributes to disease pathogenesis is unknown. In the next chapter I will describe efforts to better characterize the organellar dysfunctions caused the loss of NPC1, the mechanism by which NPC1 function regulates mTORC1 activity, and the discovery that mTORC1 dysregulation caused by loss of NPC1 function potentiates NPC disease pathogenesis.

Chapter 2

NPC1-mTORC1 Signaling Couples Cholesterol Sensing to Organelle Homeostasis and is a Targetable Pathway in Niemann-Pick Type C

A portion of the content presented in this chapter has been previously published as part of the following research article: Davis, O. B., Shin, H. R., Lim, C. Y., Wu, E. Y., Kukurugya, M., Maher, C. F., Perera, R. M., Ordoñez, M. P., Zoncu, R. NPC1-mTORC1 signaling couples cholesterol sensing to organelle homeostasis and is a targetable pathway in Neimann-Pick type C. bioRxiv 2020.08.02.233254. Preprint. (2020)

Oliver Davis, Paulina Ordoñez, and Roberto Zoncu conceived of and designed the study. Oliver Davis, Regina Shin, Chun-Yan Lim, Emma Wu, Matthew Kukurugya, Claire Maher, and Paulina Ordoñez generated key reagents and performed all experiments. Oliver Davis, Regina Shin, Chun-Yan Lim, Rushika Perera, Paulina Ordoñez, and Roberto Zoncu analyzed data and interpreted results. Oliver Davis, Paulina Ordoñez, and Roberto Zoncu wrote the manuscript. All authors read and edited the manuscript.

2.1 Chapter Summary

Lysosomes promote cellular homeostasis through macromolecular hydrolysis within their lumen and metabolic signaling by the mTORC1 kinase on their limiting membranes. Both hydrolytic and signaling functions require precise regulation of lysosomal cholesterol content. In Niemann-Pick type C (NPC), loss of the cholesterol exporter, NPC1, causes cholesterol accumulation within lysosomes, leading to mTORC1 hyperactivation, disrupted mitochondrial function and neurodegeneration. The compositional and functional alterations in NPC lysosomes, and how aberrant cholesterol-mTORC1 signaling contributes to organelle pathogenesis are not understood. Through proteomic profiling of NPC lysosomes, we find pronounced proteolytic impairment compounded with hydrolase depletion and enhanced membrane damage. Genetic and pharmacologic mTORC1 inhibition restores lysosomal proteolysis without correcting cholesterol storage, implicating aberrant mTORC1 as a pathogenic driver downstream of cholesterol accumulation. Consistently, mTORC1 inhibition reverses mitochondrial dysfunction in a neuronal model of NPC. Thus, cholesterol-mTORC1 signaling controls organelle homeostasis and is a targetable pathway in NPC.

2.2 Introduction

Lysosomes are degradative organelles that play key roles in macromolecular turnover and in recycling of cellular building blocks including amino acids, lipids and nucleotides. Through their participation in autophagy, lysosomes also help detoxify potentially harmful cellular components, such as damaged mitochondria. In addition to their recycling and degradative roles, lysosomes have been recently recognized as signaling compartments that support the activation and regulation of the master growth regulator, mechanistic Target of Rapamycin Complex 1 (mTORC1) (Liu and Sabatini, 2020; Perera and Zoncu, 2016)

The degradative and signaling roles of lysosomes are highly integrated. Intracellular nutrients drive mTORC1 translocation from the cytosol to the lysosomal limiting membrane, where growth factor signals relayed by the phosphatidylinositol 3-kinase (PI3K)-AKT pathway trigger the kinase function of mTORC1 (Castellano et al., 2017; Menon et al., 2014; Sancak et al., 2010; Wyant et al., 2017; Zoncu et al., 2011). Moreover, upon becoming activated at the lysosome by converging nutrient- and growth factor-mediated inputs, mTORC1 strongly suppresses initiation of autophagy, steering the cell toward net mass accumulation (Düvel et al., 2010; Kim et al., 2011; Puente et al., 2016; Settembre et al., 2012). The tight integration of the recycling and signaling functions of the lysosome suggests that, in diseases driven by lysosomal dysfunction, aberrant regulation of both processes may synergize to disrupt cellular homeostasis (Perera and Zoncu, 2016). However, the respective roles of aberrant lysosomal recycling and signaling, and their interplay in driving disease pathogenesis, remain largely unexplored.

Niemann-Pick type C (NPC) is one of a family of approximately 60 diseases known as lysosomal storage disorders (LSDs), in which genetic inactivation of lysosomal hydrolases or transporters triggers massive and pathogenic accumulation of their respective substrates within the lysosome (Ballabio and Gieselmann, 2009; Platt et al., 2018). NPC is triggered by inactivating mutations in NPC1, a polytopic transmembrane cholesterol transporter located on the lysosomal limiting membrane (Gong et al., 2016; Kwon et al., 2009; Li et al., 2016; Winkler et al., 2019). In conjunction with NPC2, a cholesterol-binding protein of the lysosomal lumen, NPC1 exports cholesterol released from Low-Density Lipoprotein (LDL) to acceptor compartments such as the endoplasmic reticulum (ER), the Golgi and the plasma membrane (Feltes et al., 2020; Infante and Radhakrishnan, 2017; Infante et al., 2008b; Pfeffer, 2019).

A large number of heritable mutations in the NPC1 gene lead to an unstable NPC1 protein, which fails to fold and is degraded in the ER (Schultz et al., 2018). In cells lacking NPC1, cholesterol accumulates massively within the lysosomal lumen, as well as on its limiting membrane. Cholesterol storage results in enlarged lysosomes that exhibit morphological, trafficking and functional defects. Moreover, the primary lysosomal phenotype is accompanied by dysfunction in other cellular compartments, including autophagosomes (Elrick et al., 2012; Ordonez et al., 2012; Sarkar et al., 2013), mitochondria (Kennedy et al., 2014; Ordonez, 2012; Yambire et al., 2019a; Yu et al., 2005) and peroxisomes (Schedin et al., 1997).

Mechanistically, how cholesterol accumulation caused by loss of NPC1 leads to lysosomal dysfunction remains poorly understood. There is evidence of defective degradation of autophagosomal cargo (Elrick et al., 2012; Ordonez et al., 2012), as well as defective trafficking of autophagic vesicles to lysosomes (Sarkar et al., 2013). However, the mechanistic basis for impaired lysosomal catabolism remains to be fully elucidated. Moreover, the molecular processes that connect the primary lysosomal dysfunction to the impairment of other organelle populations remain largely mysterious. It was recently reported that a faulty transcriptional circuit triggered by lipid storage compromises mitochondrial biogenesis in NPC (Yambire et al., 2019a). However, it is likely that additional lysosome-based processes may be involved in the loss of mitochondrial homeostasis.

Limiting our understanding of the pathogenic processes that drive NPC is the lack of a comprehensive view of the structural and functional alterations that occur in each membrane compartment in NPC cells. The recent development of techniques for rapid immunoisolation and systematic mass spectrometry-based profiling of intact organelles presents with an opportunity to address this critical point (Abu-Remaileh et al., 2017; Castellano et al., 2017; Sleat et al., 2013; Wyant et al., 2017, 2018; Zoncu et al., 2011).

An especially important question in understanding NPC pathogenesis is whether disruption of a common signaling pathway may underlie the multi-organellar loss of function of NPC1-defective cells. Cholesterol was recently identified as a nutrient input that regulates mTORC1 and promotes activation of its downstream biosynthetic programs as well as suppression of autophagy. Cholesterol stimulates mTORC1 activity via a protein complex also involved in amino acid-dependent mTORC1

activation and composed of the heterodimeric Rag guanosine triphosphatases (GTPases), their membrane-anchored interactor Ragulator complex, and the lysosomal amino acid permease SLC38A9 (Castellano et al., 2017; Sancak et al., 2010; Wang et al., 2015; Wyant et al., 2017). This complex responds to both extracellular cholesterol, carried by low-density lipoprotein (LDL) and to intracellular cholesterol transferred across ER-lysosome contacts by a tag team of oxysterol binding protein (OSBP) and its ER anchors, VAPA and B (Castellano et al., 2017; Dong et al., 2016; Lim et al., 2019; Mesmin et al., 2013).

In contrast to these positive activators, NPC1 appears to antagonize cholesterol-dependent mTORC1 signaling. In NPC1-deleted cells, mTORC1 signaling is elevated compared to wild-type cells and is immune to inhibition by cholesterol-depleting agents. mTORC1 dysregulation can be readily explained by the massive accumulation of lysosomal cholesterol resulting from loss of NPC1-dependent export. However, NPC1 could also play a cholesterol effector role, where it could directly regulate the mTORC1-scaffolding complex via physical interaction (Castellano et al., 2017).

mTORC1 signaling has profound effects on organelle composition and function. mTORC1 negatively regulates the basic helix-loop-helix MiT-TFE transcription factors, which are master regulators of lysosomal biogenesis and autophagy (Martina et al., 2012; Roczniak-Ferguson et al., 2012; Sardiello et al., 2009; Settembre et al., 2012). mTORC1 drives mitochondrial biogenesis and function via both transcriptional and translational mechanisms (Bentzinger et al., 2008; Cunningham et al., 2007; Morita et al., 2013), and stimulates mitochondrial metabolic programs that support cell growth and proliferation (Ben-Sahra et al., 2016; Csibi et al., 2013). Thus, dysregulation of mTORC1 signaling due to loss of NPC1 could affect organelle homeostasis via multiple mechanisms.

To shed light into the relationship between dysregulated mTORC1 signaling and organelle homeostasis in NPC, we carried out mass spectrometry-based profiling of immunopurified lysosomes combined with functional assays for mTORC1 signaling and lysosome function in both engineered cell lines and in iPSC-derived neuronal cultures lacking NPC1. We uncover a more profound disruption of lysosomal composition and function, mitochondrial homeostasis and cholesterol-mTORC1 signaling associated with NPC than previously anticipated. Importantly, pharmacological suppression of mTORC1 signaling was able to correct several aspects of organelle function independent of the primary cholesterol storage defect, thus implicating dysregulated mTORC1 signaling as a likely pathogenic driver in Niemann-Pick type C.

2.3 Results

2.3.1 NPC1-null lysosomes display extensive proteolytic defects

To investigate the molecular basis for lysosomal dysfunction in NPC, we conducted lysosome immunoprecipitation (lyso-IP) followed by label-free proteomics-based profiling from HEK-293T cells that either have intact NPC1 function or in which the NPC1 gene was targeted using CRISPR/Cas9 resulting in near-complete loss of

NPC1 protein levels and function (Abu-Remaileh et al., 2017; Castellano et al., 2017; Lim et al., 2019; Wyant et al., 2018; Zoncu et al., 2011). To identify cargo proteins being actively degraded, we incorporated additional control samples treated with the broad-spectrum hydrolase inhibitors, leupeptin and pepstatin (Figure 2.1A-2.1B). In

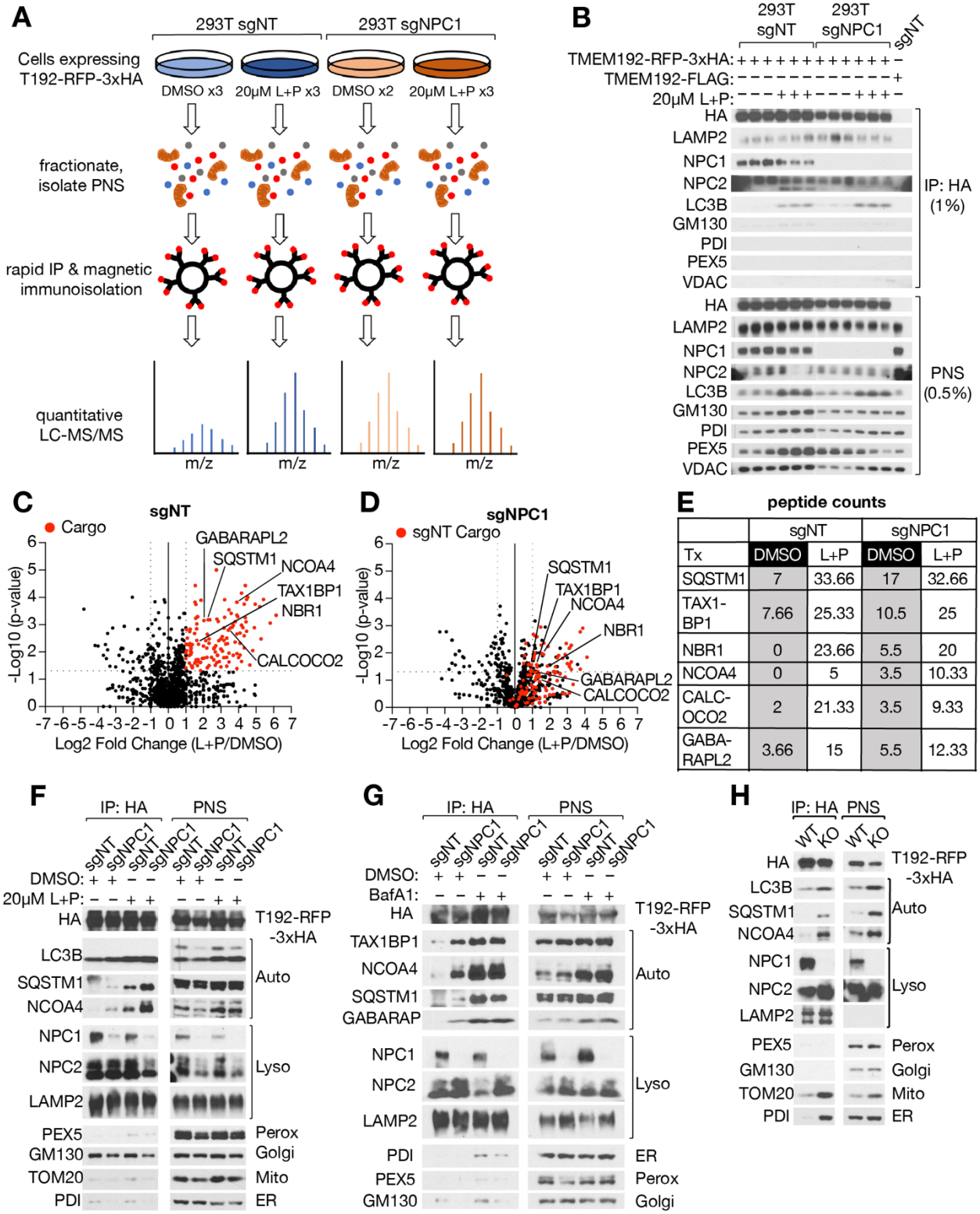

	sgNT		sgNPC1	
Tx	DMSO	L+P	DMSO	L+P
SQSTM1	7	33.66	17	32.66
TAX1-BP1	7.66	25.33	10.5	25
NBR1	0	23.66	5.5	20
NCOA4	0	5	3.5	10.33
CALC-OCO2	2	21.33	3.5	9.33
GABA-RAPL2	3.66	15	5.5	12.33

Figure 2.1 Lysosome proteomics reveals a proteolytic defect in NPC1-deficient lysosomes (on previous page)
(A) Schematic depicting protocol for proteomic analysis of lysosomal isolates generated with Lyso-IP. sgNT or sgNPC1 293Ts (expressing TMEM192-RFP-3xHA) were treated with leupeptin and pepstatin (L+P, 20μM each) or vehicle (DMSO) for 24h. Cells were mechanically fractionated and post-nuclear supernatant (PNS), containing lysosomes, was isolated by centrifugation. Intact lysosomes were purified by rapid immunoisolation, and lysosomal isolates were subjected to label-free quantitative proteomics.
(B) Immunoblots of Lyso-IP samples used for label-free quantitative proteomics. Cells expressing TMEM192-FLAG were used as a negative control (only one replicate is shown).
(C-E) Proteomic analysis of Lyso-IP samples from sgNT (NT = "non-targeting" control) and sgNPC1 293Ts. Volcano plots (-log10 p-value vs. log2 of the ratio of leupeptin+pepstatin/DMSO) for sgNT (C) and sgNPC1 (D) 293Ts. Proteins with statistically significant (p-value ≥ 0.5, two-tailed unpaired t-test) fold change L+P/DMSO > 2 ("sgNT cargo") in (A) are displayed as red circles. The sgNT cargo proteins identified in (C) are also displayed as red circles in (D). (E) Average peptide counts (raw) for selected autophagy-related proteins.
(F) Immunoblots of Lyso-IP samples and corresponding post-nuclear supernatant (PNS) from sgNT or sgNPC1 293Ts (expressing TMEM192-RFP-3xHA) treated with 20μM leupeptin and pepstatin for 24h.
(G) Immunoblots of Lyso-IP samples from sgNT or sgNPC1 293Ts (expressing TMEM192-RFP-3xHA) treated with 500nM Bafilomycin A1 (BafA1) for 4h.
(H) Immunoblots of Lyso-IP samples from sgNT or NPC1-/- (KO) MEFs (expressing TMEM192-RFP-3xHA).

lysosomes purified from control ('sgNT') cells, the abundance of resident lysosomal proteins (hydrolases, permeases, signaling components) remained unchanged. In contrast, lysosomal cargos, were enriched 2-fold or more in the leupeptin:pepstatin-treated samples (Figure 2.1C). These included autophagic adaptors, likely delivered to the lysosome via fusion with autophagosomes (Khaminets et al., 2016). Unlike lysosomes isolated from control cells, NPC1-defective lysosomes showed reduced enrichment of numerous bona fide lysosomal cargos in the leupeptin:pepstatin condition (Figure 2.1D), as most lysosomal cargo were already accumulated within NPC1-null lysosomes in the vehicle treated condition (Fig 2.1E).

To validate the proteomic data, we conducted direct immunoblotting of lysosomal immunoprecipitates from both control and NPC1-deleted HEK293T cells. We found that the steady-state levels of several autophagic adaptor proteins, including LC3, p62/SQSTM1, TAXBP1 and NCOA4 were significantly elevated in NPC1-null lysosomes compared to control lysosomes (Figure 2.1F-2.1G). Blocking lysosomal proteolysis with leupeptin:pepstatin or with the vacuolar H+ATPase (v-ATPase) inhibitor, bafilomycin A1 (BafA1) caused further buildup of autophagic substrates in both genetic backgrounds, however this buildup was significantly reduced in NPC1-null lysosomes (Figure 2.1F-2.1G). Immunoblotting of lysosomal immunoprecipitates from NPC1-knock out mouse embryonic fibroblasts (MEFs) also confirmed increased amounts of undigested autophagic substrates (Figure 2.1H).

We further confirmed accumulation of undigested autophagic material upon loss of NPC1 via immunofluorescence staining for endogenous LC3B and LAMP2, which showed strong LC3B signal within the lumen of LAMP2-positive vesicles in NPC1-depleted but not control cells (Figure 2.2A-2.2D). Consistent with defective proteolysis, BafA1 treatment caused a 5-fold increase of LC3B signal in control lysosomes, but no significant change in NPC1-defective lysosomes (Figure 2.2A-2.2B).

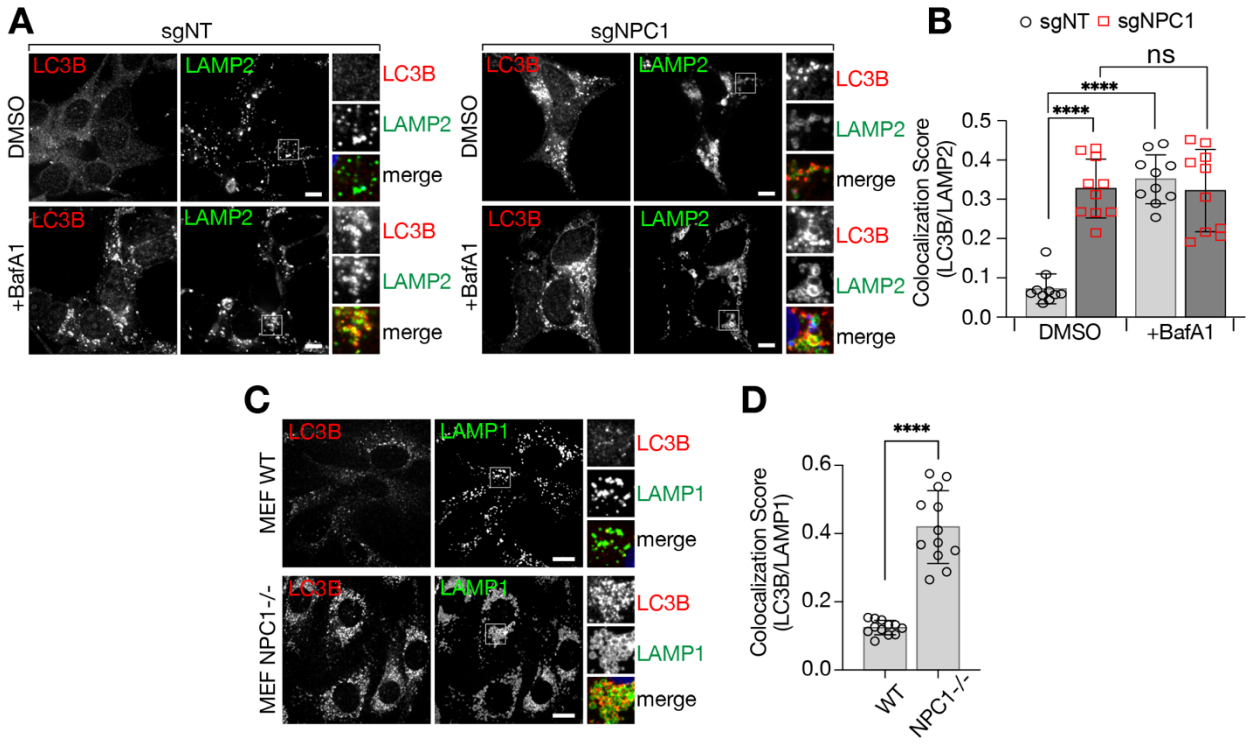

Figure 2.2 Immunofluorescence reveals undigested autophagic material in lumen of NPC1-deficient lysosomes

(A and B) sgNT and sgNPC1 293Ts were treated with 500nM bafilomycin A1for 4h before being fixed and stained with antibodies targeting LC3B and LAMP2. (A) Representative confocal micrographs for each sample. (B) Quantification of the co-localization between LC3B and LAMP2; ****P < 0.0001, ns = not significant, ANOVA with Tukey's multiple comparisons test. Scale bars are 10μm.

(C and D) WT and NPC1-/- MEFs were fixed and stained with antibodies directed against LC3B and LAMP1. (C) Representative confocal micrographs for each sample. Scale bars are 20μm. (D) Quantification of co-localization between LC3B and LAMP1; ****P < 0.0001, two-tailed unpaired t-test with Welch's correction.

The proteolytic defects characteristic of NPC1-null lysosomes are a direct consequence of ablated cholesterol-exporting activity. Reconstituting NPC1-defective cells with either wild-type NPC1 or with a mutant (D786N) that is predicted to have enhanced transport activity based on homology to the ER-resident cholesterol sensor SCAP (Gao et al., 2017; Millard et al., 2005; Yabe et al., 2002) fully rescued the LC3B accumulation defect (Figure 2.3A-2.3B). In contrast expression of several NPC1 mutant variants that either fail to export cholesterol due to impaired binding to NPC2 (F503/504A) or have impaired cholesterol binding to the putative sterol-sensing domain (SSD: P691S) (Gong et al., 2016; Li et al., 2016; Millard et al., 2005) failed to clear LC3B-positive material from the lysosomal lumen (Figure 2.3A-2.3B). F503/504A and SSD mutants were correctly targeted to the lysosome membrane (Figure 2.3C) and, as expected, failed to correct lysosomal cholesterol buildup, as shown by unchanged staining with filipin (Figure 2.3D) and with the recombinant sterol probe, mCherry-D4H*, which binds to cholesterol on the limiting membrane of the lysosome (Lim et al., 2019; Maekawa and Fairn, 2015)(Figure 2.3E-2.3F).

To dissect the molecular basis for the pronounced proteolysis defect of NPC1-null lysosomes, we quantified the abundance of resident lysosomal proteins. We found that several luminal hydrolases were decreased or undetectable in the NPC-null

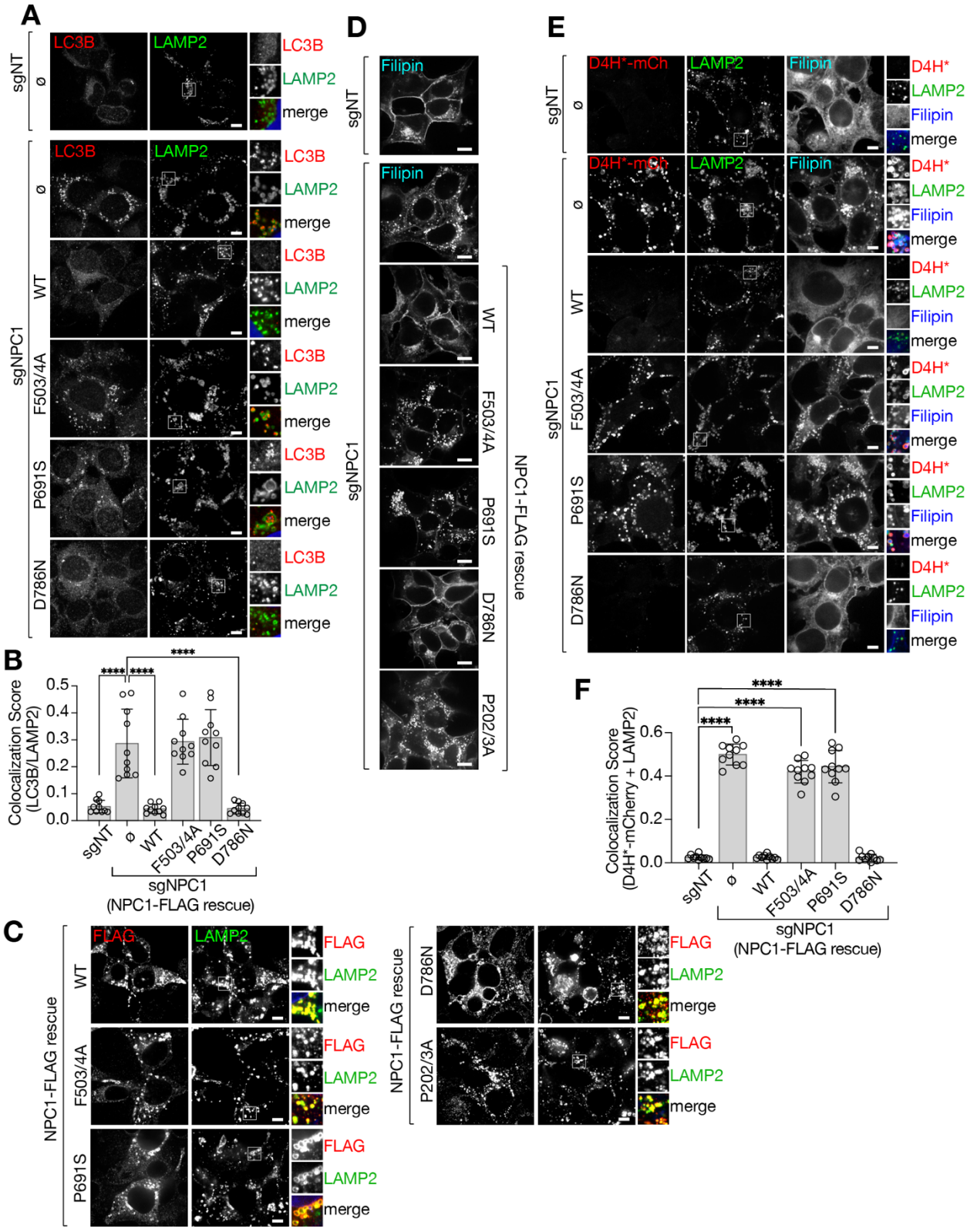

Figure 2.3 Cholesterol export by NPC1 mutants alleviates proteolytic block in NPC1-deficient cells (on previous page)
(A and B) sgNT and sgNPC1 293Ts expressing the indicated NPC1-FLAG cDNA were fixed and stained with antibodies targeting LC3B and LAMP2. (A) Representative confocal micrographs for each sample. Scale bars are 10μm. (B) Quantification of the co-localization between LC3B and LAMP2; ****P(adjusted) < 0.0001, ANOVA with Dunnett's multiple comparisons test.
(C) sgNPC1 293Ts expressing the indicated NPC1-FLAG cDNA were fixed and stained with antibodies directed against FLAG and LAMP2. Scale bars are 10μm.
(D) sgNT and sgNPC1 293Ts expressing the indicated NPC1-FLAG cDNA were fixed and cellular cholesterol deposits were stained with filipin. Scale bars are 20μm.
(E and F) sgNT and sgNPC1 293Ts expressing the indicated NPC1-FLAG cDNA were fixed and semi-permeabilized with a liquid N2 pulse, followed by cholesterol labeling with D4H*-mCherry and filipin, and staining with antibodies directed against LAMP2. (E) Representative confocal micrographs for each sample. Scale bars are 10μm. (F) Quantification of the co-localization of D4H*-mCherry and LAMP2; ****P(adjusted) < 0.0001, ANOVA with Dunnett's multiple comparisons test.

compared to control lysosomal samples. These included the Cathepsin Z protease (CTSZ), the acid lipase (LIPA), which de-esterifies LDL-derived cholesterol, and several enzymes involved in degradation of glycans and glycosphingolipids such as galactosylceramidase (GALC) and N-acetyl-alpha-glucosaminidase (NAGLU) (Figure 2.4A). A fluorescence-based reporter assay for the activity of GALC showed a marked reduction in NPC1-depleted cells compared to control cells (Figure 2.4B). Taken together, these data indicate that reduced abundance of resident lysosomal hydrolases may lead to impaired degradative capacity of NPC lysosomes and defective autophagic cargo degradation in NPC1 null cells.

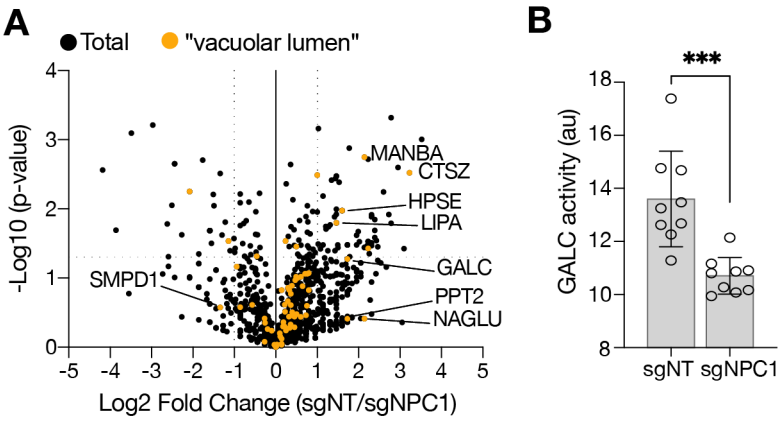

Figure 2.4 NPC1-deficient lysosomes also have reduced levels of luminal hydrolases
(A) Volcano plot of Lyso-IP proteomic data (from **2.1**) for the ratio of untreated (DMSO) sgNT/sgNPC1 LAMP1-normalized peptide counts. Proteins that are classified by the GO term "vacuolar lumen" (GO:0005775) are depicted as orange circles. Statistical analysis was performed using two-tailed unpaired t-test.
(B) Relative galactosylceramidase (GALC) activity in sgNT or sgNPC1 293Ts from cells labeled with a GALC activity probe (GalGreen) and LysoTracker Red. GalGreen fluorescence is normalized by total lysosomal content, as determined by LysoTracker Red fluorescence; ***P = 0.0004, two-tailed unpaired t-test.

2.3.2 NPC1-null lysosomes display increased susceptibility to membrane damage

Recently, it has emerged that the lysosomal limiting membrane is susceptible to damage resulting from undigested/undigestible substrates that accumulate within the lumen (Jia et al., 2020; Maejima et al., 2013; Radulovic et al., 2018; Skowyra et al., 2018). Thus, we considered possibility that defective luminal proteolysis upon loss of NPC1 function might compromise the integrity of the lysosomal membrane. An early

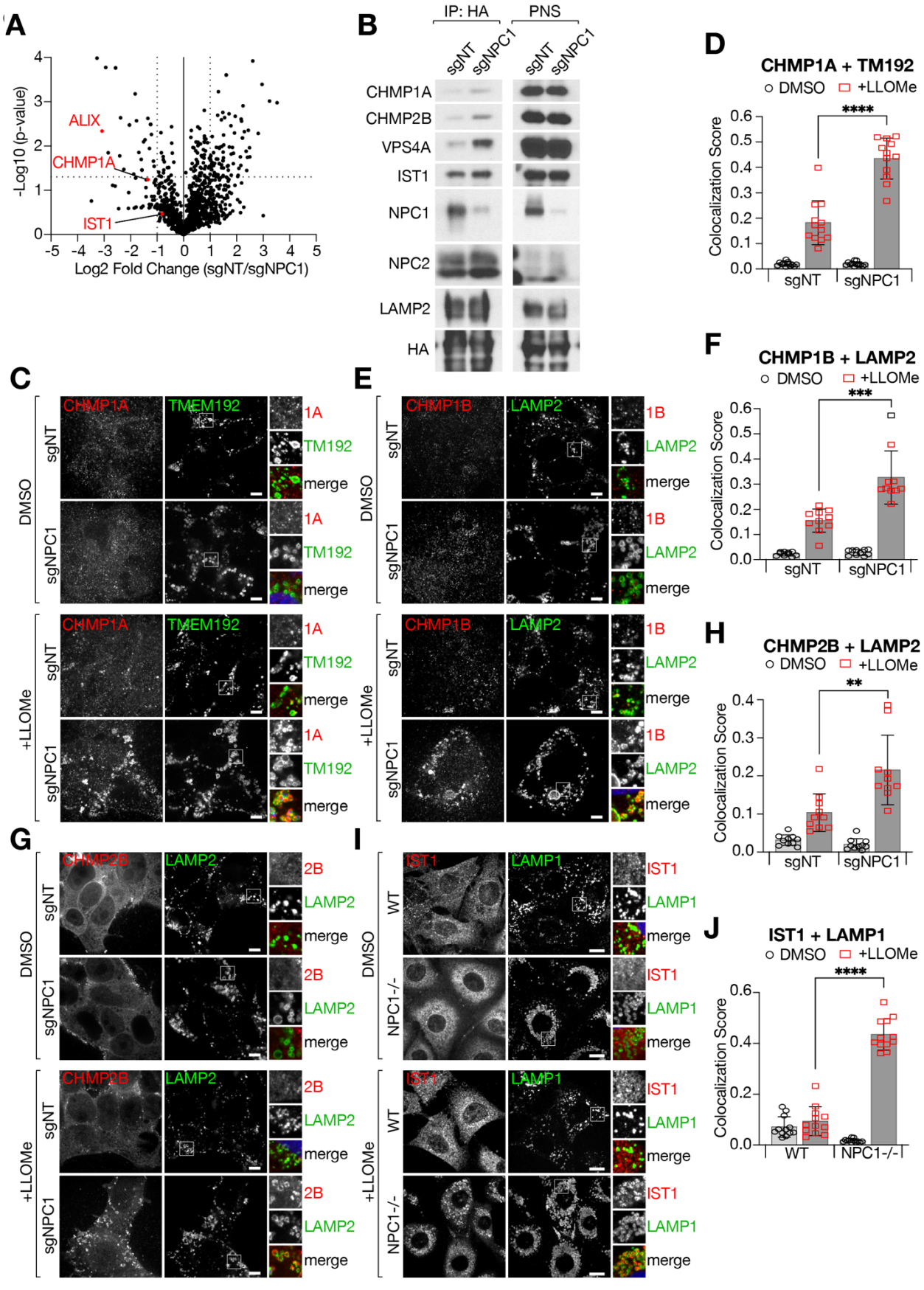
A
-Log10 (p-value)
Log2 Fold Change (sgNT/sgNPC1)
ALIX
CHMP1A
IST1
B
IP: HA
PNS
sgNT
sgNPC1
CHMP1A
CHMP2B
VPS4A
IST1
NPC1
NPC2
LAMP2
HA
C
DMSO
+LLOMe
sgNT
sgNPC1
CHMP1A
TMEM192
1A
TM192
merge
D
CHMP1A + TM192
DMSO
+LLOMe
****
Colocalization Score
E
CHMP1B
LAMP2
1B
F
CHMP1B + LAMP2
***
G
CHMP2B
2B
H
CHMP2B + LAMP2
**
I
IST1
LAMP1
WT
NPC1-/-
J
IST1 + LAMP1
****

Figure 2.5 NPC1-deficient cells have elevated levels of lysosome-associated ESCRT-III (on previous page)
(A) Volcano plot of Lyso-IP proteomic data (from **2.1**) for the ratio of untreated (DMSO) sgNT/sgNPC1 LAMP1-normalized peptide counts. Selected ESCRT proteins are depicted as red circles. Statistical analysis was performed using two-tailed unpaired t-test.
(B) Immunoblots of Lyso-IP samples from sgNT or sgNPC1 293Ts expressing TMEM192-RFP-3xHA.
(C-H) sgNT or sgNPC1 293Ts were treated with 1mM LLOMe or vehicle (DMSO) for 10m before being fixed and stained with the indicated antibodies. Representative confocal micrographs for cells stained with CHMP1A and TMEM192 (C), CHMP1B and LAMP2 (E), or CHM2B and LAMP2 (G). Scale bars are 10μm. Quantification of the co-localization between CHMP1A and TMEM192 (D), CHMP1B and LAMP2 (F), or CHMP2B and LAMP2 (H); ****P < 0.0001, ***P = 0.0005, two-tailed unpaired t-test with Welch's correction.
(I and J) WT and NPC1-/- MEFs were treated with 1mM LLOMe or vehicle (DMSO) for 10m before being fixed and stained with antibodies directed against IST1 and LAMP1. (I) Representative confocal micrographs for each sample. Scale bars are 20μm. (J) Quantification of the co-localization between IST1 and LAMP1; ****P < 0.0001, two-tailed unpaired t-test with Welch's correction.

(ESCRT) III proteins detects 'microtears' in the lysosomal membrane and repairs them via a membrane scission process that is thought to topologically resemble ESCRT III-mediated intraluminal vesicle budding during endosomal maturation (Nguyen et al., 2020; Radulovic et al., 2018; Schöneberg et al., 2016; Skowyra et al., 2018). Accordingly, our proteomics analysis found enrichment of the ESCRT III-interacting protein ALIX (also known as PDCD6IP), along with ESCRT III components CHMP1A and IST1 in NPC1-defective over wild-type lysosomes (Figure 2.5A). Together with the ESCRT I protein, TSG101, ALIX provides a recruiting platform for the assembly of coiled filaments of ESCRT III subunits, including CHMP1A and IST1, to sites of damage on lysosomal membranes (Radulovic et al., 2018; Skowyra et al., 2018).

Consistent with the proteomic data, immunoblotting of lysosomal immunoprecipitates from NPC1-defective HEK-293Ts confirmed increased lysosomal accumulation of several ESCRT III components, including CHMP1A, CHMP2B and IST1, as well as the AAA+ ATPase, VPS4A, which mediates ESCRT III polymer remodeling and disassembly (Chiaruttini et al., 2015; Schöneberg et al., 2016) (Figure 2.5B). In contrast to the clear proteomics and immunoblotting results, ESCRT III accumulation in NPC1-defective cells was not readily visible by double immunofluorescence staining for lysosomal markers and CHMP1A or CHMP1B, possibly due to limitations of the available antibodies. However, enhanced ESCRT III accumulation became evident upon induction of lysosomal damage using the membrane destabilizing agent L-leucyl-L-leucine methyl ester (LLOMe), both in NPC1-defective HEK293Ts and in NPC1-null MEFs (Figure 2.5C-2.5J). Given that lysosomal pH is not significantly compromised by loss of NPC1 (Elrick et al., 2012), the enrichment of ESCRT III components is likely not reflective of unrecoverable membrane permeabilization, but rather of higher propensity to damage events that are compensated, at least in part, by local ESCRT III polymerization.

In agreement with the notion that NPC1-deficient lysosomes are more susceptible to membrane rupture, we observed a time-dependent increase in the recruitment of Galectin-3 (Gal3) to lysosomes in cells exposed to LLOMe (Figure 2.6A-2.6B). Gal3 is a cytosolic lectin protein that is used as a marker of lysosomal damage, because it binds to glycoproteins present in the lysosomal lumen only when the limiting

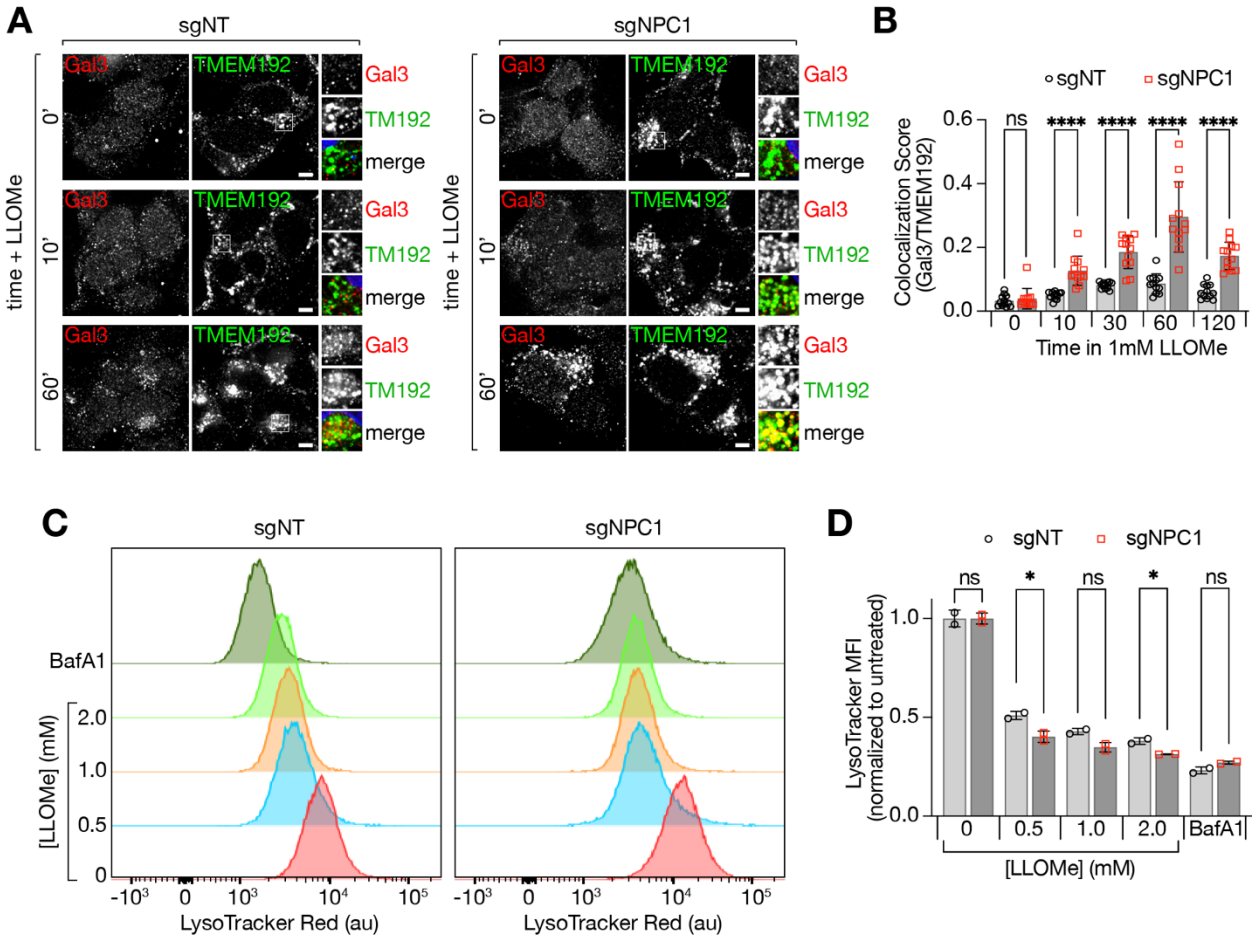

Figure 2.6 NPC1-deficient cells are more susceptible to lysosomal rupture
(A and B) sgNT or sgNPC1 293Ts were treated with 1mM LLOMe as indicated before being fixed and stained with antibodies directed against Gal3 and TMEM192. (A) Representative confocal micrographs for indicated timepoints. Scale bars are 10μm. (B) Quantification of the colocalization between Gal3 and TMEM192. ****P < 0.0001, ns = not significant, two-tailed unpaired t-test with Welch's correction.
(C and D) sgNT or sgNPC1 293Ts were treated with increasing concentrations of LLOMe for 10m (or BafA1 for 30m) before being stained with LysoTracker Red. (C) Representative histograms showing LysoTracker Red fluorescence of each population. (D) Average LysoTracker Red mean fluorescence intensity, normalized to that of untreated cells, is shown for each condition. *P < 0.05, ns = not significant, two-tailed unpaired t-test.

membrane is ruptured (Maejima et al., 2013; Paz et al., 2010). Importantly, Gal3 was not detected in the lysosomes of untreated cells, but its recruitment was enhanced at all time points in LLOMe-treated NPC1-deficient cells (Figure 2.6A-B), suggesting these cells incur greater levels of damage than cells with intact NPC1 function. We also observed that NPC1-deficient cells exhibited a greater proportional reduction in labeling with the lysosomotropic dye LysoTracker Red, which fluoresces on in acidic environments, when exposed to LLOMe in a dose-dependent manner (Figure 2.6C-2.6D). This further supports the idea that NPC1-deficient lysosomes are more sensitive to LLOMe-induced membrane rupture, resulting in increased proton leakage relative to lysosomes with functional NPC1.

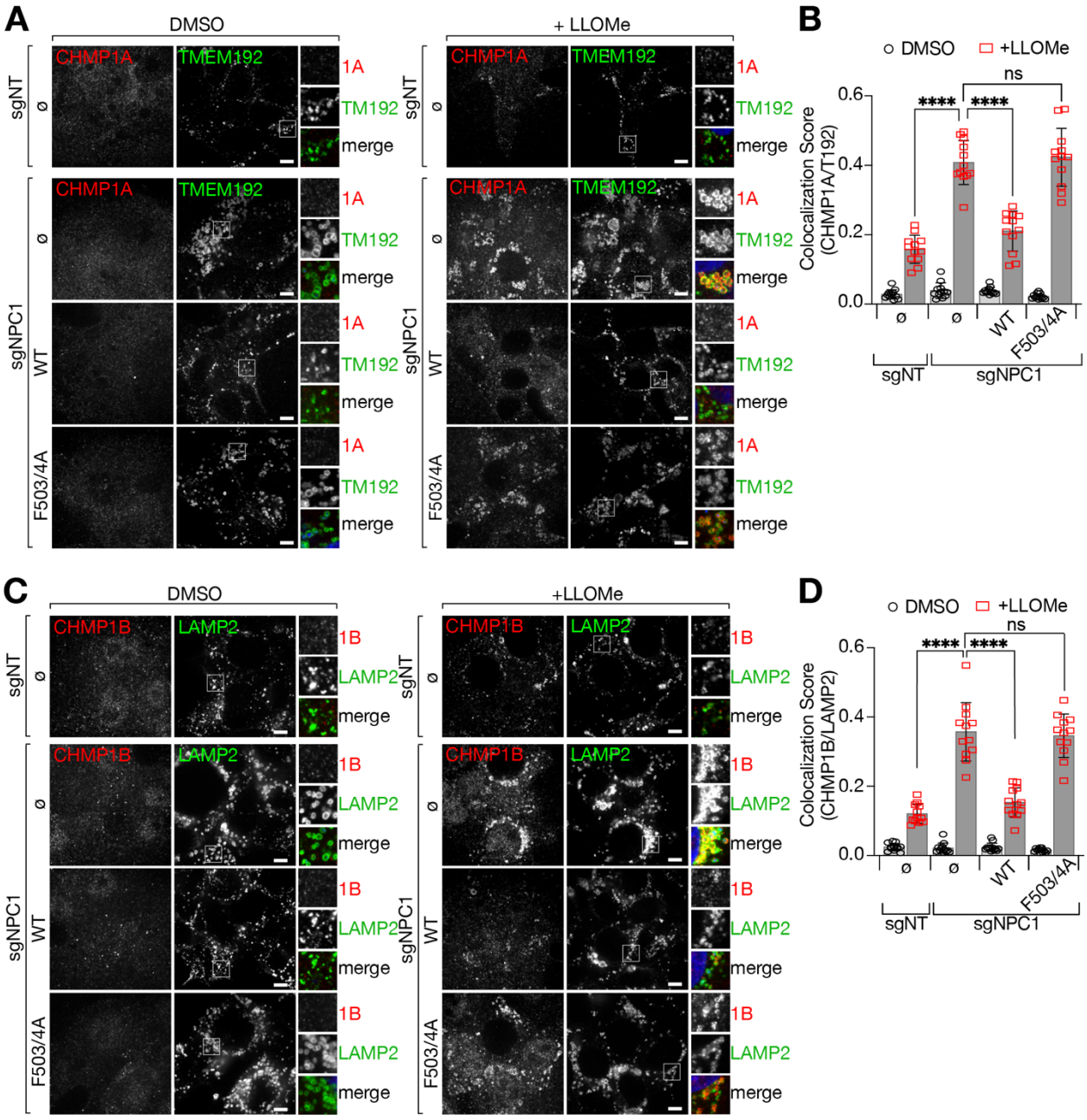

Figure 2.7 Cholesterol export by NPC1 mutants restores lysosomal membrane integrity
(A-D) sgNT and sgNPC1 293Ts expressing the indicated NPC1-FLAG cDNA were treated with 1mM LLOMe or vehicle (DMSO) for 10m before being fixed and stained with the indicated antibodies. Representative confocal micrographs for cells stained with CHMP1A and TMEM192 (A) and CHMP1B and LAMP2 (C) are shown. Scale bares are 10μm. Quantification of the co-localization between CHMP1A and TMEM192 (B) and CHMP1B and LAMP2 (D); ****P(adjusted) < 0.0001, ANOVA with Dunnett's multiple comparisons test.

As was the case for defective proteolysis, the higher propensity of NPC lysosomes to membrane damage was a direct consequence of the loss of NPC1-dependent cholesterol export. Reconstituting NPC1-deleted cells with wild-type NPC1

suppressed LLOMe-induced lysosomal CHMP1A and CHMP1B accumulation, whereas the transport-defective F503/4A mutant failed to do so (Figure 2.7A-2.7D)

Thus, our lysosomal proteomics analysis reveals that increased propensity to membrane damage accompanies defective proteolysis and loss of hydrolases following loss of NPC1-dependent cholesterol export. These defects are causally linked to cholesterol accumulation and, quite conceivably, to one another, as accumulation of undigested substrates could lead to membrane rupture through mechanical stress.

2.3.3 NPC1 regulates mTORC1 via its cholesterol-exporting function

To begin to establish a mechanistic link between the lysosomal defects described above and faulty mTORC1 regulation, we tested the ability of several sterol transport-defective NPC1 mutants to restore mTORC1 regulation by cholesterol. Reconstituting NPC1-depleted cells with wild-type NPC1 rescued the correct regulation of mTORC1 signaling upon cholesterol depletion via MCD, followed by repletion with either free cholesterol or LDL (Figure 2.8A-2.8B). Unlike wild-type, the NPC2-binding defective (F503/504A) and the sterol-sensing domain (P691S) mutants of NPC1 (expressed at nearly identical levels to the wild-type protein) were unable to restore mTORC1 regulation by cholesterol depletion-refeed (Figure 2.8A-2.8B). Another transport-incompetent mutant, caused by impaired cholesterol binding to the N-terminal luminal domain (P202/3A) (Kwon et al., 2009), also failed to restore mTORC1 sensitivity to cholesterol depletion (Figure 2.3C-2.33D and Figure 2.8A). Conversely, the transport-competent D786N mutant fully restored cholesterol- or LDL-dependent mTORC1 regulation (Figure 2.8A-2.8B). In agreement with the signaling results, the transport defective NPC1 isoforms failed to re-establish regulation of mTORC1 localization to LAMP2-positive lysosomes in response to changes in cellular cholesterol levels (Figure 2.8C-2.8D).

We previously showed that cholesterol that is transferred from the ER to the lysosome via the activity of OSBP is able to activate mTORC1 (Lim et al., 2019). In order to fully decouple the cholesterol transport role of NPC1 from any potential role in regulating mTORC1 activation by sterol-sensing, we employed the use of OSW-1, a potent chemical inhibitor of OSBP (Burgett et al., 2011; Mesmin et al., 2017). OSW-1 treatment blocks cholesterol flow from the ER, lowering the cholesterol content of the lysosomal membrane below a threshold that can promote mTORC1 activation, regardless of NPC1 function (Lim et al., 2019). As with cells lacking NPC1, OSW-1 treatment suppressed mTORC1 activity in cells re-expressing NPC1, regardless of the functionality of the isoform expressed (Figure 2.8E).

Together, these data argue against a sterol-sensing role of NPC1 in the mTORC1 pathway, and strongly suggest that the cholesterol exporting function of NPC1 is necessary and sufficient for mTORC1 regulation.

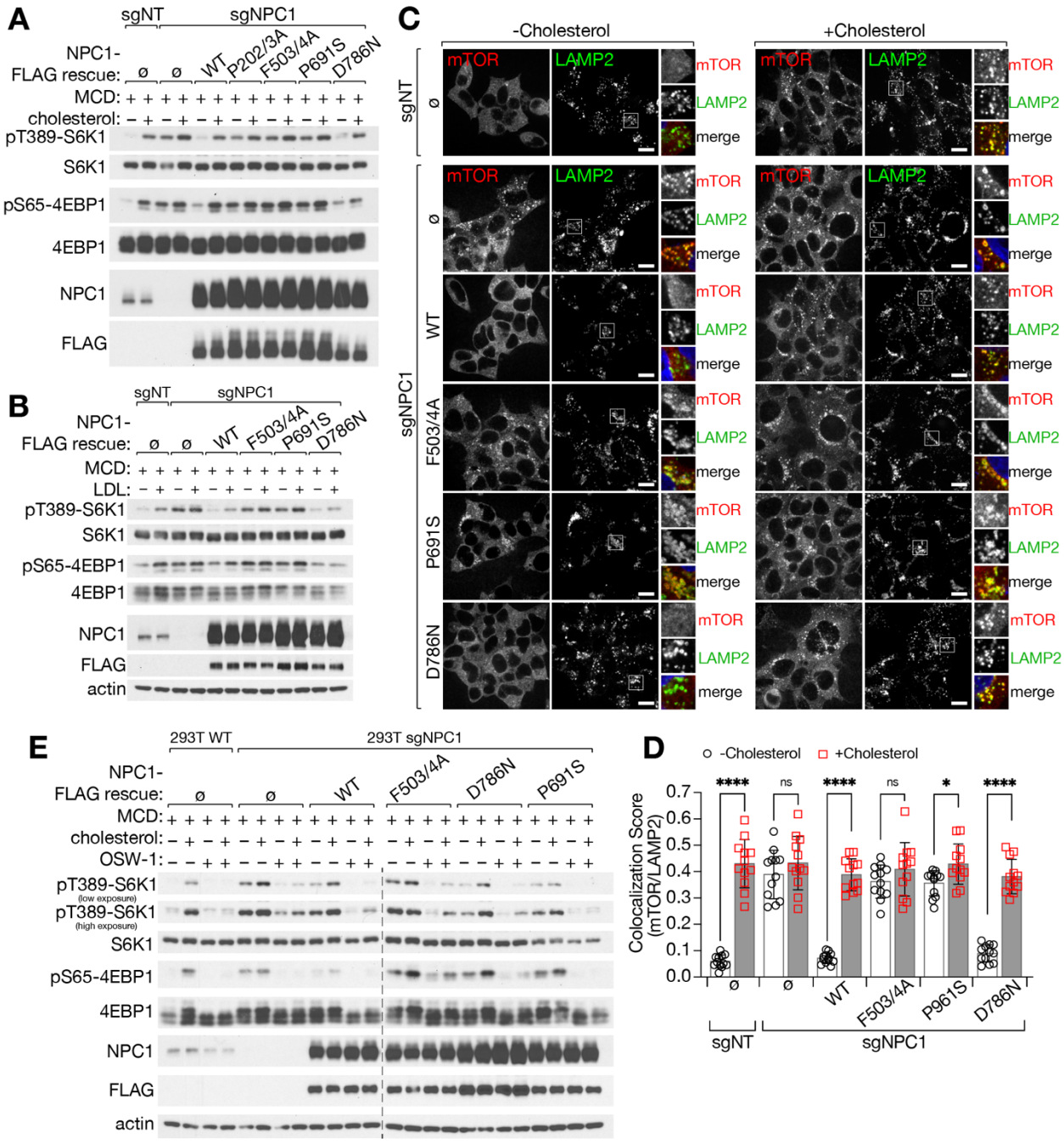

Figure 2.8 Transport by NPC1 controls mTORC1 activity in response to lysosomal cholesterol
(A and B) Immunoblots from sgNT and sgNPC1 293Ts expressing the indicated NPC1-FLAG cDNA. Cells were depleted of sterols using methyl-ß-cyclodextrin (MCD, 0.75% w/v) for 2h, followed by re-feeding for 2h with 50μM cholesterol in complex with 0.1% MCD (A), or human LDL (B), as indicated. (C and D) Cells were starved for and re-fed with cholesterol as in (A) before being fixed and stained with antibodies directed against mTOR and LAMP2. (C) Representative confocal micrographs for each sample. Scale bars are 20μm. (D) Quantification of the co-localization between mTOR and LAMP2; ****P < 0.0001, *P = 0.0121, ns = not significant, two-tailed unpaired t-test with Welch's correction.
(E) Immunoblots from sgNT and sgNPC1 293Ts expressing the indicated NPC1-FLAG cDNA were pre-treated with 10nM OSW-1 as indicated before being starved for and re-fed with cholesterol as in (A).

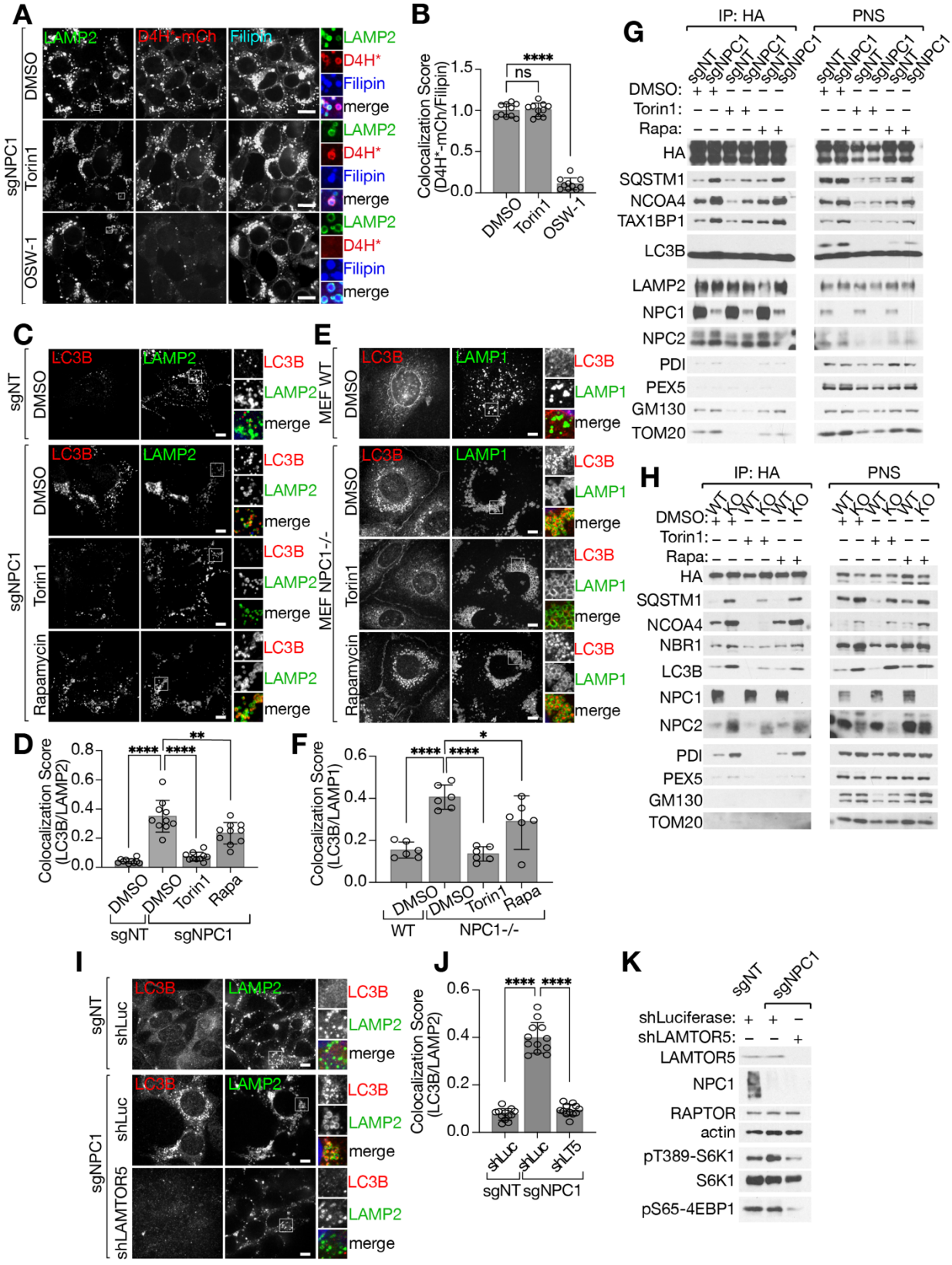
A
LAMP2
D4H*-mCh
Filipin
sgNPC1
DMSO
Torin1
OSW-1
LAMP2
D4H*
Filipin
merge
B
Colocalization Score (D4H*-mCh/Filipin)
****
ns
DMSO
Torin1
OSW-1
C
sgNT
sgNPC1
LC3B
LAMP2
merge
Rapamycin
D
Colocalization Score (LC3B/LAMP2)
****
**
DMSO
Torin1
Rapa
sgNT
sgNPC1
E
MEF WT
MEF NPC1-/-
LAMP1
F
Colocalization Score (LC3B/LAMP1)
*
WT
NPC1-/-
G
IP: HA
PNS
sgNT
sgNPC1
DMSO:
Torin1:
Rapa:
HA
SQSTM1
NCOA4
TAX1BP1
LC3B
LAMP2
NPC1
NPC2
PDI
PEX5
GM130
TOM20
H
WT
KO
NBR1
I
shLuc
shLAMTOR5
J
shLuc
shLT5
K
shLuciferase:
shLAMTOR5:
LAMTOR5
RAPTOR
actin
pT389-S6K1
S6K1
pS65-4EBP1

Figure 2.9 Inhibition of mTORC1 activity alleviates lysosomal proteolysis defect associated with loss of NPC1 (on previous page)
(A and B) sgNPC1 293Ts were treated with Torin1 (250nM, 24h), OSW-1 (10nM, 8h), or vehicle (DMSO) before being fixed and semi-permeabilized with a liquid N2 pulse, followed by cholesterol labeling with D4H*-mCherry and filipin, and staining with antibodies directed against LAMP2. (A) Representative confocal micrographs for each sample. Scale bars are 20μm. (B) Quantification of the co-localization of D4H*-mCherry and filipin-positive structures; ****P(adjusted) < 0.0001, ANOVA with Dunnett's multiple comparisons test.
(C and D) sgNT or sgNPC1 293Ts were treated with Torin1 (250nM, 24h), rapamycin (100nM, 24h), or vehicle (DMSO) as indicated before being fixed and stained for antibodies directed against LC3B and LAMP2. (C) Representative confocal micrographs for each sample. Scale bars are 10μm. (D) Quantification of co-localization between LC3B and LAMP2; ****P(adjusted) < 0.0001, **P(adjusted) = 0.0014, ANOVA with Dunnett's multiple comparisons test.
(E and F) WT and NPC1-/- MEFs were treated with Torin1 (250nM, 24h), rapamycin (100nM, 24h), or vehicle (DMSO) as indicated before being fixed and stained for antibodies directed against LC3B and LAMP1. (E) Representative confocal micrographs for each sample. Scale bars are 10μm. (F) Quantification of co-localization between LC3B and LAMP1; ****P(adjusted) < 0.0001, *P(adjusted) = 0.0426, ANOVA with Dunnett's multiple comparisons test.
(G and H) Immunoblots of Lyso-IP samples from sgNT or sgNPC1 293Ts (G), or WT and NPC1-/- MEFs (H) treated with Torin1, rapamycin, or vehicle as in (C).
(I and J) sgNT or sgNPC1 293Ts expressing control (shLuciferase) or Ragulator-specific (shLAMTOR5) shRNAs were fixed and stained with antibodies directed against LC3B and LAMP2. (I) Representative confocal micrographs for each sample. Scale bars are 10μm. (J) Quantification of co-localization between LC3B and LAMP2; ****P(adjusted) < 0.0001, ANOVA with Dunnett's multiple comparisons test.
(K) Immunoblots of cells from (I).

2.3.4 mTORC1 inhibition restores integrity and proteolytic function of NPC lysosomes downstream of cholesterol storage

We next investigated the cellular effects of aberrant mTORC1 regulation in NPC. Due to its ability to stimulate lipogenic programs (Düvel et al., 2010; Li et al., 2010; Peterson et al., 2011), conceivably mTORC1 could contribute to lysosomal cholesterol buildup in NPC1-null cells. However, treating NPC cells with the ATP-competitive mTOR inhibitor, Torin1 (Thoreen et al., 2009), did not significantly reduce cholesterol accumulation in the lysosomal lumen or limiting membrane, as indicated by unchanged staining with filipin and mCherry-D4H*, respectively (Figure 2.9A-2.9B). Thus, mTORC1 dysregulation occurs downstream of cholesterol storage and does not appear to contribute significantly to its establishment.

Due to the ability of mTORC1 to control lysosomal biogenesis and catabolism (Kim et al., 2011; Martina et al., 2012; Roczniak-Ferguson et al., 2012; Settembre et al., 2012), we next tested whether mTORC1 inhibition could alleviate at least some aspects of lysosomal dysfunction identified by our lysosomal proteomic analysis. This was clearly the case. Treating NPC1-null cells with Torin1 promoted clearance of autophagic material from the lysosomal lumen, as judged by both LC3B-LAMP2 double immunofluorescence (Figure 2.9C-2.9F) and by direct immunoblotting of immunopurified lysosomal samples from both NPC1-KO HEK-293T and MEFs (Figure 2.9G-2.9H). Also, inhibiting mTORC1 signaling via shRNA-mediated knock down of LAMTOR5, which is essential for mTORC1 recruitment to and activation at the lysosome (but is not required for mTORC2-dependent signaling) (Anandapadamanaban

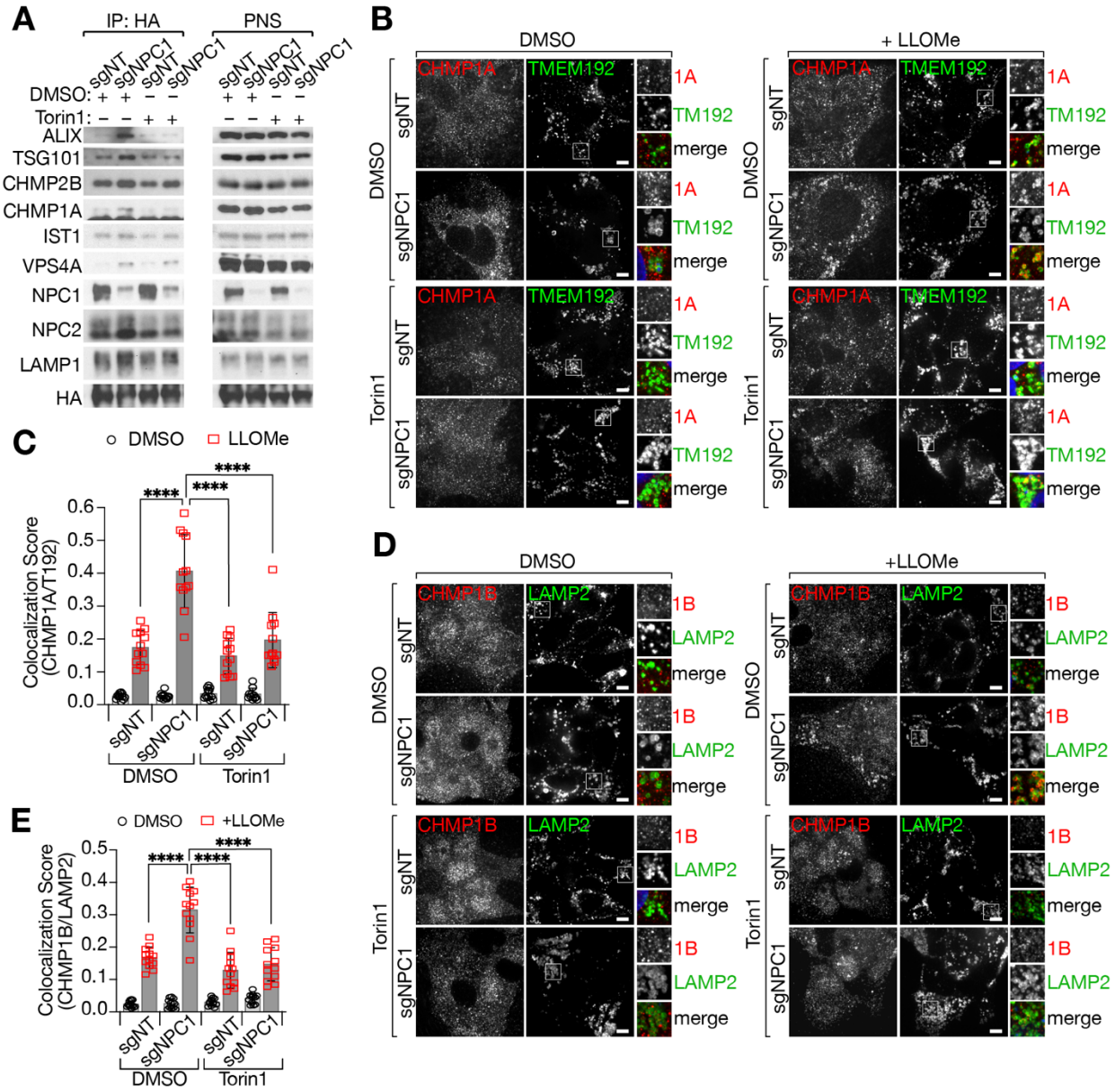

Figure 2.10 Inhibition of mTORC1 activity reduces ESCRT-III accumulation on NPC1-deficient lysosomes

(A) Immunoblots of Lyso-IP samples from sgNT or sgNPC1 293Ts treated with 250nM Torin1 or vehicle (DMSO) for 24h.

(B-E) sgNT and sgNPC1 293Ts were pre-treated with Torin1 or DMSO for 24h before being treated with LLOMe (1mM) or vehicle (DMSO) for 10m. Cells were fixed and stained with indicated antibodies. CHMP1A and TMEM192 (B) and CHMP1B and LAMP2 (D) are shown. Scale bares are 10μm. Quantification of the co-localization between CHMP1A and TMEM192 (C) and CHMP1B and LAMP2 (E) ****P(adjusted) < 0.0001, ANOVA with Dunnett's multiple comparisons test.

et al., 2019; De Araujo et al., 2017; Bar-Peled et al., 2012; Rogala et al., 2019; Su et al., 2017), led to pronounced clearance of accumulated LC3 from the lumen of LAMP2-positive NPC lysosomes (Figure 2.9I-2.9L).

In contrast to mTORC1 inhibition via Torin1 or Lamtor5 knock down, little effect on lysosomal clearance was observed when cells were treated with the allosteric

mTORC1 inhibitor, Rapamycin (Figure 2.9C-2.9H). Rapamycin incompletely inhibits mTORC1: whereas S6 kinase-dependent anabolic programs are efficiently suppressed by Rapamycin, protein synthesis triggered by mTORC1-dependent 4E-BP1 phosphorylation is largely unaffected, as is suppression of catabolic programs mediated by mTORC1-dependent phosphorylation of Unc1-like kinase (ULK1) and the master regulator of lysosomal biogenesis, transcription factor EB (TFEB) (Lawrence and Zoncu, 2019; Liu and Sabatini, 2020). The higher efficacy of Torin1 (and Lamtor5 depletion) over Rapamycin suggests that inhibition of protein synthesis and activation of the autophagy-lysosome system are both key for restoration of lysosomal proteolysis downstream of mTORC1 inhibition.

mTORC1 inhibition via Torin1 treatment also corrected the higher propensity for damage of NPC1 lysosomes, as shown by decreased recruitment of ESCRT III subunits both by immunoblotting of purified lysosomal samples and by double immunofluorescence for CHMP1A or CHMP1B and lysosomal markers (Figure 2.10A-2.10E). Given that mTORC1 inhibition reversed proteolytic failure but not cholesterol accumulation within NPC lysosomes, we conclude that the higher propensity of NPC lysosomes to undergo membrane damage primarily results from accumulation of undigested substrates within the lumen and not from altered fluidity of the membrane due to increased cholesterol content.

2.3.5 mTORC1 inhibition restores lysosomal function in iPSC-derived NPC neuronal cultures

Lysosomal dysfunction and its correction by mTORC1 inhibition were readily observed in actively proliferating cell lines. However, the cell type most compromised by loss of NPC1 are postmitotic neurons in the cerebellum, cerebral cortex and other brain regions (Walkley and Suzuki, 2004). To characterize the role of aberrant mTORC1 signaling on organelle homeostasis in a disease-relevant model of NPC, we deleted the NPC1 gene in induced pluripotent stem cells (iPSCs) using CRISPR/Cas9, and subsequently differentiated this population into neurons using a previously established method involving co-culture with a stromal cell line and FACS purification of neural populations (Ordonez et al., 2012) (Figure 2.11A-2.11B). Neural stem cells and neurons derived by this differentiation method express neuronal lineage markers (nestin, MAP2, ßIII tubulin) (Figure 2.11A-2.11B) and have been shown to be electrophysiologically active (Israel et al., 2012).

Consistent with the results in HEK-293T and MEFs and with previous reports (Elrick et al., 2012), iPSC-derived NPC neurons showed accumulation of undigested autophagic adaptors TAX1BP1 and GABARAP (Figure 2.12A-2.12D). Interestingly, unlike the HEK-293T model, iPSC-derived NPC neurons showed accumulation of autophagic adaptors both within and outside LAMP2-positive lysosomes, suggesting that defective autophagosome-lysosome fusion compounds with impaired lysosomal proteolysis in these cells (Sarkar et al., 2013). Overnight treatment of NPC neurons with Torin1 largely cleared intracellular TAX1BP1 and GABARAP aggregates, suggesting that mTORC1 inhibition is sufficient to restore the function of the autolysosomal system of neuronal cells (Figure 2.12A-2.12D).

Similar to NPC1-depleted HEK-293T cells, iPSC-derived NPC neurons also had increased sensitivity to membrane damage, as shown by enhanced recruitment of ESCRT III to lysosomes upon treatment with LLOMe (Figure 2.12E-2.12F). As seen in non-neuronal lines, the hyper-sensitivity of iPSC-derived cells to lysosomal damage was also corrected by Torin1 treatment (Figure 2.12E-2.12F).

Thus, the compositional and functional defects revealed by our lysosomal proteomics in HEK-293T cells extend to NPC1-null neurons and are corrected by mTORC1 inhibition.

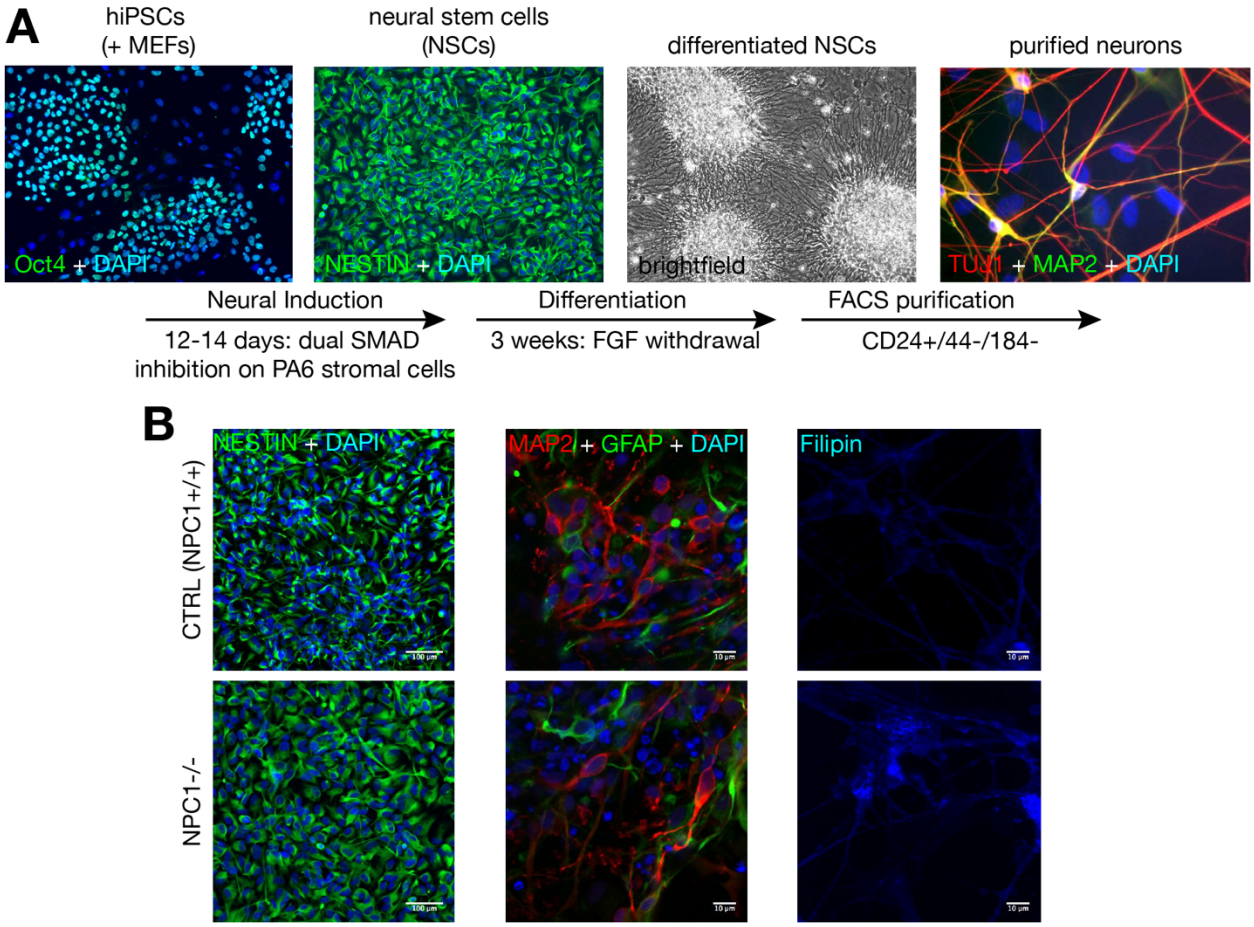

Figure 2.11 Validation of iPSC-derived neural lineage lines
(A) Schematic depicting differentiation protocol for generating neural cell lineages from human iPSCs. Representative images depicting cellular phenotypes at each stage of differentiation are shown.
(B) Validation of neural lineage differentiation for cell lines used in this study. NSCs were stained with Nestin, and differentiated neural cell populations were stained with MAP2 and GFAP. Cholesterol accumulation in NPC1-/- neural cells was validated by filipin staining.

2.3.6 mTORC1 inhibition restores defective mitochondrial function in NPC1-null cells

Given the pervasive role of the autophagy-lysosome system in cellular quality control, the defective degradative capacity of NPC1-null lysosomes is expected to affect the integrity and function of other cellular compartments. Mitochondria are especially dependent on efficient lysosome-autophagy function for their morphological

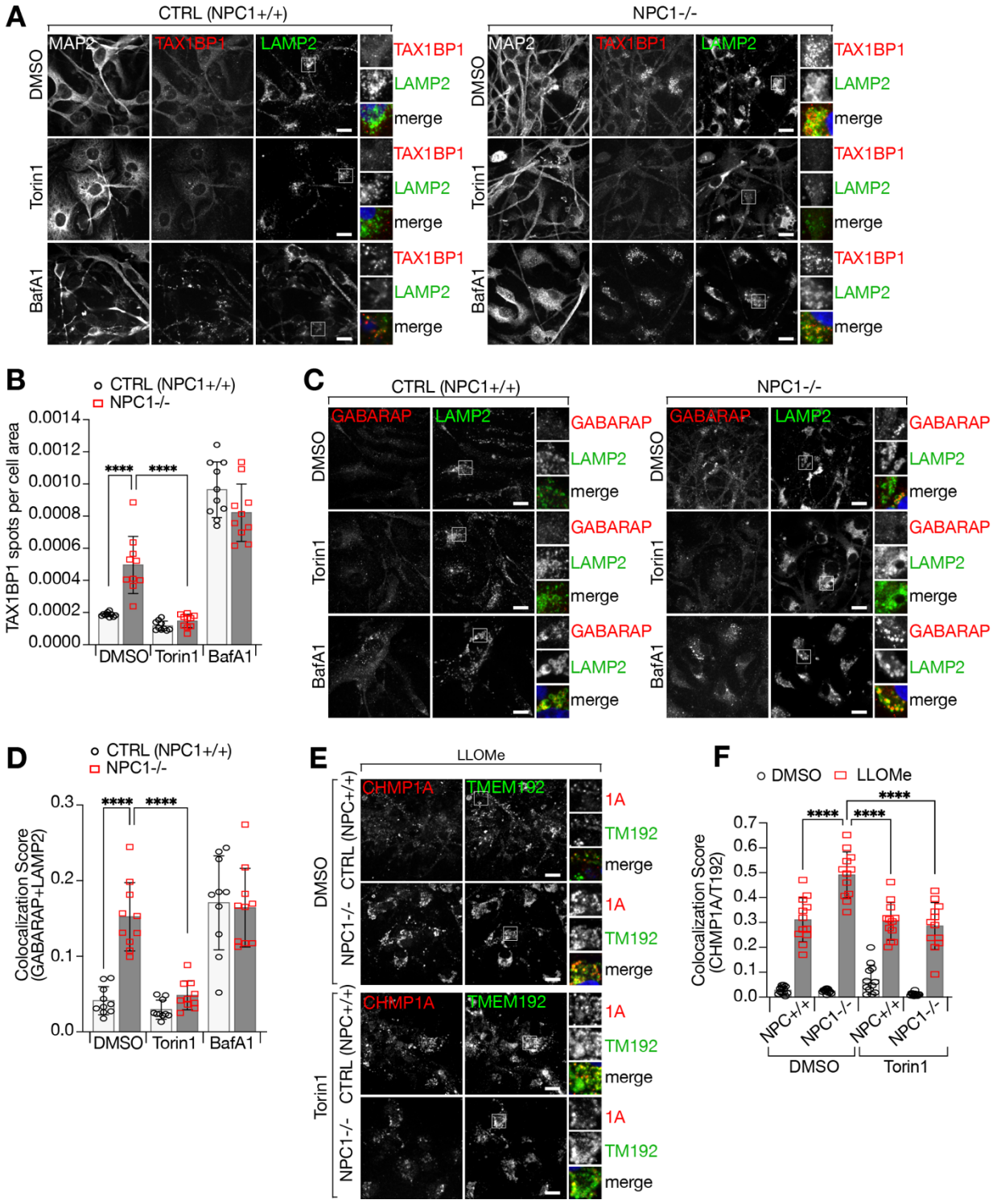

Figure 2.12 Inhibition of mTORC1 corrects lysosomal defects associated with loss of NPC1 in and iPSC-derived neuronal cell model (on previous page)
(A and B) Control or NPC1-/- iPSC-derived neural lineage cells were treated with Torin1 (250nM, 24h), BafA1 (500nM, 4h), or vehicle (DMSO) before being fixed and stained with antibodies directed against TAX1BP1, LAMP2, and MAP2. (A) Representative confocal micrographs of each sample. (B) Quantification of the number of TAX1BP1 spots per cell area (defined by MAP2); ****P(adjusted) < 0.0001, ANOVA with Dunnett's multiple comparisons test.
(C and D) Control or NPC1-/- iPSC-derived neuronal lineage cells were treated as in (A) before being fixed and stained with antibodies directed against GABARAP and LAMP2. (C) Representative confocal micrographs of each sample. (D) Quantification of the co-localization between GABARAP and LAMP2; ****P(adjusted) < 0.0001, ANOVA with Dunnett's multiple comparisons test.
(E and F) Control or NPC1-/- iPSC-derived neuronal lineage cells were pre-treated with Torin1 or DMSO for 24h before being treated with LLOMe (1mM) or vehicle (DMSO) for 10m. Cells were fixed and stained with antibodies directed against CHMP1A and TMEM192. (E) Representative confocal micrographs of LLOMe-treated cells. (F) Quantification of co-localization between CHMP1A and TMEM192; ****P(adjusted) < 0.0001, ANOVA with Dunnett's multiple comparisons test.
Scale bars in all images are 20μm.

and functional homeostasis; accordingly, severe mitochondria defects have been reported in NPC1-null cell lines and in neuronal cultures derived from human embryonic stem cells (hESCs) (Ordonez et al., 2012; Yambire et al., 2019a). Moreover, dysregulated mTORC1 activity could contribute to mitochondrial dysfunction via increased translational burden, production of reactive intermediates and morphological alterations (Ebrahimi-Fakhari et al., 2016; Morita et al., 2017).

We analyzed our lysosomal proteomic datasets for the relative representation of mitochondrial proteins, defined by MitoCarta (Calvo et al., 2016) or Gene Ontology classification. By comparing their normalized peptide abundance, we discovered that mitochondrial proteins were significantly under-represented in NPC1-defective compared to control lysosomes (Figure 2.13A). In fact, when we ranked proteins based on their preferential enrichment in wild-type over NPC1 lysosomes, approximately 50% of the proteins in the top quartile were classified as mitochondrial, whereas only 23.6% of proteins in the other three quartiles were mitochondrial (Figure 2.13B). About half of the proteins classified as mitochondrial displayed the expected behavior of substrates, where their peptide count was higher in leupeptin:pepstatin than in DMSO ("mito substrates", Figure 2.13A-2.13B). Thus, unlike other substrates that reach the lumen of NPC lysosomes but fail to be degraded, lysosomal delivery of mitochondria appears hampered in NPC, possibly reflecting disruption of the process of mitophagy (Ebrahimi-Fakhari et al., 2016; Khaminets et al., 2016; Ordonez, 2012).

Consistent with defective mitophagy, the cytoplasm of iPSC-derived NPC neurons was disseminated with fragmented mitochondria, as shown by immunostaining with the mitochondrial marker Tom20 (Figure 2.13C-2.13D). Treatment with the v-ATPase inhibitor, BafA1, induced dramatic mitochondrial fragmentation in wild-type cells, consistent with an acute requirement for the lysosome in maintaining mitochondrial function (Ordonez, 2012; Weber et al., 2020; Yambire et al., 2019b). However, BafA1 only modestly increased the already high degree of mitochondrial fragmentation observed in NPC1-null cells, implicating lysosomal dysfunction as the main driver of this process (Figure 2.13C-2.13D). Further supporting this idea, overnight treatment with Torin1 restored mean mitochondrial length of NPC1-null

neurons to wild-type levels, whereas it caused no change in mitochondria of their wild-type counterparts (Figure 2.13C-2.13D).

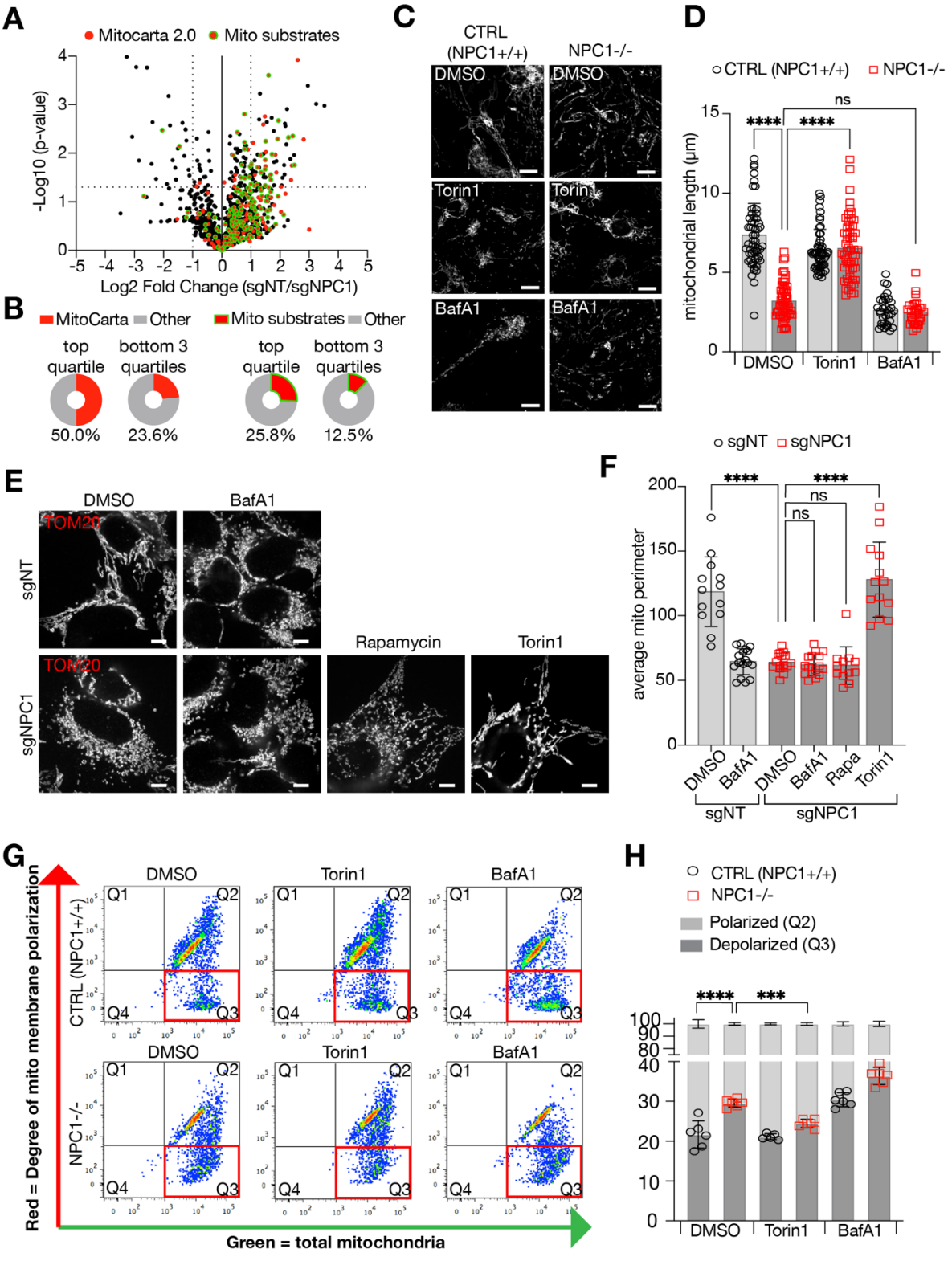

Figure 2.13 Mitochondrial morphology and function are disrupted by loss of NPC1 and is restored by inhibition of mTORC1 (on previous page)
(A) Volcano plot of Lyso-IP proteomic data (from **2.1**) for the ratio of untreated (DMSO) sgNT/sgNPC1 LAMP1-normalized peptide counts. Proteins identified as mitochondrial, based on the human MitoCarta 2.0 database (Calvo et al., 2016), are shown as red circles. The subset of mitochondrial proteins that behave as substrates for lysosomal proteolysis are highlighted with a green outline.
(B) Percentages of MitoCarta or "mito substrates" proteins that are in the top quartile (>75% enrichment) or remaining three quartiles (<75% enrichment) of proteins enriched in sgNT over sgNPC1 lysosomes. Total number of proteins is 1254, total number in top quartile is 62.
(C and D) Control or NPC1-/- iPSC-derived neuronal lineage cells were treated with Torin1 (250nM, 24h), BafA1 (500nM, 4h), or vehicle (DMSO) before being fixed and stained with antibodies directed against TOM20. (C) Representative confocal micrographs of each sample. (D) Lengths of individual mitochondria were measured and quantified.
(E and F) sgNT and sgNPC1 293Ts were treated with BafA1 (500nM, 4h), Rapamycin (100nM, 24h), Torin1 (250nM, 24h) or vehicle (DMSO) as indicated, before being fixed and stained with antibodies directed against TOM20. (E) Representative confocal micrographs for each sample. Scale bars are 10μm. (F) Quantification of average mitochondrial perimeter measured from TOM20 stained bodies. Number of cells in each condition are shown as individual points; ****P(adjusted) < 0.0001, ns = not significant, ANOVA with Dunnett's multiple comparisons test.
(G and H) Control or NPC1-/- iPSC-derived neuronal lineage cells were treated with Torin1, BafA1, or vehicle as in (C) before being stained with the ratiometric mitochondrial membrane potential dye JC-10. (G) Dot plots showing fluorescence distribution of individual cells from one representative experiment. MMP-independent ("green") fluorescence is shown on the x-axis and MMP-dependent ("red") fluorescence is shown on the y-axis. (H) Percentages of cells classified as depolarized (Q3: green^{high}, red^{low}) or polarized (Q3: green^{high}, red^{high}). Values from individual replicates are shown as points, bars represent average values across all replicates.

Similar to iPSC-derived NPC neurons, mitochondria of NPC1-deleted HEK293T cells were highly fragmented, and their fragmentation was not further increased by BafA1-mediated v-ATPase inhibition (Figure 2.13E-2.13F). Treating NPC1-deleted HEK-293T cells with Torin1 re-established the tubular morphology of mitochondria, whereas rapamycin was largely ineffective (Figure 2.13E-2.13F).

Loss of mitochondrial integrity is often indicative of decreased mitochondrial membrane potential (MMP). Indeed, consistent with previous reports, mitochondria from NPC1-null iPSC-derived neurons showed significantly reduced MMP compared to wild-type cells, as determined by flow cytometry analysis of iPSC-derived neurons co-stained with the ratiometric MMP indicator, JC-10 (Figure 2.13G-2.13H). BafA1 treatment decreased the MMP of wild-type neurons, whereas it had a smaller effect on the MMP of NPC cells. Similar to mitochondrial fragmentation, Torin1 significantly rescued the MMP of NPC neurons, whereas it had a negligible effect on wild-type cultures. Thus, dysregulated mTORC1 signaling contributes to mitochondrial impairment in NPC neurons, and its pharmacological modulation is sufficient to restore both morphological and functional aspects of these organelles.

2.4 Discussion

Taken together, our results support a central role for the NPC1-cholesterol-mTORC1 signaling axis in the maintenance of organelle function and cellular homeostasis (Figure 2.14). Export of lysosomal cholesterol by NPC1 is essential for

optimal regulation of mTORC1 signaling outputs. In turn, mTORC1 signaling plays a critical role in sustaining the hydrolytic activities of the lysosome, the integrity of its limiting membranes, and the morphology and polarization of mitochondria.

A key point that we address concerns the mechanisms via which NPC1 regulates mTORC1. We had previously shown that, in cells lacking NPC1, mTORC1 could not be switched off by cholesterol depletion, a phenotype consistent with both a cholesterol-transporting and a cholesterol-sensing role for NPC1 (Castellano et al., 2017; Lim et al., 2019). To determine which of these mechanisms is more likely to be correct, we systematically rescued NPC1-deleted cells with different NPC1 mutants that lack cholesterol-exporting activities. These studies reveal a tight correlation between the cholesterol transporting function of NPC1 and its ability to regulate mTORC1 signaling, supporting a model in which NPC1 functions upstream of cholesterol, not downstream of it, in the mTORC1 pathway. The ability of OSW-1, which depletes cholesterol in the lysosome limiting membrane by blocking transport from the ER, to abrogate mTORC1 activation in response to cholesterol independently of NPC1 function, further supports a model where cholesterol export by NPC1 is required to suppress mTORC1 activity in response to depletion of cellular cholesterol. In turn, dysregulated mTORC1 signaling emerges as a key driver of organelle dysfunction downstream of NPC1 loss and the resulting lysosomal cholesterol buildup.

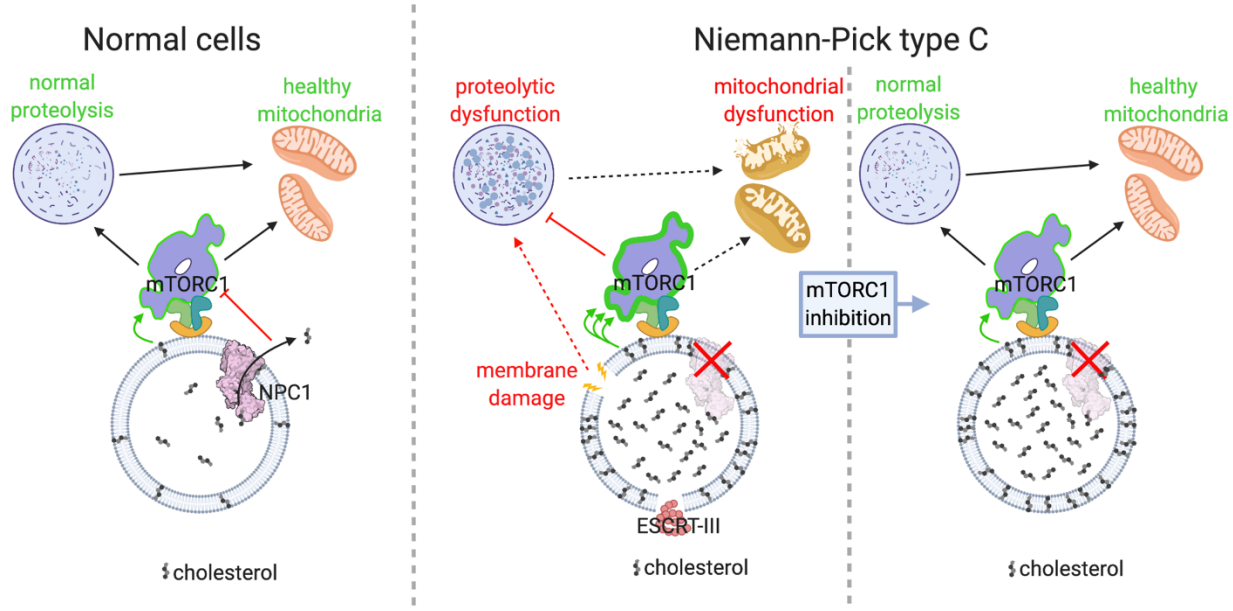

Figure 2.14 Model illustrating the relationship between NPC1, lysosomal cholesterol, mTORC1 signaling and organelle homeostasis in both normal and NPC cells.

This is shown by genetic and pharmacologic inhibition of mTORC1, which failed to correct cholesterol storage in the lysosomal lumen or on its limiting membrane but effectively corrected compositional and functional defects of the lysosome. How the lysosomal defects that we uncovered relate to each other will require further investigation. The depletion of several hydrolases (including proteases such as Cathepsin Z) provides a likely explanation for the profound proteolytic impairment of NPC lysosome revealed by accumulation of autophagic substrates. In turn, hydrolase

depletion could stem from transcriptional inhibition or from their defective trafficking to the lysosome (Kobayashi et al., 1999; Saftig and Klumperman, 2009; Sleat et al., 2013). Alternatively, it is tempting to speculate that the increased propensity of NPC lysosomes to undergo membrane damage could result in leakage of luminal contents, including resident hydrolases, a phenomenon suggested to occur in NPC as well as other physiological and pathological contexts (Chung et al., 2016; Hämälistö et al., 2020; Maejima et al., 2013; Sakamachi et al., 2017).

The primary factors driving membrane damage in NPC remain to be determined. In principle, alterations in membrane fluidity caused by the massive cholesterol accumulation on the limiting membrane of NPC lysosomes (as revealed by mCherry-D4H*) could increase the probability of membrane rupture, possibly through discontinuities between cholesterol-rich, crystalline-like microdomains and the surrounding membrane (Toulmay and Prinz, 2013; Tsuji et al., 2017). Damage could also result from undigested cargo accumulating within the lumen, a mechanism more similar to that induced by LLOMe, which assembles into membrane-piercing polymers within the acidic lysosomal lumen (Maejima et al., 2013; Radulovic et al., 2018; Skowyra et al., 2018). The observation that mTORC1 inhibition in NPC cells corrects lysosomal membrane damage and defective proteolysis without altering the cholesterol content of the lysosomal limiting membrane favors the latter possibility.

The observation that hydrolases mutated in other lysosomal storage disorders, such as acid lipase, beta-glucosidase and galactosidase are depleted from NPC lysosomes suggests the intriguing possibility that NPC compounds the pathogenic consequences of cholesterol storage with those of other diseases such as Wolman, Krabbe and Mucopolysaccharidosis III (Ballabio and Gieselmann, 2009) and could provide a mechanistic basis for the accumulation of neurofibrillary tangles, a pathogenic trait of Alzheimer Disease, in NPC brains (Walkley and Suzuki, 2004). More generally, hydrolase loss may be a common trait of several LSDs (Danyukova et al., 2018; Platt et al., 2018), a possibility that can be tested through the use of lysosomal profiling in cellular models of those diseases.

Given that mTORC1 inhibition decouples cholesterol storage from proteolytic failure and lysosomal membrane damage, a question that remains to be addressed is how NPC1-mTORC1 signaling controls these important functions of the lysosome. mTORC1 lies upstream of anabolic programs that could increase the proteolytic load of the lysosome, such as protein synthesis and ribosome biogenesis, while actively suppressing catabolic programs that could help restore lysosomal function, such as synthesis of lysosomal hydrolases and v-ATPase subunits by the MiT/TFE factors, TFEB and TFE3 (Düvel et al., 2010; Perera and Zoncu, 2016; Settembre et al., 2012). The failure of rapamycin, a partial mTORC1 inhibitor, at restoring lysosomal function in NPC cells suggests that simultaneous inhibition of biosynthetic programs and activation of catabolic ones downstream of mTORC1 may be required.

In our hands, overnight mTORC1 inhibition by Torin1 was sufficient to boost lysosomal proteolysis and correct susceptibility to damage. An interesting question is whether mTORC1 inhibition restores the function of pre-existing, cholesterol-filled lysosomes or rather promotes the formation of new ones. Answering this question,

which may have implications for the use of mTORC1 inhibitors in clinical settings, will require follow-up analysis with single-organelle resolution.

Another important finding from this work concerns the role of mTORC1 signaling in maintaining mitochondrial morphology and function in NPC. Mitochondria are known to be severely impacted in many neurodegenerative diseases, and mitochondrial dysfunction is a major contributor to neuronal cell death observed in these contexts. However, there is limited understanding of the molecular processes that disrupt mitochondrial composition and function. mTORC1 stimulates translation of multiple nuclear-encoded mitochondrial transcripts (Morita et al., 2013), stimulates energy production as well as generation of anabolic intermediates in mitochondria (Ben-Sahra et al., 2016; Cunningham et al., 2007; Morita et al., 2013) and can indirectly promote mitochondrial fission (Morita et al., 2017). Moreover, by inhibiting autophagic initiation, elevated mTORC1 signaling can suppress the capture and clearance of damaged mitochondria, an observation in line with our lysosomal proteomic data (Ebrahimi-Fakhari et al., 2016; Perera and Zoncu, 2016). Thus, the ability of catalytic mTORC1 inhibitors to restore mitochondrial morphology and membrane potential likely stems from a combination of decreased translational burden and activity (associated with dampened production of reactive intermediates) and increased repair due to restoration of lysosomal proteolysis.

The restorative effects of mTORC1 inhibition on key functions in NPC cells suggests the attractive possibility that inhibiting this pathway could have therapeutic value. Our data clearly indicate that clinical derivatives of rapamycin (rapalogues) are unlikely to be beneficial, whereas the more potent and complete ATP-competitive inhibitors may be effective. However, the applicability of this class of inhibitors is limited by poor bioavailability and toxic off-target inhibition of mTORC2, which may lead to insulin resistance and other complications (Lamming et al., 2012; Liu and Sabatini, 2020). The recent development of new-generation, mTORC1-specific inhibitors with more complete inhibitory profiles than rapamycin (Chung et al., 2019; Mahoney et al., 2018; Rodrik-Outmezguine et al., 2016; Schreiber et al., 2019) may provide an avenue for safe and effective mTORC1 modulation in NPC and other lysosomal diseases.

2.5 Methods

2.5.1 Mammalian Cell Culture

HEK293T sgNT, HEK293T sgNPC1, MEF SGNT, and MEF NPC1-/- cells were maintained in DMEM (Gibco, 11995) supplemented with 10% (v/v) fetal bovine serum (Sigma, F0926) and 100 U/ml penicillin, and 100 µg/ml streptomycin (Gibco, 15140-122). All cells were cultured at 37ºC in 5% CO2. Cells were free of mycoplasma and routinely tested using MycoAlert Mycoplasma Detection Kit (Lonza, LT07-318).

Drug treatments were performed as follows unless otherwise specified. Leupeptin (Alfa Aesar, J61188) and pepstatin A (MP Biologicals, 195368) were used at 20 µM each for 24 h. Bafilomycin A1 (Alfa Aesar, J61835) was used at 500 nM for 4 h.

LLOMe (Sigma, L7393) was used at 1 mM for 10 m. Torin1 (Tocris, 4247) was used at 250 nM for 24 h, and rapamycin (Calbiochem, 553210) was used at 100 nM for 24 h.

2.5.2 Cloning and Generation of Stable Cell Lines

A synthetic cDNA encoding TMEM192-RFP-3xHA (Lim et al., 2019) was cloned into the pLJM1 lentiviral vector. TMEM192-FLAG was cloned also cloned in the pLJM1 vector by amplifying the TMEM192 cDNA using primers to append a DYKDDDK ("FLAG") peptide to the c-terminus of the resulting protein. Codon-optimized NPC1 cDNA containing a FLAG tag (Castellano, et al.) was subcloned into the pLVX lentiviral vector (Clontech). All NPC1 mutants were generated using the QuikChange II Site-Directed Mutagenesis Kit (Agilent, 200524).

Short-hairpin oligonucleotides (shRNAs) directed against LAMTOR5 (TRCN0000153443) or Luciferase (TRCN0000072243, used as a non-targeting control) were cloned into the pLKO.1 lentiviral vector (The RNAi Consortium, Broad Institute) according to the manufacturer's instructions.

Expression of protein-encoding cDNAs or shRNA constructs was performed by stable lentiviral transduction. Lentivirus was generated by co-transfection of lentiviral vector carrying the construct of interest with lentiviral packaging plasmids (pMD2.G, Addgene 12259; and psPAX2, Addgene 12260) in a 5:3.75:1.25 ratio, respectively, using polyethylenimine (PEI). Viral supernatant was harvested 48 h after transfection, cleared by centrifugation, and concentrated using Lenti-X Concentrator (Clontech, 631231) according to the manufacturer's instructions. Target cells were plated in 6-well plates in media supplemented with 8 µg/ml polybrene (Millipore, TR-1003-G) and concentrated virus. Virus-containing media was removed after 24 h and replaced with media containing 1.5 µg/ml puromycin. Protein expression or knockdown was confirmed by immunoblotting. For shRNA knockdown, cells were maintained in selective media for 3 days before use in assays in order to ensure complete knockdown.

2.5.3 Lysosome Immunoprecipitation (Lyso-IP)

Lysosomes from cells expressing TMEM192-RFP-3xHA were purified as previously described (Lim et al., 2019). Briefly, cells were seeded in a 15cm at a density appropriate for them to reach confluency after 24h. All subsequent steps were performed on ice or at 4ºC unless otherwise noted. Media was removed, cell monolayers were rinsed with ice-cold KPBS buffer (136 mM KCl, 10m M KH2PO4, pH 7.25, supplemented with Pierce Protease Inhibitor Tablets (Thermo, A32965)), scraped into 10 ml of KPBS and collected by centrifugation at 1500 rpm for 5 min. Pelleted cells were resuspended in a total volume of 1ml KPBS (supplemented with 3.6% (w/v) OptiPrep (Sigma, D1556)) and fractionated by passing through a 23G syringe 5 times followed by centrifugation at 2700 rpm for 10 min. Post-nuclear supernatant was harvested and incubated with 40 µl of anti-HA magnetic beads (Thermo, 88836, prewashed with KPBS buffer) with end-over-end rotation for 10 min. Lysosome-bound beads were washed two times with KPBS(+ OptiPrep) and two times with KPBS. For immunoblotting, samples were incubated with a 1:1 mixture of KPBS and 2x urea sample buffer (150 mM Tris, pH 6.5, 6 M urea, 6% SDS, 25% glycerol, 5% □-

mercaptoethanol, 0.02% bromophenol blue) for 30 min at 37ºC. For proteomics experiments, lysosomal immunoprecipitates were eluted from beads using 0.1% NP-40 in PBS for 30 min at 37ºC, beads were removed and the resulting eluate was snap-frozen with LN2.

2.5.4 Proteomics Analysis

For comparative analysis between treatment conditions and genotypes, minimum peptide abundance was set to 1 for all replicates. Experimental datasets were first compared to the proteomic dataset generated from anti-HA Lyso-IP performed on cells expressing TMEM192-FLAG ("blank" samples). Only proteins present with a combined average peptide abundance across both experimental samples >1.5-fold enrichment over blank samples were included in further analysis. Fold changes between experimental samples were then calculated, and the significance of these fold changes were calculated using a two-tailed unpaired t-test. For comparative analysis between genotypes, peptide counts from each replicate were additionally normalized to the peptide abundance of LAMP1 within each replicate, before calculation of fold changes and significance values. Data in all volcano plots are displayed as the log2 of the fold change, and the -log10 of the p-value.

The list of "cargo" proteins was generated by identifying all proteins whose abundance increased ≥2-fold upon inhibition of lysosomal proteolysis (leupeptin/pepstatin treatment). This list was cross-referenced to the dataset comparing leupeptin/pepstatin-treated to vehicle-treated sgNPC1 cells.

To analyze mitochondrial proteins present in Lyso-IP samples, the filtered datasets were cross-referenced with the Human MitoCarta 2.0 database (Calvo, et al., 2015; Pagliarini, et al., 2008). This list was further refined by eliminating proteins that did not obey expected behavior upon lysosomal proteolysis inhibition (i.e. any protein whose abundance decreased upon leupeptin/pepstatin treatment in either genotype was excluded) to generate the "mito substrates" subset. Quartile analysis is based on the enrichment of proteins in sgNT samples over sgNPC1 samples, where "top quartile" are proteins with an enrichment of >75% in sgNT samples, and "bottom three quartiles" are all other proteins. Percentages shown in pie charts represent the fraction of proteins identified in MitoCarta 2.0 database, or as "mito substrates".

2.5.5 Immunofluorescence

Cells were seeded on fibronectin-coated glass coverslips in 12-well plates at 150,000-300,000 cells per well, and allowed to attach overnight. Cells were treated with compounds at the specified concentrations and length of time as indicated before being fixed and stained. For LC3B, GABARAP, and TAX1BP1 staining cells were first fixed and permeabilized with ice-cold 100% methanol for 5 min at -20ºC and then rinsed three times with PBS. For all other stainings, cells were first fixed with 4% paraformaldehyde (PFA) in PBS for 15 min at room temperature, rinsed three times with PBS, permeabilized with 0.1% (w/v) saponin in PBS for 10 min at room temperature, and rinsed three times with PBS. Primary antibodies were diluted into 5% normal donkey serum (Jackson ImmunoResearch, 017-000-121) and coverslips were labeled with this solution overnight at 4ºC. Coverslips were rinsed three times with PBS

and then labeled with fluorescently-conjugated secondary antibodies (diluted 1:400 in 5% normal donkey serum, PBS) for 45 min at room temperature, protected from light. Coverslips were rinsed with PBS six times (incubating in every other wash for 5 min at room temperature) and then mounted on glass slides using VECTASHIELD Antifade Mounting Medium with DAPI (Vector Laboratories, H-1200).

2.5.6 Microscopy

All confocal microscopy was performed on a spinning-disk Nikon Ti-E inverted microscope (Nikon Instruments) system using a Plan Apo 60x oil objective. Images of fine cellular detail were acquired with an additional 1.5x magnifier. All images were acquired with an Andor Zyla-4.5 scientific complementary metal-oxide-semiconductor camera (Andor Technology) using iQ3 acquisition software (Andor Technology).

2.5.7 Image analysis

For quantification of co-localization, 10-12 non-overlapping images were acquired from each coverslip. Raw, unprocessed images were imported into FIJI v.2.0.0-rc-69/1.52i and converted to 8-bit images, and images of individual channels were thresholded independently to exclude background and non-specific staining noise and converted to binary masks. Co-localization between lysosomes and the marker of interest was determined using the “AND” function of the image calculator. Data are plotted as the fraction of lysosomes that are positive for the marker of interest (the “Colocalization Score”).

For quantification of TAX1BP1 aggregates, thresholded images of the channel corresponding to MAP2 staining were used to generate a binary mask to define and measure the total area occupied by MAP2+ cells. Masks were then applied to independently thresholded images of channel corresponding to TAX1BP1 staining to exclude signal outside the defined cell area. Individual TAX1BP1 aggregates in the resulting image were counted using the “Analyze Particles” function, and data from individual frames are plotted as the average number of TAX1BP1 spots per MAP2+ cell area.

For mitochondrial perimeter measurements, individual cells were isolated into separate images and blinded before analysis. Each image was individually thresholded and converted to binary masks. The “Analyze Particles” function was used to identify and measure the perimeter of every particle in the resulting mask. Data are plotted as the average mitochondrial perimeter per cell analyzed. For mitochondrial length measurements, images were first blinded and then the length of individual mitochondria was measured manually. Data are plotted as the length of every individual mitochondria in each condition.

2.5.8 Measurement of GALC activity

HEK293T cells were seeded at 10,000 cells per well in fibronectin-coated flat-bottom black 96-well plates with clear bottom (Greiner, 655090) and allowed to adhere overnight. Media was aspirated and then replaced with fresh complete growth media supplemented with 15 μM LysoLive GalGreen fluorogenic substrate (MarkerGene Technologies, M2776) and 50 nM LysoTracker Red DND-99 (Thermo Scientific, L7528)

and incubated at 37ºC for 2 h. Media was aspirated, wells were rinsed once with warm PBS, and then replaced with Imaging Buffer (136 mM NaCl, 2.5 mM KCl, 2 mM CaCl2, 1.3 mM MgCl2, 10 mM HEPES, pH 7.4). Endpoint fluorescence was measured on a Bio-Tek Synergy HT Multi-Mode Microplate Reader, using 485 nm/20 nm excitation with 528 nm/20 nm emission, and 570 nm/9 nm excitation with 590 nm/9 nm emission, read through the bottom of the plate. GalGreen fluorescence was normalized per well to LysoTracker Red fluorescence, and values from individual wells are plotted as points.

2.5.9 Cholesterol starvation and replenishment

HEK293T cells were seeded in fibronectin coated culture dishes so they would reach 80-90% confluency at the start of the assay. For cholesterol depletion, cells were incubated in DMEM supplemented with 0.75% (w/v) methyl-ß-cyclodextrin (MCD, Sigma C4555) and 0.5% (v/v) lipid-depleted serum (LDS) for 2 h. For cholesterol re-feeding cells were incubated with DMEM supplemented with 0.1% MCD and 0.5% LDS containing either 50 µM cholesterol (Sigma, C3045) or 100 mg/ml human LDL (Alfa Aesar, J65039), as indicated.

2.5.10 Cell lysis and immunoblotting

Cells were incubated in lysis buffer (1% Triton X-100, 10 mM □-glycerol phosphate, 10 mM sodium pyrophosphate, 4 mM EDTA, 40 mM HEPES, pH 7.4, supplemented with Pierce protease inhibitor tablets) for 30 min at 4ºC with rocking to ensure complete lysis. Lysates were harvested and cleared by centrifuging at 17,000g for 10 min at 4ºC, protein concentration in the supernatant was measured by Bradford assay. Samples of equalized concentration were prepared for SDS-PAGE by addition of 2x Urea samples buffer or 5x sample buffer (235 mM Tris, pH 6.8, 10% SDS, 25% glycerol, 25% ß-mercaptoethanol, 0.1% bromophenol blue). 5 µg of total protein from per sample was loaded per lane in a 12% Tris-Glycine gel (Thermo Scientific, XP00122) and resolved by electrophoresis in a Tris-Glycine running buffer (25 mM Tris, 190 mM glycine, 0.1% (w/v) SDS). For Lyso-IP samples 10% of the total immunoprecipitated material was loaded per lane, and 0.5% of total PNS was loaded per lane. Proteins were transferred to a PVDF membrane (Millipore IPVH00010), blocked with 5% non-fat milk in TBS-T, and incubated in primary antibodies (diluted in 5% milk in TBS-T) overnight at 4ºC. Membranes were rinsed with TBS-T and incubated with horseradish peroxidase conjugated anti-rabbit or anti-mouse secondary antibodies (diluted in 5% milk in TBS-T) for 1 h at room temperature. Membranes were washed again with TBS-T and incubated with Pierce ECL Western Blotting Substrate (Thermo Scientific, 32109) before being exposed to ProSignal ECL Blotting Film (Genesee Scientific, 30-810L). For phosphorylation site specific antibodies, PBS-T was used in place of TBS-T for all steps, and antibodies were diluted in 5% BSA in PBS-T.

2.5.11 Cholesterol labeling in situ with D4H*-mCherry and filipin

Recombinantly expressed GST-D4H*-mCherry was purified from BL21 E. coli as previously described (Lim et al., 2019). Labeling with D4H*-mCherry and filipin was also performed as previously detailed (Lim et al., 2019). Briefly, cells were plated on

fibronectin-coated coverslips and treated as indicated before being fixed with 4% PFA in PBS for 15 min at room temperature. Coverslips were rinsed in PBS, and then selectively permeabilized by immersion in LN2 for 25 sec. Coverslips were then blocked with 1% BSA in PBS for 1 h at room temperature, followed by incubation in D4H*-mCherry, diluted 1:50 in 1% BSA/PBS, for 2 h at room temperature, protected from light. Coverslips were rinsed with PBS and then fixed again with 4% PFA/PBS for 10 min at room temperature. Coverslips were rinsed with PBS and filipin labeling was performed simultaneously with immunofluorescent staining of LAMP2. Primary and secondary antibodies were diluted in 1% BSA in PBS supplemented with 0.5 mg/ml filipin (Sigma, F9765) and performed each for 1 h at room temperature, rinsing the coverslips with PBS after each incubation. Coverslips were mounted on glass slides in VECTASHEILD Antifade Mounting Media (Vector Laboratories, H-1000).

2.5.12 Measurement of lysosomal permeability

LLOMe treatment, LysoTracker Red staining, and flow cytometry were performed according to previously published protocols (Repnik et al., 2016). Briefly, HEK293T cells were harvested and transferred to 5mL polystyrene tubes and treated with the indicated concentration of LLOMe for 10 minutes at 37ºC. Cells were then centrifuged to pellet, resuspended in complete media containing 50 nM LysoTracker Red DND-99, and incubated at 37ºC for 15 minutes. Cells were centrifuged again and resuspended in 1X PBS before flow cytometry analysis. Cytometry was performed on an LSR Fortessa instrument (BD Biosciences). Forward and side scatter parameters were collected, and LysoTracker Red was excited using a 561nm laser line and collected with a 586/15nm emission filter. Cell aggregates were discriminated by gating FSC area against FSC height, and 100,000 single cell events were collected per condition.

2.5.13 hIPSC generation and neuronal differentiation

Control hIPSC lines were derived from fibroblasts obtained from one healthy adult (J. Craig Venter) whose genome is fully sequenced and published. hIPSC lines are generated by four-factor reprogramming as previously described (Israel et al., 2012). Cell lines are examined for pluripotency by labeling with lineage specific markers Tra 1-81 (BD Bioscience), Oct-4 and Nanog (Santa Cruz). Pluripotency is assessed by embryoid body formation and staining for the 3 germ layers, endoderm (Alpha-fetoprotein, DAKO), mesoderm (smooth muscle actin, Millipore) and ectoderm (Nestin, Millipore). NSC and neurons were generated using previously described protocols and purified by FACS (Yuan et al., 2011). NSCs are stained for Nestin (Millipore) Sox1, Sox2 and Pax 6. Neurons are stained for MAP2 and TUJ. For each experiment involving hIPSC derived neurons, neurons from at least two independent differentiations were examined in duplicate or triplicate format.

2.5.14 Generation of NPC1 knock-out hIPSCs

CRISPR/Cas9 gene editing was used to generate an NPC1 knock-out (KO) in the Craig Venter control hIPSC line. We inserted a frame-shift mutation in Exon 4 that engineered a premature stop codon leading to complete ablation of NPC1. Transfected

hIPSCs were sorted based on GFP and Tra181 expression and sparsely plated onto 10cm MEF plates. Individual colonies were picked manually and transferred to 96-well plates. Candidates were screened by PCR and TOPO cloning, and positive hits were karyotyped to ensure genetic stability. Digital karyotype was normal. A microamplification on chromosome 1p was visually observed in parental CV line and NPC1 KO line but this was below threshold and considered to be an artifact. Ablation of NPC1 was confirmed by RTqPCR and Western Blot.

Chapter 3

Characterization of NPC2 function in regulation of mTORC1 activity

3.1 Chapter Summary

Some of the work I present in Chapter 2 relates to the regulation of mTORC1 activity, and the role that the cholesterol transport function of NPC1 plays in negatively regulating mTORC1 in response to lysosomal cholesterol. While it appears that NPC1 acts in this capacity mainly by exporting an activating ligand, cholesterol, away from sensors that communicate its presence to mTORC1, the role of NPC2 in this process remains incompletely characterized. In this chapter I present some preliminary evidence that NPC2 also functions as a negative regulator of mTORC1's cholesterol-regulated activity, likely via the same cholesterol export pathway as NPC1, although the precise mechanism by which this occurs remains to be determined.

3.2 Introduction

NPC2 is a small soluble protein that functions in the lysosomal lumen to bind and mobilize cholesterol between internal pools and membranes and acceptor membranes and proteins (Storch and Xu, 2009). The primary function of NPC2 appears to be to transfer cholesterol to NPC1 for export from the lysosome, as mutations inactivating NPC2 have been identified as the other cause of Niemann Pick type C disease, responsible for ~5% of total identified cases (Naureckiene et al., 2000; Storch and Xu, 2009). Recent biochemical and structural studies have validated this role for NPC2, and have elucidated the mechanism of NPC1-NPC2 binding and cholesterol transport (Qian et al., 2020; Winkler et al., 2019). Biochemical assays of NPC2 function have suggested that in addition to being able to transfer cholesterol to NPC1, it also is able to transfer cholesterol rapidly between donor and acceptor membranes (Babalola et al., 2007), as well as to other proteins that might act as lysosomal cholesterol reservoirs, such as LAMP1 and 2 (Li and Pfeffer, 2016).

Recent work from the Zoncu laboratory, as well as some of the work presented in Chapter 2, strongly suggests that the pool of cholesterol that is present in the limiting membrane of the lysosome is directly sensed by machinery responsible for the activation of mTORC1 (Castellano et al., 2017; Lim et al., 2019). The function of NPC1 appears to be to export cholesterol from the lysosome and away from these sensors (Castellano *et al.*, 2017; Lim *et al.*, 2019, and Chapter 2). How the activity of NPC2 affects the regulation of this cholesterol-mTORC1 axis has previously been uncharacterized. Whether or not cholesterol transport by NPC2 is required for NPC1-mediated regulation of mTORC1, and whether or not NPC2 is required for cholesterol export from the lysosomal limiting membrane remain open questions.

To begin to address these questions I generated cells that do not express NPC2, and interrogated the effects of this knockout on cholesterol-regulated mTORC1 signaling and downstream effects of this activity on NPC-disease associated cellular phenotypes. While technical limitations impaired my ability to execute a more detailed investigation of the molecular mechanisms of NPC2-mediated regulation of mTORC1 activity, preliminary data presented here suggest that NPC2 acts in the same pathway as NPC1 in regulating mTORC1.

3.3 Results

3.3.1 Loss of NPC2 causes cholesterol accumulation in the lysosomal limiting membrane and render mTORC1 cholesterol insensitive

To generate cells lacking functional NPC2, CRISPR/Cas9 was used to target the first exon of the NPC2 gene. Clonal cell populations were isolated and screened for NPC2 expression by western blot, resulting in the isolation of several clones with no detectable NPC2 protein (data not shown). We next interrogated the responsiveness of

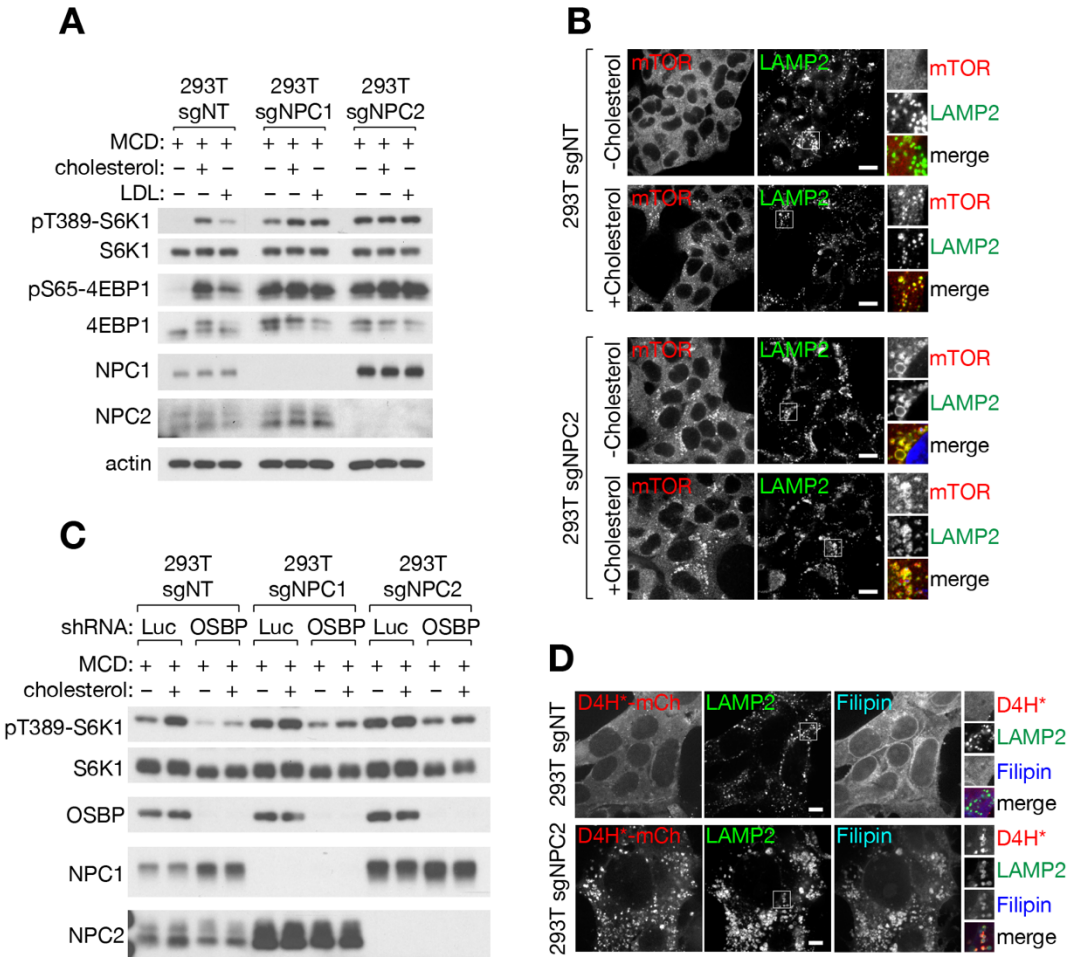

Figure 3.1 NPC2-null cells have dysregulated mTORC1 signaling caused by elevated cholesterol present on the limiting membrane of the lysosome
(A) Immunoblots from sgNT, sgNPC1, and sgNPC2 293Ts that were depleted of sterols using methyl-ß-cyclodextrin (MCD, 0.75% w/v) for 2h, followed by re-feeding for 2h with 50μM cholesterol in complex with 0.1% MCD, or human LDL, as indicated.
(B) Cells were starved for and re-fed with cholesterol as in (A) before being fixed and stained with antibodies directed against mTOR and LAMP2. Representative confocal micrographs for each sample are shown. Scale bars are 20μm.
(C) Immunoblots from sgNT, sgNPC1, and sgNPC2 293Ts expressing control (shLuciferase, Luc) or OSBP-directed shRNAs. Cells were depleted and re-fed with cholesterol as in (A).
(D) sgNT or sgNPC2 293Ts were fixed and semi-permeabilized with a liquid N2 pulse, followed by cholesterol labeling with D4H*-mCherry and filipin, and staining with antibodies directed against LAMP2. Representative confocal micrographs for each sample are shown. Scale bars are 10μm.

mTORC1 to depletion of cellular cholesterol using methyl-ß-cyclodextrin (MCD) and subsequent refeeding with free cholesterol in complex with MCD or with human LDL. In comparison to cells treated with a non-targeting guide RNA sequence (sgNT), cells lacking NPC2 (sgNPC2) showed no reduction in phosphorylation of the mTORC1 targets S6K1 and 4EBP1 upon depletion of cellular cholesterol, similar to the dynamics observed in cells lacking functional NPC1 (sgNPC1) (Figure 3.1A). In agreement with the signaling results, the loss of NPC2 also failed to promote the dissociation of mTOR from LAMP2-positive lysosomes upon cholesterol depletion (Figure 3.1B).

It is well established that loss of NPC2 function results in a massive accumulation of cholesterol in the lysosomal lumen (refs), but whether or not this also causes accumulation of cholesterol in the limiting membrane of the lysosome is unclear. We sought to clarify this by first disrupting OSBP-mediated cholesterol transport from the ER to the lysosome, a tactic that has been previously shown to lower the elevated cholesterol content in the limiting membrane of NPC1-null lysosomes below the threshold that renders mTORC1 insensitive to cellular cholesterol depletion (Lim et al., 2019). As in NPC1-deficient cells, inhibition of OSBP by shRNA-mediated knockdown lowered mTORC1 activity and blunted its response to cholesterol upon re-feeding (Figure 3.1C). We confirmed that cholesterol levels were elevated in the limiting membrane of the lysosomes of sgNPC2 cells using the recombinant sterol probe mCherry-D4H* (Lim et al., 2019; Maekawa and Fairn, 2015), which strongly labeled the limiting membrane of filipin- and LAMP2-positive lysosomes in sgNPC2 cells (Figure 3.1D). Thus, as is the case with NPC1, the loss of NPC2 appears to disrupt the balance of cholesterol transport by blocking the export of cholesterol from the limiting membrane of the lysosome, resulting in the accumulation of an ER-derived mTORC1-activating cholesterol pool.

3.3.2 Lysosomal and mitochondrial perturbations caused by loss of NPC2 are remediated by inhibition of mTORC1

To further assess the role of NPC2 in mTORC1-dependent regulation of cellular homeostasis, we next investigated whether NPC2-null cells exhibit the same phenotypic perturbations as previously observed in NPC1-null cells. Indeed, cells lacking NPC2 also appear to suffer from a block in lysosomal proteolysis, as judged by the presence of undigested aggregates of LC3B present in the lumen of the lysosomes of untreated cells (Figure 3.2A). Similarly, mitochondrial morphology appeared to be perturbed in NPC2-null cells, which showed a highly fragmented mitochondrial network (Figure 3.2B). In both cases these phenotypes appear to be dependent on lysosomal function, as treatment with the v-ATPase inhibitor bafilomycin A1 (BafA1) caused luminal LC3B aggregates to form and induced mitochondrial fragmentation in sgNT cells but did not appreciably worsen these phenotypes in sgNPC2 cells (Figure 3.2A-3.2B). Consistent with the observation that mTORC1 hyperactivation occurs in NPC2-deficient cells via the same (or highly similar) pathway as in NPC1-deficient cells, treatment of sgNPC2 cells with the ATP-competitive mTOR inhibitor Torin1 appeared to markedly remediate the observed LC3B aggregation and mitochondrial fragmentation in these cells (Figure 3.2A-3.2B). Therefore, it appears that like in NPC1-

deficient cells, hyperactivation of mTORC1 exacerbates lysosomal and mitochondrial dysfunctions present in cells lacking NPC2 as well.

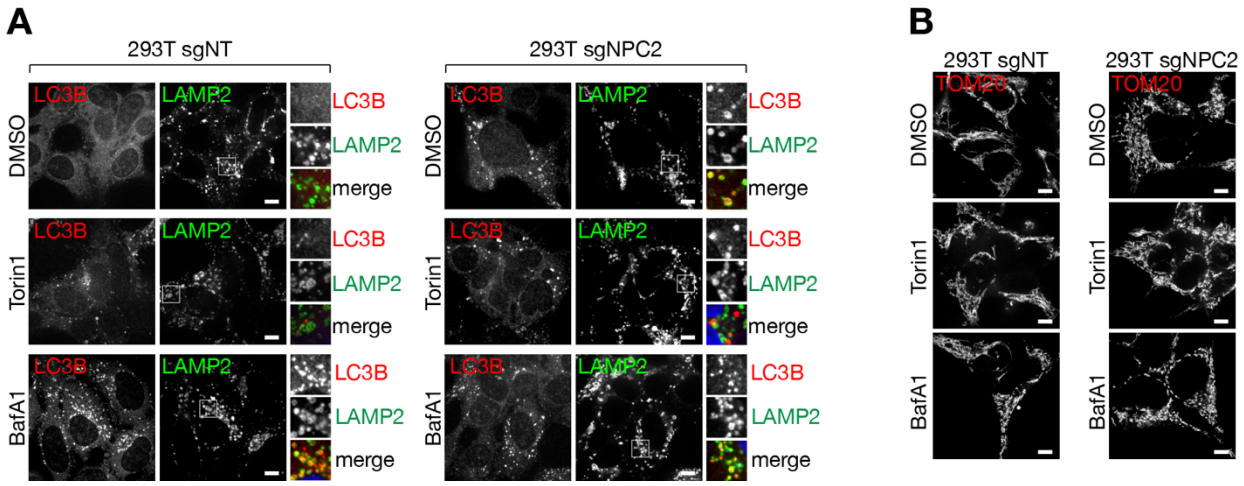

Figure 3.2 NPC2-null cells exhibit a block in lysosomal proteolysis and increased mitochondrial fragmentation that are corrected by mTOR inhibition
(A) sgNT or sgNPC2 293Ts were treated with Torin1 (250nM, 24h), BafA1 (500nM, 4h), or vehicle (DMSO) as indicated before being fixed and stained for antibodies directed against LC3B and LAMP2. Representative confocal micrographs for each sample are shown. Scale bars are 10μm.
(B) sgNT or sgNPC2 293Ts were treated as in (A) before being fixed and stained with an antibody directed against TOM20. Representative confocal micrographs for each sample are shown. Scale bars are 10μm.

3.4 Discussion

Collectively the results presented here suggest a role for NPC2 that is identical to that of NPC1 in the regulation of lysosomal cholesterol export with respect to the activation of mTORC1. NPC2-null cells display similar dynamics of mTORC1 signaling and lysosomal recruitment in response to cholesterol as NPC1-null cells do. Furthermore, the pool of cholesterol that activates mTORC1 in NPC2-null cells appears to be ER-derived, as in NPC1-null cells where it accumulates on the lysosomal limiting membrane as a result of a block in lysosomal cholesterol export. Lastly, the phenotypic overlap, with respect to lysosomal proteolysis and mitochondrial morphology, between NPC1- and NPC2-null cells, along with the fact that both appear to be downstream of mTORC1 activation in both genetic backgrounds, further suggests a common mechanism is responsible for the observed disruption of organelle homeostasis.

The exact mechanism by which NPC2 promotes the clearance of cholesterol from the limiting membrane of the lysosome remains unclear. The fact that the loss of NPC2 results in accumulation of cholesterol in the lumen of the lysosome is well established, but why NPC2 located in the lumen of the lysosome is required for export of cholesterol from the limiting membrane is unknown. It is tempting to speculate that binding of NPC2 by NPC1 is required to allosterically activate the cholesterol efflux capabilities of NPC1. This hypothesis is in line with the observation that NPC1-deficient cells reconstituted with a NPC2-binding defective NPC1 mutant (F503A/Y504A)

functionally behave as NPC1-null cells (see Chapter 2, Figures 2.2, 2.7, and 2.8). Alternatively, it is possible that NPC2 is required to first extract cholesterol from the limiting membrane before it can be transferred to NPC1 for export away from the lysosome.

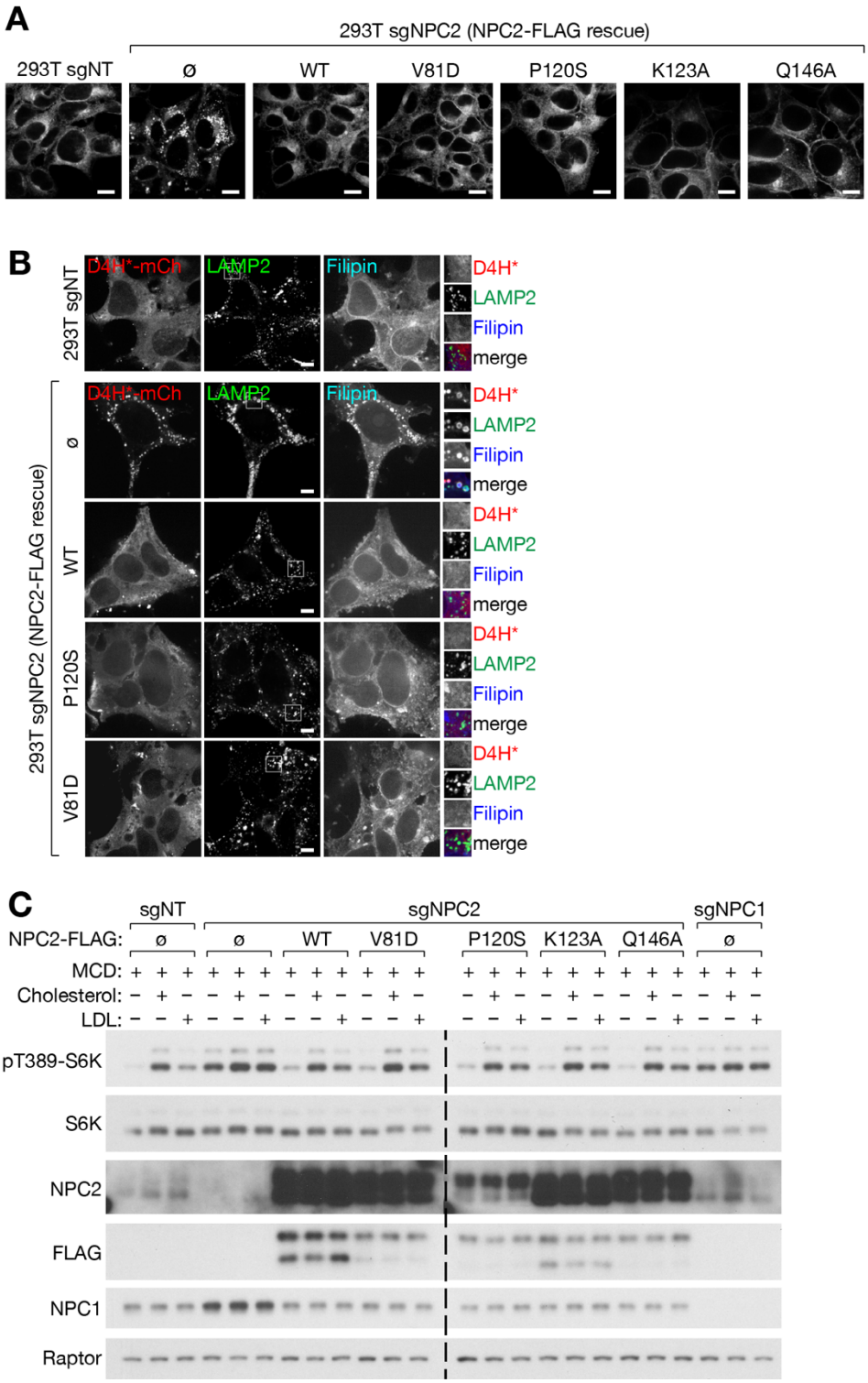

Figure 3.3 NPC2-null cells reconstituted with mutant NPC2 isoforms exhibit phenotypic inconsistencies with published results (on previous page)
(A) sgNT or sgNPC2 cells expressing the indicated NPC2-FLAG cDNA were fixed and stained for free cholesterol with filipin. Representative confocal micrographs for each sample are shown. Scale bars are 20μm.
(B) sgNT or sgNPC2 cells expressing the indicated NPC2-FLAG cDNA were fixed and semi-permeabilized with a liquid N2 pulse, followed by cholesterol labeling with D4H*-mCherry and filipin, and staining with antibodies directed against LAMP2. Representative confocal micrographs for each sample are shown. Scale bars are 10μm.
(C) Immunoblots from sgNT, sgNPC1, and sgNPC2 cells expressing the indicated NPC2-FLAG cDNA. Cells were depleted of sterols using methyl-ß-cyclodextrin (MCD, 0.75% w/v) for 2h, followed by re-feeding for 2h with 50μM cholesterol in complex with 0.1% MCD, or human LDL, as indicated.

Unfortunately, a more detailed investigation of the mechanism of NPC2 function was hampered for technical reasons involving the creation of reconstituted NPC2 mutant cell lines. As we did with NPC1, we attempted to create a panel of NPC2 mutants known to disrupt cholesterol binding (P120S), transfer (V81D) (Infante et al., 2008b; Wang et al., 2010), or suspected to be involved in binding to NPC1 (K123A and Q146A) (Li et al., 2016). Phenotypically however, these mutants did not behave as expected – all mutants appeared to support cholesterol export from the lysosome as judged by filipin staining or mCherry-D4H* labeling (Figure 3.3A-3.3B). This appeared not to be a technical issue related to the staining because all NPC2 mutants tested also appeared to restore sensitivity of mTORC1 to changes in cellular cholesterol as well (Figure 3.3C). These results are difficult to reconcile with published findings demonstrating that some of these NPC2 mutations are unable to rescue lysosomal cholesterol export, especially given that both the V81D and P120S mutants were first identified in patients with NPC disease (Infante et al., 2008b; Wang et al., 2010). It is possible that the observed phenotypes are an artifact caused by the overexpression of NPC2 that allow it to bind and mask cholesterol from dyes or cellular sensing machinery. Furthermore, we were unable to verify that overexpressed NPC2 was correctly targeted to the lysosomal lumen, so it remains a formal possibility that the mistargeting of these NPC2 isoforms is in some way responsible for the observed phenotypic incongruencies. Future studies that employ a gene-editing approach to knock-in these NPC2 mutations at the endogenous genomic locus would be useful in clarifying the mechanisms of NPC2-dependent cholesterol transport and regulation of mTORC1.

3.5 Methods

Details of all methods used in experiments described in this chapter are previously described in the methodology for Chapter 2. shRNAs targeting OSBP were previously described (Lim et al., 2019), and cDNA encoding human NPC2 was a kind gift of Dr. Ofer Moldavski.

References

Abu-Remaileh, M., Wyant, G.A., Kim, C., Laqtom, N.N., Abbasi, M., Chan, S.H., Freinkman, E., and Sabatini, D.M. (2017). Lysosomal metabolomics reveals V-ATPase- and mTOR-dependent regulation of amino acid efflux from lysosomes. Science (80-.). *358*, 807–813.

An, H., Ordureau, A., Paulo, J.A., Shoemaker, C.J., Denic, V., and Harper, J.W. (2019). TEX264 Is an Endoplasmic Reticulum-Resident ATG8-Interacting Protein Critical for ER Remodeling during Nutrient Stress. Mol. Cell *74*, 891-908.e10.

Anandapadamanaban, M., Masson, G.R., Perisic, O., Berndt, A., Kaufman, J., Johnson, C.M., Santhanam, B., Rogala, K.B., Sabatini, D.M., and Williams, R.L. (2019). Architecture of human Rag GTPase heterodimers and their complex with mTORC1. Science (80-.). *366*, 203–210.

Anding, A.L., and Baehrecke, E.H. (2017). Cleaning House: Selective Autophagy of Organelles. Dev. Cell *41*, 10–22.

De Araujo, M.E.G., Naschberger, A., Fürnrohr, B.G., Stasyk, T., Dunzendorfer-Matt, T., Lechner, S., Welti, S., Kremser, L., Shivalingaiah, G., Offterdinger, M., et al. (2017). Crystal structure of the human lysosomal mTORC1 scaffold complex and its impact on signaling. Science (80-.). *358*, 377–381.

Babalola, J.O., Wendeler, M., Breiden, B., Arenz, C., Schwarzmann, G., Locatelli-Hoops, S., and Sandhoff, K. (2007). Development of an assay for the intermembrane transfer of cholesterol by Niemann-Pick C2 protein. Biol. Chem. *388*, 617–626.

Ballabio, A., and Gieselmann, V. (2009). Lysosomal disorders: From storage to cellular damage. Biochim. Biophys. Acta - Mol. Cell Res. *1793*, 684–696.

Bar-Peled, L., Schweitzer, L.D., Zoncu, R., and Sabatini, D.M. (2012). Ragulator is a GEF for the rag GTPases that signal amino acid levels to mTORC1. Cell *150*, 1196–1208.

Bar-Peled, L., Chantranupong, L., Cherniack, A.D., Chen, W.W., Ottina, K. a, Grabiner, B.C., Spear, E.D., Carter, S.L., Meyerson, M., and Sabatini, D.M. (2013). A Tumor suppressor complex with GAP activity for the Rag GTPases that signal amino acid sufficiency to mTORC1. Science *340*, 1100–1106.

Behrends, C., Sowa, M.E., Gygi, S.P., and Harper, J.W. (2010). Network organization of the human autophagy system. Nature *466*, 68–76.

Ben-Sahra, I., Howell, J.J., Asara, J.M., and Manning, B.D. (2013). Stimulation of de Novo Pyrimidine Synthesis by Growth Signaling Through mTOR and S6K1. Science (80-.). *339*, 1323–1328.

Ben-Sahra, I., Hoxhaj, G., Ricoult, S.J.H., Asara, J.M., and Manning, B.D. (2016). mTORC1 induces purine synthesis through control of the mitochondrial tetrahydrofolate cycle. Science (80-.). *351*, 728–733.

Bentzinger, C.F., Romanino, K., Cloëtta, D., Lin, S., Mascarenhas, J.B., Oliveri, F., Xia, J., Casanova, E., Costa, C.F., Brink, M., et al. (2008). Skeletal Muscle-Specific Ablation of raptor, but Not of rictor, Causes Metabolic Changes and Results in Muscle Dystrophy. Cell Metab. *8*, 411–424.

Binda, M., Péli-Gulli, M.P., Bonfils, G., Panchaud, N., Urban, J., Sturgill, T.W., Loewith, R., and De Virgilio, C. (2009). The Vam6 GEF Controls TORC1 by Activating the EGO Complex. Mol. Cell *35*, 563–573.

Brunn, G.J., Hudson, C.C., Sekulić, A., Williams, J.M., Hosoi, H., Houghton, P.J., Lawrence, J.C., and Abraham, R.T. (1997). Phosphorylation of the translational repressor PHAS-I by the mammalian target of rapamycin. Science (80-.). *277*, 99–101.

Burgett, A.W.G., Poulsen, T.B., Wangkanont, K., Anderson, D.R., Kikuchi, C., Shimada, K., Okubo, S., Fortner, K.C., Mimaki, Y., Kuroda, M., et al. (2011). Natural products reveal cancer cell dependence on oxysterol-binding proteins. Nat. Chem. Biol. *7*, 639–647.

Calvo, S.E., Clauser, K.R., and Mootha, V.K. (2016). MitoCarta2.0: An updated inventory of mammalian mitochondrial proteins. Nucleic Acids Res. *44*, D1251–D1257.

Castellano, B.M., Thelen, A.M., Moldavski, O., Feltes, M., van der Welle, R.E.N., Mydock-McGrane, L., Jiang, X., van Eijkeren, R.J., Davis, O.B., Louie, S.M., et al. (2017). Lysosomal cholesterol activates mTORC1 via an SLC38A9–Niemann-Pick C1 signaling complex. Science (80-.). *355*, 1306–1311.

Chantranupong, L., Scaria, S.M., Saxton, R.A., Gygi, M.P., Shen, K., Wyant, G.A., Wang, T., Harper, J.W., Gygi, S.P., and Sabatini, D.M. (2016). The CASTOR Proteins Are Arginine Sensors for the mTORC1 Pathway. Cell 153–164.

Chapel, a., Kieffer-Jaquinod, S., Sagne, C., Verdon, Q., Ivaldi, C., Mellal, M., Thirion, J., Jadot, M., Bruley, C., Garin, J., et al. (2013). An Extended Proteome Map of the Lysosomal Membrane Reveals Novel Potential Transporters. Mol. Cell. Proteomics *12*, 1572–1588.

Chiaruttini, N., Redondo-Morata, L., Colom, A., Humbert, F., Lenz, M., Scheuring, S., and Roux, A. (2015). Relaxation of Loaded ESCRT-III Spiral Springs Drives Membrane Deformation. Cell *163*, 866–879.

Chu, B.B., Liao, Y.C., Qi, W., Xie, C., Du, X., Wang, J., Yang, H., Miao, H.H., Li, B.L., and Song, B.L. (2015). Cholesterol transport through lysosome-peroxisome membrane contacts. Cell *161*, 291–306.

Chung, C., Puthanveetil, P., Ory, D.S., and Lieberman, A.P. (2016). Genetic and pharmacological evidence implicates cathepsins in Niemann-Pick C cerebellar degeneration. Hum. Mol. Genet. *25*, 1434–1446.

Chung, C.Y.S., Shin, H.R., Berdan, C.A., Ford, B., Ward, C.C., Olzmann, J.A., Zoncu, R., and Nomura, D.K. (2019). Covalent targeting of the vacuolar H+-ATPase activates autophagy via mTORC1 inhibition. Nat. Chem. Biol. *15*, 776–785.

Csibi, A., Fendt, S.M., Li, C., Poulogiannis, G., Choo, A.Y., Chapski, D.J., Jeong, S.M., Dempsey, J.M., Parkhitko, A., Morrison, T., et al. (2013). The mTORC1 pathway stimulates glutamine metabolism and cell proliferation by repressing SIRT4. Cell *153*, 840–854.

Cuervo, A.M., and Dice, J.F. (1996). A receptor for the selective uptake and degradation of proteins by lysosomes. Science (80-.). *273*, 501–503.

Cunningham, J.T., Rodgers, J.T., Arlow, D.H., Vazquez, F., Mootha, V.K., and Puigserver, P. (2007). mTOR controls mitochondrial oxidative function through a YY1-PGC-1α transcriptional complex. Nature *450*, 736–740.

Dos D. Sarbassov, Ali, S.M., Kim, D.-H., Guertin, D.A., Latek, R.R., Erdjument-Bromage, H., Tempst, P., and Sabatini, D.M. (2004). Rictor, a Novel Binding Partner of mTOR, Defines a Rapamycin-Insensitive and Raptor-Independent Pathway that Regulates the Cytoskeleton. Curr. Biol. *14*, 1296–1302.

Danyukova, T., Ariunbat, K., Thelen, M., Brocke-Ahmadinejad, N., Mole, S.E., and Storch, S. (2018). Loss of CLN7 results in depletion of soluble lysosomal proteins and impaired mTOR reactivation. Hum. Mol. Genet. *27*, 1711–1722.

Davidson, S.M., and Vander Heiden, M.G. (2017). Critical Functions of the Lysosome in Cancer Biology. Annu. Rev. Pharmacol. Toxicol. *57*, 481–507.

Deffieu, M.S., and Pfeffer, S.R. (2011). Niemann – Pick type C 1 function requires lumenal domain residues that mediate cholesterol-dependent NPC2 binding. 18932–18936.

Derler, I., Jardin, I., Stathopulos, P.B., Muik, M., Fahrner, M., Zayats, V., Pandey, S.K., Poteser, M., Lackner, B., Absolonova, M., et al. (2016). Cholesterol modulates Orai1 channel function. Sci. Signal. *9*, 1–11.

Dikic, I., and Elazar, Z. (2018). Mechanism and medical implications of mammalian autophagy. Nat. Rev. Mol. Cell Biol. *19*, 349–364.

Doherty, G.J., and McMahon, H.T. (2009). Mechanisms of Endocytosis. Annu. Rev. Biochem. *78*, 857–902.

Dokudovskaya, S., Waharte, F., Schlessinger, A., Pieper, U., Devos, D.P., Cristea, I.M.,

Williams, R., Salamero, J., Chait, B.T., Sali, A., et al. (2011). A conserved coatomer-related complex containing Sec13 and Seh1 dynamically associates with the vacuole in Saccharomyces cerevisiae. Mol. Cell. Proteomics *10*, 1–17.

Dong, R., Saheki, Y., Swarup, S., Lucast, L., Harper, J.W., and De Camilli, P. (2016). Endosome-ER Contacts Control Actin Nucleation and Retromer Function through VAP-Dependent Regulation of PI4P. Cell *166*, 408–423.

Dowling, R.J.O., Topisirovic, I., Alain, T., Bidinosti, M., Fonseca, B.D., Petroulakis, E., Wang, X., Larsson, O., Selvaraj, A., Liu, Y., et al. (2010). mTORC1-Mediated Cell Proliferation, But Not Cell Growth, Controlled by the 4E-BPs. Science (80-.). *328*, 1172–1176.

Du, X., Kumar, J., Ferguson, C., Schulz, T.A., Ong, Y.S., Hong, W., Prinz, W.A., Parton, R.G., Brown, A.J., and Yang, H. (2011). A role for oxysterol-binding protein-related protein 5 in endosomal cholesterol trafficking. J. Cell Biol. *192*, 121–135.

de Duve, C. (2005). The lysosome turns fifty. Nat. Cell Biol. *7*, 847–849.

Düvel, K., Yecies, J.L., Menon, S., Raman, P., Lipovsky, A.I., Souza, A.L., Triantafellow, E., Ma, Q., Gorski, R., Cleaver, S., et al. (2010). Activation of a Metabolic Gene Regulatory Network Downstream of mTOR Complex 1. Mol. Cell *39*, 171–183.

Ebrahimi-Fakhari, D., Saffari, A., Wahlster, L., Di Nardo, A., Turner, D., Lewis, T.L., Conrad, C., Rothberg, J.M., Lipton, J.O., Kölker, S., et al. (2016). Impaired Mitochondrial Dynamics and Mitophagy in Neuronal Models of Tuberous Sclerosis Complex. Cell Rep. *17*, 1053–1070.

Efeyan, A., Zoncu, R., Chang, S., Gumper, I., Snitkin, H., Wolfson, R.L., Kirak, O., Sabatini, D.D., and Sabatini, D.M. (2013). Regulation of mTORC1 by the Rag GTPases is necessary for neonatal autophagy and survival. Nature *493*, 679–683.

Elrick, M.J., Yu, T., Chung, C., and Lieberman, A.P. (2012). Impaired proteolysis underlies autophagic dysfunction in Niemann-Pick type C disease. Hum. Mol. Genet. *21*, 4876–4887.

Emmanuel, N., Ragunathan, S., Shan, Q., Wang, F., Giannakou, A., Huser, N., Jin, G., Myers, J., Abraham, R.T., and Unsal-Kacmaz, K. (2017). Purine Nucleotide Availability Regulates mTORC1 Activity through the Rheb GTPase. Cell Rep. *19*, 2665–2680.

Eskelinen, E.-L., Schmidt, C.K., Neu, S., Willenborg, M., Fuertes, G., Salvador, N., Tanaka, Y., Lüllmann-Rauch, R., Hartmann, D., Heeren, J., et al. (2004). Disturbed Cholesterol Traffic but Normal Proteolytic Function in LAMP-1/LAMP-2 Double-deficient Fibroblasts. Mol. Biol. Cell *15*, 3132–3145.

Essner, E., and Novikoff, A.B. (1961). Activity of Acid By Means in Hepatic of Electron

Microscopy. *9*, 773–784.

Feltes, M., Gale, S.E., Moores, S., Ory, D.S., and Schaffer, J.E. (2020). Monitoring the itinerary of lysosomal cholesterol in Niemann-Pick Type C1-deficient cells after cyclodextrin treatment. J. Lipid Res. *61*, 403–412.

Feng, Y., He, D., Yao, Z., and Klionsky, D.J. (2014). The machinery of macroautophagy. Cell Res. *24*, 24–41.

Forgac, M. (2007). Vacuolar ATPases: Rotary proton pumps in physiology and pathophysiology. Nat. Rev. Mol. Cell Biol. *8*, 917–929.

Friedland, N., Liou, H.L., Lobel, P., and Stock, A.M. (2003). Structure of a cholesterol-binding protein deficient in Niemann-Pick type C2 disease. Proc. Natl. Acad. Sci. U. S. A. *100*, 2512–2517.

Gao, S., Casey, A.E., Sargeant, T.J., and Mäkinen, V.P. (2018). Genetic variation within endolysosomal system is associated with late-onset Alzheimer's disease. Brain *141*, 2711–2720.

Gao, Y., Zhou, Y., Goldstein, J.L., Brown, M.S., and Radhakrishnan, A. (2017). Cholesterol-induced conformational changes in the sterolsensing domain of the Scap protein suggest feedback mechanism to control cholesterol synthesis. J. Biol. Chem. *292*, 8729–8737.

Gatica, D., Lahiri, V., and Klionsky, D.J. (2018). Cargo recognition and degradation by selective autophagy. Nat. Cell Biol. *20*, 233–242.

Gegg, M.E., Cooper, J.M., Chau, K.Y., Rojo, M., Schapira, A.H.V., and Taanman, J.W. (2010). Mitofusin 1 and mitofusin 2 are ubiquitinated in a PINK1/parkin-dependent manner upon induction of mitophagy. Hum. Mol. Genet. *19*, 4861–4870.

Gingras, A., Gygi, S.P., Raught, B., Polakiewicz, R.D., Abraham, R.T., Hoekstra, M.F., Aebersold, R., and Sonenberg, N. (1999). Regulation of 4E-BP1 phosphorylation : a novel two-step mechanism. 1422–1437.

Goh, L.K., and Sorkin, A. (2013). Endocytosis of receptor tyrosine kinases. Cold Spring Harb. Perspect. Med. *3*, 1–18.

Goldstein, J.L., and Brown, M.S. (2015). Review A Century of Cholesterol and Coronaries : From Plaques to Genes to Statins. Cell *161*, 161–172.

Gong, X., Qian, H., and Zhou, X. (2016). Mediated Cholesterol Transfer and Ebola Infection Article Structural Insights into the Niemann-Pick. Cell *165*, 1467–1478.

Gu, X., Orozco, J.M., Saxton, R.A., Condon, K.J., Liu, G.Y., Krawczyk, P.A., Scaria, S.M., Wade Harper, J., Gygi, S.P., and Sabatini, D.M. (2017). SAMTOR is an S-

adenosylmethionine sensor for the mTORC1 pathway. Science (80-.). *358*, 813–818.

Hämälistö, S., Stahl, J.L., Favaro, E., Yang, Q., Liu, B., Christoffersen, L., Loos, B., Guasch Boldú, C., Joyce, J.A., Reinheckel, T., et al. (2020). Spatially and temporally defined lysosomal leakage facilitates mitotic chromosome segregation. Nat. Commun. *11*.

Hara, K., Yonezawa, K., Kozlowski, M.T., Sugimoto, T., Andrabi, K., Weng, Q.P., Kasuga, M., Nishimoto, I., and Avruch, J. (1997). Regulation of eIF-4E BP1 phosphorylation by mTOR. J. Biol. Chem. *272*, 26457–26463.

Hara, K., Yonezawa, K., Weng, Q.P., Kozlowski, M.T., Belham, C., and Avruch, J. (1998). Amino acid sufficiency and mTOR regulate p70 S6 kinase and eIF-4E BP1 through a common effector mechanism. J. Biol. Chem. *273*, 14484–14494.

Hara, T., Nakamura, K., Matsui, M., Yamamoto, A., Nakahara, Y., Suzuki-Migishima, R., Yokoyama, M., Mishima, K., Saito, I., Okano, H., et al. (2006). Suppression of basal autophagy in neural cells causes neurodegenerative disease in mice. Nature *441*, 885–889.

Harayama, T., and Riezman, H. (2018). Understanding the diversity of membrane lipid composition. Nat. Rev. Mol. Cell Biol. *19*, 281–296.

He, C., and Klionsky, D.J. (2009). Regulation Mechanisms and Signaling Pathways of Autophagy. Annu. Rev. Genet. *43*, 67–93.

He, L., Gomes, A.P., Wang, X., Yoon, S.O., Lee, G., Nagiec, M.J., Cho, S., Chavez, A., Islam, T., Yu, Y., et al. (2018). mTORC1 Promotes Metabolic Reprogramming by the Suppression of GSK3-Dependent Foxk1 Phosphorylation. Mol. Cell *70*, 949-960.e4.

Heitman, J., Movva, N., and Hall, M. (1991). Targets for cell cycle arrest by the immunosuppressant rapamycin in yeast. Science (80-.). *253*, 905–909.

Heybrock, S., Kanerva, K., Meng, Y., Ing, C., Liang, A., Xiong, Z.J., Weng, X., Ah Kim, Y., Collins, R., Trimble, W., et al. (2019). Lysosomal integral membrane protein-2 (LIMP-2/SCARB2) is involved in lysosomal cholesterol export. Nat. Commun. *10*.

Höglinger, D., Burgoyne, T., Sanchez-Heras, E., Hartwig, P., Colaco, A., Newton, J., Futter, C.E., Spiegel, S., Platt, F.M., and Eden, E.R. (2019). NPC1 regulates ER contacts with endocytic organelles to mediate cholesterol egress. Nat. Commun. *10*, 1–14.

Hosokawa, N., Hara, T., Kaizuka, T., Kishi, C., Takamura, A., Miura, Y., Iemura, S., Natsume, T., Takehana, K., Yamada, N., et al. (2009). Nutrient-dependent mTORC1 association with the ULK1-Atg13-FIP200 complex required for autophagy. Mol. Biol. Cell *20*, 1981–1991.

Hoxhaj, G., Hughes-Hallett, J., Timson, R.C., Ilagan, E., Yuan, M., Asara, J.M., Ben-Sahra, I., and Manning, B.D. (2017). The mTORC1 Signaling Network Senses Changes in Cellular Purine Nucleotide Levels. Cell Rep. *21*, 1331–1346.

Hulce, J.J., Cognetta, A.B., Niphakis, M.J., Tully, S.E., and Cravatt, B.F. (2013). Proteome-wide mapping of cholesterol-interacting proteins in mammalian cells. Nat. Methods *10*, 259–264.

Hurley, J.H., and Schulman, B.A. (2014). Atomistic autophagy: The structures of cellular self-digestion. Cell *157*, 300–311.

Ikonen, E. (2008). Cellular cholesterol trafficking and compartmentalization. Nat. Rev. Mol. Cell Biol. *9*, 125–138.

Infante, R.E., and Radhakrishnan, A. (2017). Continuous transport of a small fraction of plasma membrane cholesterol to endoplasmic reticulum regulates total cellular cholesterol. Elife *6*, 1–23.

Infante, R.E., Radhakrishnan, A., Abi-Mosleh, L., Kinch, L.N., Wang, M.L., Grishin, N. V., Goldstein, J.L., and Brown, M.S. (2008a). Purified NPC1 protein II. Localization of sterol binding to a 240-amino acid soluble luminal loop. J. Biol. Chem. *283*, 1064–1075.

Infante, R.E., Wang, M.L., Radhakrishnan, A., Kwon, H.J., Brown, M.S., and Goldstein, J.L. (2008b). NPC2 facilitates bidirectional transfer of cholesterol between NPC1 and lipid bilayers, a step in cholesterol egress from lysosomes. Proc. Natl. Acad. Sci. *105*, 15287–15292.

Inoki, K., Li, Y., Zhu, T., Wu, J., and Guan, K.L. (2002). TSC2 is phosphorylated and inhibited by Akt and suppresses mTOR signalling. Nat. Cell Biol. *4*, 648–657.

Inoki, K., Li, Y., Xu, T., and Guan, K.L. (2003a). Rheb GTpase is a direct target of TSC2 GAP activity and regulates mTOR signaling. Genes Dev. *17*, 1829–1834.

Inoki, K., Zhu, T., and Guan, K.-L. (2003b). TSC2 mediates cellular energy response to control cell growth and survival. Cell *115*, 577–590.

Inoki, K., Ouyang, H., Zhu, T., Lindvall, C., Wang, Y., Zhang, X., Yang, Q., Bennett, C., Harada, Y., Stankunas, K., et al. (2006). TSC2 Integrates Wnt and Energy Signals via a Coordinated Phosphorylation by AMPK and GSK3 to Regulate Cell Growth. Cell *126*, 955–968.

Israel, M.A., Yuan, S.H., Bardy, C., Reyna, S.M., Mu, Y., Herrera, C., Hefferan, M.P., Van Gorp, S., Nazor, K.L., Boscolo, F.S., et al. (2012). Probing sporadic and familial Alzheimer's disease using induced pluripotent stem cells. Nature *482*, 216–220.

Jeźégou, A., Llinares, E., Anne, C., Kieffer-Jaquinod, S., O'Regan, S., Aupetit, J.,

Chabli, A., Sagné, C., Debacker, C., Chadefaux-Vekemans, B., et al. (2012). Heptahelical protein PQLC2 is a lysosomal cationic amino acid exporter underlying the action of cysteamine in cystinosis therapy. Proc. Natl. Acad. Sci. U. S. A. *109*.

Jia, J., Claude-Taupin, A., Gu, Y., Choi, S.W., Peters, R., Bissa, B., Mudd, M.H., Allers, L., Pallikkuth, S., Lidke, K.A., et al. (2020). Galectin-3 Coordinates a Cellular System for Lysosomal Repair and Removal. Dev. Cell *52*, 69-87.e8.

Jung, J., Genau, H.M., and Behrends, C. (2015). Amino Acid-Dependent mTORC1 Regulation by the Lysosomal Membrane Protein SLC38A9. Mol. Cell. Biol. *35*, 2479–2494.

Kalatzis, V., Cherqui, S., Antignac, C., and Gasnier, B. (2001). Cystinosin, the protein defective in cystinosis, is a H+-driven lysosomal cystine transporter. EMBO J. *20*, 5940–5949.

Kalender, A., Selvaraj, A., Kim, S.Y., Gulati, P., Brûlé, S., Viollet, B., Kemp, B.E., Bardeesy, N., Dennis, P., Schlager, J.J., et al. (2010). Metformin, independent of AMPK, inhibits mTORC1 in a rag GTPase-dependent manner. Cell Metab. *11*, 390–401.

Kaushik, S., and Cuervo, A.M. (2018). The coming of age of chaperone-mediated autophagy. Nat. Rev. Mol. Cell Biol. *19*, 365–381.

Kennedy, B.E., Madreiter, C.T., Vishnu, N., Malli, R., Graier, W.F., and Karten, B. (2014). Adaptations of energy metabolism associated with increased levels of mitochondrial cholesterol in Niemann-Pick type C1-deficient cells. J. Biol. Chem. *289*, 16278–16289.

Khaminets, A., Heinrich, T., Mari, M., Grumati, P., Huebner, A.K., Akutsu, M., Liebmann, L., Stolz, A., Nietzsche, S., Koch, N., et al. (2015). Regulation of endoplasmic reticulum turnover by selective autophagy. Nature *522*, 354–358.

Khaminets, A., Behl, C., and Dikic, I. (2016). Ubiquitin-Dependent And Independent Signals In Selective Autophagy. Trends Cell Biol. *26*, 6–16.

Kim, D.H., Sarbassov, D.D., Ali, S.M., King, J.E., Latek, R.R., Erdjument-Bromage, H., Tempst, P., and Sabatini, D.M. (2002). mTOR interacts with raptor to form a nutrient-sensitive complex that signals to the cell growth machinery. Cell *110*, 163–175.

Kim, E., Goraksha-Hicks, P., Li, L., Neufeld, T.P., and Guan, K.L. (2008a). Regulation of TORC1 by Rag GTPases in nutrient response. Nat. Cell Biol. *10*, 935–945.

Kim, J., Kundu, M., Viollet, B., and Guan, K.L. (2011). AMPK and mTOR regulate autophagy through direct phosphorylation of Ulk1. Nat. Cell Biol. *13*, 132–141.

Kim, P.K., Hailey, D.W., Mullen, R.T., and Lippincott-Schwartz, J. (2008b). Ubiquitin

signals autophagic degradation of cytosolic proteins and peroxisomes. Proc. Natl. Acad. Sci. U. S. A. *105*, 20567–20574.

Kim, Y.M., Jung, C.H., Seo, M., Kim, E.K., Park, J.M., Bae, S.S., and Kim, D.H. (2015). MTORC1 phosphorylates UVRAG to negatively regulate autophagosome and endosome maturation. Mol. Cell *57*, 207–218.

Kirkin, V., Lamark, T., Sou, Y.S., Bjørkøy, G., Nunn, J.L., Bruun, J.A., Shvets, E., McEwan, D.G., Clausen, T.H., Wild, P., et al. (2009). A Role for NBR1 in Autophagosomal Degradation of Ubiquitinated Substrates. Mol. Cell *33*, 505–516.

Kitada, T., Asakawa, S., Hattori, N., Matsumine, H., Yamamura, Y., Minoshima, S., Yokochi, M., Mizuno, Y., and Shimizu, N. (1998). Mutations in the parkin gene cause autosomal recessive juvenile parkinsonism. Nature *392*, 605–608.

Kobayashi, T., Beuchat, M.H., Lindsay, M., Frias, S., Palmiter, R.D., Sakuraba, H., Parton, R.G., and Gruenberg, J. (1999). Late endosomal membranes rich in lysobisphosphatidic acid regulate cholesterol transport. Nat. Cell Biol. *1*, 113–118.

Komatsu, M., Waguri, S., Chiba, T., Murata, S., Iwata, J.I., Tanida, I., Ueno, T., Koike, M., Uchiyama, Y., Kominami, E., et al. (2006). Loss of autophagy in the central nervous system causes neurodegeneration in mice. Nature *441*, 880–884.

Komatsu, M., Waguri, S., Koike, M., Sou, Y. shin, Ueno, T., Hara, T., Mizushima, N., Iwata, J. ichi, Ezaki, J., Murata, S., et al. (2007). Homeostatic Levels of p62 Control Cytoplasmic Inclusion Body Formation in Autophagy-Deficient Mice. Cell *131*, 1149–1163.

Kuo, C.J., Chung, J., Fiorentino, D.F., Flanagan, W.M., Blenis, J., and Crabtree, G.R. (1992). Rapamycin selectively inhibits interleukin-2 activation of p70 S6 kinase. Nature *358*, 70–73.

Kwon, H.J., Abi-Mosleh, L., Wang, M.L., Deisenhofer, J., Goldstein, J.L., Brown, M.S., and Infante, R.E. (2009). Structure of N-Terminal Domain of NPC1 Reveals Distinct Subdomains for Binding and Transfer of Cholesterol. Cell *137*, 1213–1224.

Lamming, D.W., Ye, L., Katajisto, P., Goncalves, M.D., Saitoh, M., Stevens, D.M., Davis, J.G., Salmon, A.B., Richardson, A., Ahima, R.S., et al. (2012). Rapamycin-Induced Insulin Resistance Is Mediated by mTORC2 Loss and Uncoupled from Longevity. Science (80-.). *335*, 1638–1643.

Lawrence, R.E., and Zoncu, R. (2019). The lysosome as a cellular centre for signalling, metabolism and quality control. Nat. Cell Biol. *21*, 133–142.

Lawrence, R.E., Cho, K.F., Rappold, R., Thrun, A., Tofaute, M., Kim, D.J., Moldavski, O., Hurley, J.H., and Zoncu, R. (2018). A nutrient-induced affinity switch controls

mTORC1 activation by its Rag GTPase–Ragulator lysosomal scaffold. Nat. Cell Biol. *20*, 1052–1063.

Lazarou, M., Sliter, D.A., Kane, L.A., Sarraf, S.A., Wang, C., Burman, J.L., Sideris, D.P., Fogel, A.I., and Youle, R.J. (2015). The ubiquitin kinase PINK1 recruits autophagy receptors to induce mitophagy. Nature *524*, 309–314.

Li, J., and Pfeffer, S.R. (2016). Lysosomal membrane glycoproteins bind cholesterol and contribute to lysosomal cholesterol export. Elife *5*, 1–16.

Li, S.C., and Kane, P.M. (2009). The yeast lysosome-like vacuole: Endpoint and crossroads. Biochim. Biophys. Acta - Mol. Cell Res. *1793*, 650–663.

Li, S., Brown, M.S., and Goldstein, J.L. (2010). Bifurcation of insulin signaling pathway in rat liver: mTORC1 required for stimulation of lipogenesis, but not inhibition of gluconeogenesis. Proc. Natl. Acad. Sci. *107*, 3441–3446.

Li, X., Saha, P., Li, J., Blobel, G., and Pfeffer, S.R. (2016). Clues to the mechanism of cholesterol transfer from the structure of NPC1 middle lumenal domain bound to NPC2. Proc. Natl. Acad. Sci. *113*, 10079–10084.

Lim, C.Y., Davis, O.B., Shin, H.R., Zhang, J., Berdan, C.A., Jiang, X., Counihan, J.L., Ory, D.S., Nomura, D.K., and Zoncu, R. (2019). ER–lysosome contacts enable cholesterol sensing by mTORC1 and drive aberrant growth signalling in Niemann–Pick type C. Nat. Cell Biol. *21*, 1206–1218.

Liu, G.Y., and Sabatini, D.M. (2020). mTOR at the nexus of nutrition, growth, ageing and disease. Nat. Rev. Mol. Cell Biol. *21*, 183–203.

Liu, B., Du, H., Rutkowski, R., Gartner, A., and Wang, X. (2012). LAAT-1 Is the Lysosomal Lysine/Arginine Transporter That Maintains Amino Acid Homeostasis. Science (80-.). *337*, 351–354.

Loewith, R., Jacinto, E., Wullschleger, S., Lorberg, A., Crespo, J.L., Bonenfant, D., Oppliger, W., Jenoe, P., and Hall, M.N. (2002). Two TOR complexes, only one of which is rapamycin sensitive, have distinct roles in cell growth control. Mol. Cell *10*, 457–468.

Long, T., Qi, X., Hassan, A., Liang, Q., De Brabander, J.K., and Li, X. (2020). Structural basis for itraconazole-mediated NPC1 inhibition. Nat. Commun. *11*, 1–11.

Long, X., Lin, Y., Ortiz-Vega, S., Yonezawa, K., and Avruch, J. (2005). Rheb binds and regulates the mTOR kinase. Curr. Biol. *15*, 702–713.

Lu, F., Liang, Q., Abi-Mosleh, L., Das, A., de Brabander, J.K., Goldstein, J.L., and Brown, M.S. (2015). Identification of NPC1 as the target of U18666A, an inhibitor of lysosomal cholesterol export and Ebola infection. Elife *4*, 1–16.

Luzio, J.P., Pryor, P.R., and Bright, N.A. (2007). Lysosomes: Fusion and function. Nat. Rev. Mol. Cell Biol. *8*, 622–632.

Luzio, J.P., Parkinson, M.D.J., Gray, S.R., and Bright, N.A. (2009). The delivery of endocytosed cargo to lysosomes. Biochem. Soc. Trans. *37*, 1019–1021.

Ma, L., Chen, Z., Erdjument-Bromage, H., Tempst, P., and Pandolfi, P.P. (2005). Phosphorylation and functional inactivation of TSC2 by Erk: Implications for tuberous sclerosis and cancer pathogenesis. Cell *121*, 179–193.

Maejima, I., Takahashi, A., Omori, H., Kimura, T., Takabatake, Y., Saitoh, T., Yamamoto, A., Hamasaki, M., Noda, T., Isaka, Y., et al. (2013). Autophagy sequesters damaged lysosomes to control lysosomal biogenesis and kidney injury. EMBO J. *32*, 2336–2347.

Maekawa, M., and Fairn, G.D. (2015). Complementary probes reveal that phosphatidylserine is required for the proper transbilayer distribution of cholesterol. J. Cell Sci. *128*, 1422–1433.

Mahoney, S.J., Narayan, S., Molz, L., Berstler, L.A., Kang, S.A., Vlasuk, G.P., and Saiah, E. (2018). A small molecule inhibitor of Rheb selectively targets mTORC1 signaling. Nat. Commun. *9*, 1–12.

Mancias, J.D., Wang, X., Gygi, S.P., Harper, J.W., and Kimmelman, A.C. (2014). Quantitative proteomics identifies NCOA4 as the cargo receptor mediating ferritinophagy. Nature *508*, 105–109.

Manning, B.D., Tee, A.R., Logsdon, M.N., Blenis, J., and Cantley, L.C. (2002). Identification of the tuberous sclerosis complex-2 tumor suppressor gene product tuberin as a target of the phosphoinositide 3-kinase/Akt pathway. Mol. Cell *10*, 151–162.

Marshall, R.S., Hua, Z., Mali, S., McLoughlin, F., and Vierstra, R.D. (2019). ATG8-Binding UIM Proteins Define a New Class of Autophagy Adaptors and Receptors. Cell *177*, 766-781.e24.

Martina, J.A., Chen, Y., Gucek, M., and Puertollano, R. (2012). MTORC1 functions as a transcriptional regulator of autophagy by preventing nuclear transport of TFEB. Autophagy *8*, 903–914.

Meng, Y., Heybrock, S., Neculai, D., and Saftig, P. (2020). Cholesterol Handling in Lysosomes and Beyond. Trends Cell Biol. *30*, 452–466.

Menon, S., Dibble, C.C., Talbott, G., Hoxhaj, G., Valvezan, A.J., Takahashi, H., Cantley, L.C., and Manning, B.D. (2014). Spatial control of the TSC complex integrates insulin and nutrient regulation of mtorc1 at the lysosome. Cell *156*, 1771–1785.

Menzies, F.M., Fleming, A., Caricasole, A., Bento, C.F., Andrews, S.P., Ashkenazi, A., Füllgrabe, J., Jackson, A., Jimenez Sanchez, M., Karabiyik, C., et al. (2017). Autophagy and Neurodegeneration: Pathogenic Mechanisms and Therapeutic Opportunities. Neuron *93*, 1015–1034.

Mesmin, B., Bigay, J., Moser Von Filseck, J., Lacas-Gervais, S., Drin, G., and Antonny, B. (2013). A four-step cycle driven by PI(4)P hydrolysis directs sterol/PI(4)P exchange by the ER-Golgi Tether OSBP. Cell *155*.

Mesmin, B., Bigay, J., Polidori, J., Jamecna, D., Lacas-Gervais, S., and Antonny, B. (2017). Sterol transfer, PI 4P consumption, and control of membrane lipid order by endogenous OSBP . EMBO J. *36*, 3156–3174.

Millard, E.E., Gale, S.E., Dudley, N., Zhang, J., Schaffer, J.E., and Ory, D.S. (2005). The sterol-sensing domain of the Niemann-Pick C1 (NPC1) protein regulates trafficking of low density lipoprotein cholesterol. J. Biol. Chem. *280*, 28581–28590.

Mindell, J.A. (2012). Lysosomal Acidification Mechanisms. Annu. Rev. Physiol. *74*, 69–86.

Morita, M., Gravel, S.P., Chénard, V., Sikström, K., Zheng, L., Alain, T., Gandin, V., Avizonis, D., Arguello, M., Zakaria, C., et al. (2013). MTORC1 controls mitochondrial activity and biogenesis through 4E-BP-dependent translational regulation. Cell Metab. *18*, 698–711.

Morita, M., Prudent, J., Basu, K., Goyon, V., Katsumura, S., Hulea, L., Pearl, D., Siddiqui, N., Strack, S., McGuirk, S., et al. (2017). mTOR Controls Mitochondrial Dynamics and Cell Survival via MTFP1. Mol. Cell *67*, 922-935.e5.

Naureckiene, S., Sleat, D.E., Lacklan, H., Fensom, A., Vanier, M.T., Wattiaux, R., Jadot, M., and Lobel, P. (2000). Identification of HE1 as the second gene of Niemann-Pick C disease. Science (80-.). *290*, 2298–2301.

Nguyen, H.C., Talledge, N., McCullough, J., Sharma, A., Moss, F.R., Iwasa, J.H., Vershinin, M.D., Sundquist, W.I., and Frost, A. (2020). Membrane constriction and thinning by sequential ESCRT-III polymerization. Nat. Struct. Mol. Biol. *27*, 392–399.

Nicastro, R., Sardu, A., Panchaud, N., and De Virgilio, C. (2017). The architecture of the Rag GTPase signaling network. Biomolecules *7*, 1–21.

Noda, N.N., Kumeta, H., Nakatogawa, H., Satoo, K., Adachi, W., Ishii, J., Fujioka, Y., Ohsumi, Y., and Inagaki, F. (2008). Structural basis of target recognition by Atg8/LC3 during selective autophagy. Genes to Cells *13*, 1211–1218.

Ohgami, N., Kot, D.C., Thomas, M., Scott, M.P., Chang, C.C.Y., and Chang, T.Y. (2004). Binding between the Niemann-Pick C1 protein and a photoactiviatable

cholesterol analog requires a functional sterol-sensing domain. Proc. Natl. Acad. Sci. U. S. A. *101*, 12473–12478.

Ohgane, K., Karaki, F., Dodo, K., and Hashimoto, Y. (2013). Discovery of oxysterol-derived pharmacological chaperones for NPC1: Implication for the existence of second sterol-binding site. Chem. Biol. *20*, 391–402.

Ordonez, M.P. (2012). Defective mitophagy in human Niemann-Pick type C1 neurons is due to abnormal autophagy activation. Autophagy *8*, 1157–1158.

Ordonez, M.P., Roberts, E.A., Kidwell, C.U., Yuan, S.H., Plaisted, W.C., and Goldstein, L.S.B. (2012). Disruption and therapeutic rescue of autophagy in a human neuronal model of Niemann Pick type C1. Hum. Mol. Genet. *21*, 2651–2662.

Orozco, J.M., Krawczyk, P.A., Scaria, S.M., Cangelosi, A.L., Chan, S.H., Kunchok, T., Lewis, C.A., and Sabatini, D.M. (2020). Dihydroxyacetone phosphate signals glucose availability to mTORC1. Nat. Metab.

Palmieri, M., Impey, S., Kang, H., di Ronza, A., Pelz, C., Sardiello, M., and Ballabio, A. (2011). Characterization of the CLEAR network reveals an integrated control of cellular clearance pathways. Hum. Mol. Genet. *20*, 3852–3866.

Panchaud, N., Péli-Gulli, M.P., and De Virgilio, C. (2013). Amino acid deprivation inhibits TORC1 through a GTPase-activating protein complex for the Rag family GTPase Gtr1. Sci. Signal. *6*, 1–7.

Pankiv, S., Clausen, T.H., Lamark, T., Brech, A., Bruun, J.A., Outzen, H., Øvervatn, A., Bjørkøy, G., and Johansen, T. (2007). p62/SQSTM1 binds directly to Atg8/LC3 to facilitate degradation of ubiquitinated protein aggregates by autophagy*[S]. J. Biol. Chem. *282*, 24131–24145.

Patterson, M.C., and Walkley, S.U. (2017). Niemann-Pick disease, type C and Roscoe Brady. Mol. Genet. Metab. *120*, 34–37.

Paz, I., Sachse, M., Dupont, N., Mounier, J., Cederfur, C., Enninga, J., Leffler, H., Poirier, F., Prevost, M.C., Lafont, F., et al. (2010). Galectin-3, a marker for vacuole lysis by invasive pathogens. Cell. Microbiol. *12*, 530–544.

Peake, K.B., and Vance, J.E. (2010). Defective cholesterol trafficking in Niemann-Pick C-deficient cells. FEBS Lett. *584*, 2731–2739.

Péli-Gulli, M.-P., Sardu, A., Panchaud, N., Raucci, S., and De Virgilio, C. (2015). Amino Acids Stimulate TORC1 through Lst4-Lst7, a GTPase-Activating Protein Complex for the Rag Family GTPase Gtr2. Cell Rep. 1–7.

Perera, R.M., and Bardeesy, N. (2015). Pancreatic cancer metabolism: Breaking it down to build it back up. Cancer Discov. *5*, 1247–1261.

Perera, R.M., and Zoncu, R. (2016). The Lysosome as a Regulatory Hub. Annu. Rev. Cell Dev. Biol. *32*, 223–253.

Peterson, T.R., Sengupta, S.S., Harris, T.E., Carmack, A.E., Kang, S.A., Balderas, E., Guertin, D.A., Madden, K.L., Carpenter, A.E., Finck, B.N., et al. (2011). mTOR Complex 1 Regulates Lipin 1 Localization to Control the SREBP Pathway. Cell *146*, 408–420.

Petit, C.S., Roczniak-Ferguson, a., and Ferguson, S.M. (2013). Recruitment of folliculin to lysosomes supports the amino acid-dependent activation of Rag GTPases. J. Cell Biol. *202*, 1107–1122.

Pfeffer, S.R. (2019). NPC intracellular cholesterol transporter 1 (NPC1)-mediated cholesterol export from lysosomes. J. Biol. Chem. *294*, 1706–1709.

Platt, F.M. (2018). Emptying the stores: Lysosomal diseases and therapeutic strategies. Nat. Rev. Drug Discov. *17*, 133–150.

Platt, F.M., d'Azzo, A., Davidson, B.L., Neufeld, E.F., and Tifft, C.J. (2018). Lysosomal storage diseases. Nat. Rev. Dis. Prim. *4*.

Porstmann, T., Santos, C.R., Griffiths, B., Cully, M., Wu, M., Leevers, S., Griffiths, J.R., Chung, Y.-L., and Schulze, A. (2008). SREBP Activity Is Regulated by mTORC1 and Contributes to Akt-Dependent Cell Growth. Cell Metab. *8*, 224–236.

Price, D., Grove, Calvo, V., Avruch, J., and Bierer, B. (1992). Rapamycin-induced inhibition of the 70-kilodalton S6 protein kinase. Science (80-.). *257*, 973–977.

Pu, J., Schindler, C., Jia, R., Jarnik, M., Backlund, P., and Bonifacino, J.S. (2015). BORC, a Multisubunit Complex that Regulates Lysosome Positioning. Dev. Cell *33*, 176–188.

Puente, C., Hendrickson, R.C., and Jiang, X. (2016). Nutrient-regulated phosphorylation of ATG13 inhibits starvation-induced autophagy. J. Biol. Chem. *291*, 6026–6035.

Qian, H., Wu, X., Du, X., Yao, X., Zhao, X., Lee, J., Yang, H., and Yan, N. (2020). Structural Basis of Low-pH-Dependent Lysosomal Cholesterol Egress by NPC1 and NPC2. Cell *182*, 98-111.e18.

Radulovic, M., Schink, K.O., Wenzel, E.M., Nähse, V., Bongiovanni, A., Lafont, F., and Stenmark, H. (2018). ESCRT -mediated lysosome repair precedes lysophagy and promotes cell survival . EMBO J. *37*, 1–15.

Rebsamen, M., Pochini, L., Stasyk, T., de Araújo, M.E.G., Galluccio, M., Kandasamy, R.K., Snijder, B., Fauster, A., Rudashevskaya, E.L., Bruckner, M., et al. (2015). SLC38A9 is a component of the lysosomal amino acid sensing machinery that controls mTORC1. Nature *519*, 477–481.

Repnik, U., Česen, M.H., and Turk, B. (2016). The use of lysosomotropic dyes to exclude lysosomal membrane permeabilization. Cold Spring Harb. Protoc. *2016*, 447–452.

Riboldi, G.M., and Di Fonzo, A.B. (2019). GBA, Gaucher Disease, and Parkinson's Disease: From Genetic to Clinic to New Therapeutic Approaches. Cells *8*, 364.

Riggi, M., Bourgoint, C., Macchione, M., Matile, S., Loewith, R., and Roux, A. (2019). TORC2 controls endocytosis through plasma membrane tension. J. Cell Biol. *218*, 2265–2276.

Rispal, D., Eltschinger, S., Stahl, M., Vaga, S., Bodenmiller, B., Abraham, Y., Filipuzzi, I., Movva, N.R., Aebersold, R., Helliwell, S.B., et al. (2015). Target of rapamycin complex 2 regulates actin polarization and endocytosis via multiple pathways. J. Biol. Chem. *290*, 14963–14978.

Robak, L.A., Jansen, I.E., Rooij, J. van, Uitterlinden, A.G., Kraaij, R., Jankovic, J., Heutink, P., Shulman, J.M., Nalls, M.A., Plagnol, V., et al. (2017). Excessive burden of lysosomal storage disorder gene variants in Parkinson's disease. Brain *140*, 3191–3203.

Robitaille, A.M., Christen, S., Shimobayashi, M., Cornu, M., Fava, L.L., Moes, S., Prescianotto-Baschong, C., Sauer, U., Jenoe, P., and Hall, M.N. (2013). Quantitative Phosphoproteomics Reveal mTORC1 Activates de Novo Pyrimidine Synthesis. Science (80-.). *339*, 1320–1323.

Rocha, N., Kuijl, C., Van Der Kant, R., Janssen, L., Houben, D., Janssen, H., Zwart, W., and Neefjes, J. (2009). Cholesterol sensor ORP1L contacts the ER protein VAP to control Rab7-RILP-p150Glued and late endosome positioning. J. Cell Biol. *185*, 1209–1225.

Roczniak-Ferguson, A., Petit, C.S., Froehlich, F., Qian, S., Ky, J., Angarola, B., Walther, T.C., and Ferguson, S.M. (2012). The transcription factor TFEB links mTORC1 signaling to transcriptional control of lysosome homeostasis. Sci. Signal. *5*, ra42.

Rodrik-Outmezguine, V.S., Okaniwa, M., Yao, Z., Novotny, C.J., McWhirter, C., Banaji, A., Won, H., Wong, W., Berger, M., de Stanchina, E., et al. (2016). Overcoming mTOR resistance mutations with a new-generation mTOR inhibitor. Nature *534*, 272–276.

Roelants, F.M., Breslow, D.K., Muir, A., Weissman, J.S., and Thorner, J. (2011). Protein kinase Ypk1 phosphorylates regulatory proteins Orm1 and Orm2 to control sphingolipid homeostasis in Saccharomyces cerevisiae. Proc. Natl. Acad. Sci. U. S. A. *108*, 19222–19227.

Rogala, K.B., Gu, X., Kedir, J.F., Abu-Remaileh, M., Bianchi1, L.F., Bottino1, A.M.S., Dueholm1, R., Niehaus1, A., Overwijn1, D., Priso Fils1, A.C., et al. (2019). Structural

basis for the docking of mTORC1 on the lysosomal surface. Science (80-.). *366*, 468–475.

Rong, Y., McPhee, C., Denga, S., Huanga, L., Chen, L., Liu, M., Tracy, K., Baehreck, E.H., Yu, L., and Lenardo, M.J. (2011). Spinster is required for autophagic lysosome reformation and mTOR reactivation following starvation. Proc. Natl. Acad. Sci. U. S. A. *108*, 7826–7831.

Russnak, R., Konczal, D., and McIntire, S.L. (2001). A Family of Yeast Proteins Mediating Bidirectional Vacuolar Amino Acid Transport. J. Biol. Chem. *276*, 23849–23857.

Sabatini, D.M., Erdjument-Bromage, H., Lui, M., Tempst, P., and Snyder, S.H. (1994). RAFT1: A mammalian protein that binds to FKBP12 in a rapamycin-dependent fashion and is homologous to yeast TORs. Cell *78*, 35–43.

Saftig, P., and Klumperman, J. (2009). Lysosome biogenesis and lysosomal membrane proteins: Trafficking meets function. Nat. Rev. Mol. Cell Biol. *10*, 623–635.

Sagné, C., Agulhon, C., Ravassard, P., Darmon, M., Hamon, M., El Mestikawy, S., Gasnier, B., and Giros, B. (2001). Identification and characterization of a lysosomal transporter for small neutral amino acids. Proc. Natl. Acad. Sci. U. S. A. *98*, 7206–7211.

Sakamachi, Y., Morioka, S., Mihaly, S.R., Takaesu, G., Foley, J.F., Fessler, M.B., and Ninomiya-Tsuji, J. (2017). TAK1 regulates resident macrophages by protecting lysosomal integrity. Cell Death Dis. *8*, 1–11.

Sancak, Y., Peterson, T.R., Shaul, Y.D., Lindquist, R.A., Thoreen, C.C., Bar-Peled, L., and Sabatini, D.M. (2008). The Rag GTPases Bind Raptor and Mediate Amino Acid Signaling to mTORC1. Science (80-.). *320*, 1496–1501.

Sancak, Y., Bar-Peled, L., Zoncu, R., Markhard, A.L., Nada, S., and Sabatini, D.M. (2010). Ragulator-rag complex targets mTORC1 to the lysosomal surface and is necessary for its activation by amino acids. Cell *141*, 290–303.

Sarbassov, D.D., Guertin, D.A., Ali, S.M., and Sabatini, D.M. (2005). Phosphorylation and regulation of Akt/PKB by the rictor-mTOR complex. Science (80-.). *307*, 1098–1101.

Sardiello, M., Palmieri, M., di Ronza, A., Medina, D.L., Valenza, M., Gennarino, V.A., Di Malta, C., Donaudy, F., Embrione, V., Polishchuk, R.S., et al. (2009). A Gene Network Regulating Lysosomal Biogenesis and Function. Science (80-.). *53*, 1–30.

Sarkar, S., Carroll, B., Buganim, Y., Maetzel, D., Ng, A.H.M., Cassady, J.P., Cohen, M.A., Chakraborty, S., Wang, H., Spooner, E., et al. (2013). Impaired autophagy in the

lipid-storage disorder niemann-pick type c1 disease. Cell Rep. *5*, 1302–1315.

Saxton, R.A., and Sabatini, D.M. (2017). mTOR Signaling in Growth, Metabolism, and Disease. Cell *168*, 960–976.

Saxton, R.A., Knockenhauer, K.E., Wolfson, R.L., Chantranupong, L., Pacold, M.E., Wang, T., Schwartz, T.U., and Sabatini, D.M. (2016a). Structural basis for leucine sensing by the Sestrin2-mTORC1 pathway. Science (80-.). *351*, 53–58.

Saxton, R.A., Chantranupong, L., Knockenhauer, K.E., Schwartz, T.U., and Sabatini, D.M. (2016b). Mechanism of arginine sensing by CASTOR1 upstream of mTORC1. Nature *536*, 229–233.

Schedin, S., Sindelar, P.J., Pentchev, P., Brunk, U., and Dallner, G. (1997). Peroxisomal impairment in Niemann-Pick type C disease. J. Biol. Chem. *272*, 6245–6251.

Schneede, A., Schmidt, C.K., Hölttä-Vuori, M., Heeren, J., Willenborg, M., Blanz, J., Domanskyy, M., Breiden, B., Brodesser, S., Landgrebe, J., et al. (2011). Role for LAMP-2 in endosomal cholesterol transport. J. Cell. Mol. Med. *15*, 280–295.

Schöneberg, J., Lee, I.H., Iwasa, J.H., and Hurley, J.H. (2016). Reverse-topology membrane scission by the ESCRT proteins. Nat. Rev. Mol. Cell Biol. *18*, 5–17.

Schreiber, K.H., Arriola Apelo, S.I., Yu, D., Brinkman, J.A., Velarde, M.C., Syed, F.A., Liao, C.Y., Baar, E.L., Carbajal, K.A., Sherman, D.S., et al. (2019). A novel rapamycin analog is highly selective for mTORC1 in vivo. Nat. Commun. *10*, 1–12.

Schultz, M.L., Krus, K.L., Kaushik, S., Dang, D., Chopra, R., Qi, L., Shakkottai, V.G., Cuervo, A.M., and Lieberman, A.P. (2018). Coordinate regulation of mutant NPC1 degradation by selective ER autophagy and MARCH6-dependent ERAD. Nat. Commun. *9*.

Sekito, T., Fujiki, Y., Ohsumi, Y., and Kakinuma, Y. (2008). Novel families of vacuolar amino acid transporters. IUBMB Life *60*, 519–525.

Seranova, E., Connolly, K.J., Zatyka, M., Rosenstock, T.R., Barrett, T., Tuxworth, R.I., and Sarkar, S. (2017). Dysregulation of autophagy as a common mechanism in lysosomal storage diseases. Essays Biochem. *61*, 733–749.

Settembre, C., Fraldi, A., Jahreiss, L., Spampanato, C., Venturi, C., Medina, D., de Pablo, R., Tacchetti, C., Rubinsztein, D.C., and Ballabio, A. (2008a). A block of autophagy in lysosomal storage disorders. Hum. Mol. Genet. *17*, 119–129.

Settembre, C., Fraldi, A., Rubinsztein, D.C., and Ballabio, A. (2008b). Lysosomal storage diseases as disorders of autophagy. Autophagy *4*, 113–114.

Settembre, C., Di Malta, C., Polito, V.A., Arencibia, M.G., Vetrini, F., Erdin, S., Erdin,

S.U., Huynh, T., Medina, D., Colella, P., et al. (2011). TFEB Links Autophagy to Lysosomal Biogenesis. Science (80-.). *332*, 1429–1433.

Settembre, C., Zoncu, R., Medina, D.L., Vetrini, F., Erdin, S., Erdin, S., Huynh, T., Ferron, M., Karsenty, G., Vellard, M.C., et al. (2012). A lysosome-to-nucleus signalling mechanism senses and regulates the lysosome via mTOR and TFEB. EMBO J. *31*, 1095–1108.

Settembre, C., Fraldi, A., Medina, D.L., and Ballabio, A. (2013). Signals from the lysosome: a control centre for cellular clearance and energy metabolism. Nat. Rev. Mol. Cell Biol. *14*, 283–296.

Shen, K., and Sabatini, D.M. (2018). Ragulator and SLC38A9 activate the Rag GTPases through noncanonical GEF mechanisms. Proc. Natl. Acad. Sci. U. S. A. *115*, 9545–9550.

Shin, H.R., and Zoncu, R. (2020). The Lysosome at the Intersection of Cellular Growth and Destruction. Dev. Cell *54*, 226–238.

Singh, R., and Cuervo, A.M. (2011). Autophagy in the cellular energetic balance. Cell Metab. *13*, 495–504.

Skowyra, M.L., Schlesinger, P.H., Naismith, T. V., and Hanson, P.I. (2018). Triggered recruitment of ESCRT machinery promotes endolysosomal repair. Science (80-.). *360*, eaar5078.

Sleat, D.E., Sun, P., Wiseman, J.A., Huang, L., El-Banna, M., Zheng, H., Moore, D.F., and Lobel, P. (2013). Extending the Mannose 6-Phosphate Glycoproteome by High Resolution/Accuracy Mass Spectrometry Analysis of Control and Acid Phosphatase 5-Deficient Mice. Mol. Cell. Proteomics *12*, 1806–1817.

Storch, J., and Xu, Z. (2009). Niemann-Pick C2 (NPC2) and intracellular cholesterol trafficking. Biochim. Biophys. Acta - Mol. Cell Biol. Lipids *1791*, 671–678.

Su, M.Y., Morris, K.L., Kim, D.J., Fu, Y., Lawrence, R., Stjepanovic, G., Zoncu, R., and Hurley, J.H. (2017). Hybrid Structure of the RagA/C-Ragulator mTORC1 Activation Complex. Mol. Cell *68*, 835-846.e3.

Tee, A.R., Manning, B.D., Roux, P.P., Cantley, L.C., and Blenis, J. (2003). Tuberous Sclerosis Complex Gene Products, Tuberin and Hamartin, Control mTOR Signaling by Acting as a GTPase-Activating Protein Complex toward Rheb. Curr. Biol. *13*, 1259–1268.

Thelen, A.M., and Zoncu, R. (2017). Emerging Roles for the Lysosome in Lipid Metabolism. Trends Cell Biol. 1–18.

Thoreen, C.C., Kang, S.A., Chang, J.W., Liu, Q., Zhang, J., Gao, Y., Reichling, L.J.,

Sim, T., Sabatini, D.M., and Gray, N.S. (2009). An ATP-competitive mammalian target of rapamycin inhibitor reveals rapamycin-resistant functions of mTORC1. J. Biol. Chem. *284*, 8023–8032.

Thumm, M., Egner, R., Koch, B., Schlumpberger, M., Straub, M., Veenhuis, M., and Wolf, D.H. (1994). Isolation of autophagocytosis mutants of Saccharomyces cerevisiae. FEBS Lett. *349*, 275–280.

Toulmay, A., and Prinz, W. a. (2013). Direct imaging reveals stable, micrometer-scale lipid domains that segregate proteins in live cells. J. Cell Biol. *202*, 35–44.

Trinh, M.N., Lu, F., Li, X., Das, A., Liang, Q., De Brabander, J.K., Brown, M.S., and Goldstein, J.L. (2017). Triazoles inhibit cholesterol export from lysosomes by binding to NPC1. Proc. Natl. Acad. Sci. *114*, 89–94.

Tsuji, T., Fujimoto, M., Tatematsu, T., Cheng, J., Orii, M., Takatori, S., and Fujimoto, T. (2017). Niemann-Pick type C proteins promote microautophagy by expanding raft-like membrane domains in the yeast vacuole. Elife *6*, 1–23.

Tsukada, M., and Ohsumi, Y. (1993). Isolation and characterization of autophagy-defective mutants of Saccharomyces cerevisiae. FEBS Lett. *333*, 169–174.

Tsun, Z.-Y., Bar-Peled, L., Chantranupong, L., Zoncu, R., Wang, T., Kim, C., Spooner, E., and Sabatini, D.M. (2013). The Folliculin Tumor Suppressor Is a GAP for the RagC/D GTPases That Signal Amino Acid Levels to mTORC1. Mol. Cell *52*, 495–505.

Valente, E.M., Abou-Sleiman, P.M., Caputo, V., Muqit, M.M.K., Harvey, K., Gispert, S., Ali, Z., Del Turco, D., Bentivoglio, A.R., Healy, D.G., et al. (2004). Hereditary early-onset Parkinson's disease caused by mutations in PINK1. Science *304*, 1158–1160.

Valvezan, A.J., and Manning, B.D. (2019). Molecular logic of mTORC1 signalling as a metabolic rheostat. Nat. Metab. *1*, 321–333.

Verdon, Q., Boonen, M., Ribes, C., Jadot, M., Gasnier, B., and Sagné, C. (2017). SNAT7 is the primary lysosomal glutamine exporter required for extracellular protein-dependent growth of cancer cells. Proc. Natl. Acad. Sci. U. S. A. *114*, E3602–E3611.

Walkley, S.U., and Suzuki, K. (2004). Consequences of NPC1 and NPC2 loss of function in mammalian neurons. Biochim. Biophys. Acta - Mol. Cell Biol. Lipids *1685*, 48–62.

Wang, M.L., Motamed, M., Infante, R.E., Abi-Mosleh, L., Kwon, H.J., Brown, M.S., and Goldstein, J.L. (2010). Identification of surface residues on Niemann-Pick C2 essential for hydrophobic handoff of cholesterol to NPC1 in lysosomes. Cell Metab. *12*, 166–173.

Wang, S., Tsun, Z.-Y., Wolfson, R.L., Shen, K., Wyant, G.A., Plovanich, M.E., Yuan,

E.D., Jones, T.D., Chantranupong, L., Comb, W., et al. (2015). Lysosomal amino acid transporter SLC38A9 signals arginine sufficiency to mTORC1. Science (80-.). *347*, 188–194.

Weber, R.A., Yen, F.S., Nicholson, S.P.V., Alwaseem, H., Bayraktar, E.C., Alam, M., Timson, R.C., La, K., Abu-Remaileh, M., Molina, H., et al. (2020). Maintaining Iron Homeostasis Is the Key Role of Lysosomal Acidity for Cell Proliferation. Mol. Cell *77*, 645-655.e7.

Wilhelm, L.P., Wendling, C., Védie, B., Kobayashi, T., Chenard, M., Tomasetto, C., Drin, G., and Alpy, F. (2017). STARD3 mediates endoplasmic reticulum-to-endosome cholesterol transport at membrane contact sites. EMBO J. *36*, 1412–1433.

Winkler, M.B.L., Kidmose, R.T., Szomek, M., Thaysen, K., Rawson, S., Muench, S.P., Wüstner, D., and Pedersen, B.P. (2019). Structural Insight into Eukaryotic Sterol Transport through Niemann-Pick Type C Proteins. Cell *179*, 485-497.e18.

Wolfson, R.L., Chantranupong, L., Saxton, R.A., Shen, K., Scaria, S.M., Cantor, J.R., and Sabatini, D.M. (2016). Sestrin2 is a leucine sensor for the mTORC1 pathway. Science (80-.). *351*, 43–48.

Wolfson, R.L., Chantranupong, L., Wyant, G.A., Gu, X., Orozco, J.M., Shen, K., Condon, K.J., Petri, S., Kedir, J., Scaria, S.M., et al. (2017). KICSTOR recruits GATOR1 to the lysosome and is necessary for nutrients to regulate mTORC1. Nature.

Wyant, G.A., Abu-Remaileh, M., Wolfson, R.L., Chen, W.W., Freinkman, E., Danai, L. V., Vander Heiden, M.G., and Sabatini, D.M. (2017). mTORC1 Activator SLC38A9 Is Required to Efflux Essential Amino Acids from Lysosomes and Use Protein as a Nutrient. Cell *171*, 642-654.e12.

Wyant, G.A., Abu-Remaileh, M., Frenkel, E.M., Laqtom, N.N., Dharamdasani, V., Lewis, C.A., Chan, S.H., Heinze, I., Ori, A., and Sabatini, D.M. (2018). Nufip1 is a ribosome receptor for starvation-induced ribophagy. Science (80-.). *360*, 751–758.

Xu, S., Benoff, B., Liou, H.L., Lobel, P., and Stock, A.M. (2007). Structural basis of sterol binding by NPC2, a lysosomal protein deficient in Niemann-Pick type C2 disease. J. Biol. Chem. *282*, 23525–23531.

Yabe, D., Xia, Z.P., Adams, C.M., and Rawson, R.B. (2002). Three mutations in sterol-sensing domain of SCAP block interaction with insig and render SREBP cleavage insensitive to sterols. Proc. Natl. Acad. Sci. U. S. A. *99*, 16672–16677.

Yambire, K.F., Fernandez-Mosquera, L., Steinfeld, R., Mühle, C., Ikonen, E., Milosevic, I., and Raimundo, N. (2019a). Mitochondrial biogenesis is transcriptionally repressed in lysosomal lipid storage diseases. Elife *8*, 1–29.

Yambire, K.F., Rostosky, C., Watanabe, T., Pacheu-Grau, D., Torres-Odio, S.,

Sanchez-Guerrero, A., Senderovich, O., Meyron-Holtz, E.G., Milosevic, I., Frahm, J., et al. (2019b). Impaired lysosomal acidification triggers iron deficiency and inflammation in vivo. Elife *8*, 1–36.

Yang, H., Jiang, X., Li, B., Yang, H.J., Miller, M., Yang, A., Dhar, A., and Pavletich, N.P. (2017). Mechanisms of mTORC1 activation by RHEB and inhibition by PRAS40. Nature.

Yim, W.W.Y., and Mizushima, N. (2020). Lysosome biology in autophagy. Cell Discov. *6*.

Yu, W., Gong, J.S., Ko, M., Garver, W.S., Yanagisawa, K., and Michikawa, M. (2005). Altered cholesterol metabolism in Niemann-Pick type C1 mouse brains affects mitochondrial function. J. Biol. Chem. *280*, 11731–11739.

Zhao, K., and Ridgway, N.D. (2017). Oxysterol-Binding Protein-Related Protein 1L Regulates Cholesterol Egress from the Endo-Lysosomal System. Cell Rep. *19*, 1807–1818.

Zhao, Y.G., and Zhang, H. (2019). Autophagosome maturation: An epic journey from the ER to lysosomes. J. Cell Biol. *218*, 757–770.

Zoncu, R., Bar-Peled, L., Efeyan, A., Wang, S., Sancak, Y., and Sabatini, D.M. (2011). mTORC1 Senses Lysosomal Amino Acids Through an Inside-Out Mechanism That Requires the Vacuolar H+-ATPase. Science (80-.). *334*, 678–683.